NASA Conference Publication 10147

NASA Lewis Research Center Workshop on Forced Response in Turbomachinery

Proceedings of a conference sponsored by the
NASA Lewis Research Center
and held at the NASA Lewis Research Center
Cleveland, Ohio
August 11, 1993

National Aeronautics and
Space Administration

Office of Management

Scientific and Technical
Information Program

1994

C1717

PREFACE

This document serves as a summary of the NASA Lewis Research Center (LeRC) Workshop on Forced Response in Turbomachinery in August of 1993. The workshop was sponsored by the following NASA organizations: Structures, Space Propulsion Technology, and Propulsion Systems Divisions of the NASA Lewis Research Center and the Aeronautics and Advanced Concepts & Technology Offices of NASA Headquarters. In addition, the workshop was held in conjunction with the GUIde (Government/Industry/Universities) Consortium on Forced Response. The workshop was specifically designed to receive suggestions and comments from industry on current research at NASA LeRC in the area of forced vibratory response of turbomachinery blades which includes both computational and experimental approaches. There were eight presentations and a code demonstration. Major areas of research included aeroelastic response, steady and unsteady fluid dynamics, mistuning, and corresponding experimental work.

Forced response in turbomachinery blades is one of the most important issues in blade design. Controlling the forced response of turbomachinery blades is crucial for reliable operation of rocket and aircraft engines. Yet a major vacuum exists in predicting dynamic stresses in turbomachinery blades due to forced response. Furthermore, with the next generation engines being conceived for advanced aircraft, such as the high speed civil transport, forced response problems will have a major impact on their design and development. The acuteness of the problem is further emphasized by the willingness of all the engine companies to work together in the GUIde Consortium.

Representatives from the U.S. aerospace engine companies (Textron Lycoming, General Electric, Rocketdyne, Pratt & Whitney Rocket Engine Group, Pratt & Whitney Aircraft Engine Group, and United Technologies Research Center), numerous universities, the U.S. Air Force, and NASA LeRC attended the one-day workshop. In addition, the representatives from these companies, government agencies, and universities form the nucleus of the GUIde Consortium. The consortium was created to perform basic research on forced response of turbomachinery. This research work will improve the durability of turbomachinery and prevent engine failures.

An excellent dialogue took place in which many suggestions were given in a round-table discussion following each presentation. Action items from the participants were evaluated and incorporated into future work. An industry sub-committee was created to guide the FREPS (Forced REsponse Prediction System) development. Currently, FREPS is being modified to formulate a workstation version in order for industry to access the code for their design requirements. The industry representatives unanimously decided to participate in the Forced Response workshop every two years to evaluate NASA's research efforts in this area.

TABLE OF CONTENTS

PRECEDING PAGE BLANK NOT FILMED

OMIT TO P.13

16P

WORKSHOP ORGANIZERS

G. L. Stefko
NASA Lewis Research Center/Structural Dynamics Branch
21000 Brookpark Road M.S. 23-3
Cleveland, Ohio 44135
Phone: (216) 433-3920

D. V. Murthy
University of Toledo/Structural Dynamics Branch
21000 Brookpark Road M.S. 23-3
Cleveland, Ohio 44135
Phone: (216) 433-6714

M. R. Morel
NYMA, Inc./Structural Dynamics Branch
NASA Lewis Research Center Group
2001 Aerospace Parkway
Brookpark, Ohio 44142
Phone: (216) 977-1109

D. Hoyniak
NASA Lewis Research Center/Turbomachinery Technology Branch
21000 Brookpark Road M.S. 77-6
Cleveland, Ohio 44135
Phone: (216) 433-3789

J. W. Gauntner
NASA Lewis Research Center/Launch Vehicle Propulsion Branch
21000 Brookpark Road M.S. SPT-D2
Cleveland, Ohio 44135
Phone: (216) 433-7435

ATTENDEES

Dr. Reza Abhari
Textron Lycoming
Department LSD11
550 South Main Street
Stratford, CT 06497-2452

Dr. Andrew Chuang
General Electric Aircraft Engines
Mail Drop A334
One Neumann Way
Cincinnati, OH 45215

Mr. Charles J. Cross
WL/POTC
Room D133
1921 Sixth Street
Wright Patterson AFB, OH 45433-7649

Mr. Gary Davis
Rockwell International
Rocketdyne Division
6633 Canoga Avenue
Canoga Park, CA 91309-7922

Dr. Earl Dowell
Duke University
Dean School of Engineering
Durham, NC 27706

Professor Sanford Fleeter
Purdue University
School of Mechanical Engineering
Chaffee Hall
West Lafayette, IN 47907

Mr. Jim Gauntner
NASA Lewis Research Center
21000 Brookpark Road M.S. SPT-D2
Cleveland, Ohio 44135

Dr. Jerry Griffin
Carnegie Mellon University
Department of Mechanical Engineering
Pittsburgh, PA 15213

Dr. Kenneth Hall
Department Of Mechanical Engineering
Box 90300
Duke University
Durham, NC 27708-0300

Mr. Gary R. Hilbert
Pratt & Whitney
Mail Code 163-09
400 Main Street
East Hartford, CT 06108

Dr. Dan Hoyniak
NASA Lewis Research Center
21000 Brookpark Road M.S. 77-6
Cleveland, Ohio 44135

Dr. Robert E. Kielb
General Electric Aircraft Engines
Mail Drop A334
One Neumann Way
Cincinnati, OH 45215

Dr. A. P. Kurkov
NASA Lewis Research Center
21000 Brookpark Road M.S. 23-3
Cleveland, Ohio 44135

Ms. Barb Lucci
NASA Lewis Research Center
21000 Brookpark Road M.S. 5-11
Cleveland, Ohio 44135

Dr. A. Mahajan
University of Toledo/NASA Lerc
21000 Brookpark Road M.S. 23-3
Cleveland, Ohio 44135

Mr. Steve Manwaring
General Electric Aircraft Engines
Mail Drop A323
One Neumann Way
Cincinnati, OH 45215-6301

Mr. Bill McAllister
General Electric Aircraft Engines
Mail Drop N203
One Neumann Way
Cincinnati, OH 45215

Mr. Michael Morel
NYMA Inc./NASA LeRC
2001 Aerospace Parkway
Brook Park, OH 44142

Dr. Durbha Murthy
University of Toledo/NASA LeRC
21000 Brookpark Road M.S. 23-3
Cleveland, Ohio 44135

Mr. Joseph Osani
General Electric
24950 Great Northern Corporate Ctr.
Suite 215
North Olmsted, OH 44070

Mr. Joe Panovski
General Electric Aircraft Engines
Mail Drop X406
1 Neumann Way
Cincinnati, OH 45215-6301

Professor Christophe Pierre
Department of Mechanical Engineering and Applied Mechanics
3104 G.G. Brown Building
The University of Michigan
Ann Arbor, MI 48109-2125

Dr. T. S. R. Reddy
University of Toledo/NASA LeRC
21000 Brookpark Road M.S. 23-3
Cleveland, Ohio 44135

Mr. Scott Richardson
WL/POTX
Room D133
1921 Sixth Street
Wright Patterson AFB, OH 45433-7649

Mr. Richard J. Rowey
Pratt & Whitney
Mail Stop 715-92
P. O. Box 109600
West Palm Beach, FL 33410-9600

Dr. Ram Sharma
Pratt & Whitney Canada
Dynamics, Mail 01SA4
1000, Marie-Victorin
Longueuil, Quebec J4G 1A1

Mr. George Stefko
NASA Lewis Research Center
21000 Brookpark Road M.S. 23-3
Cleveland, Ohio 44135

Mr. Richard Stockton
Textron Lycoming
Department LSB10
550 South Main Street
Stratford, CT 06497-2452

Dr. Joseph M. Verdon
MF-20
United Technologies Research Center
Silverlane
East Hartford CT 06108

Dr. Brian C. Watson
University Of Virginia
Mail Stop 210
NASA Langley Research Center
Hampton, VA 23681

Dr. Dan Winterscheidt
Institute for Computational Mechanics in Propulsion (ICOMP)
22800 Cedar Point Road M.S. OAI
Brookpark, Ohio 4142

PRESENTATIONS

The following pages contain the presentations made at the Forced Response Workshop. Readers are encouraged to contact the researchers for further information. All researchers are listed in the Attendees list on pgs. iv-vi.

PROGRAM OVERVIEW

G.L. Stefko
NASA Lewis Research Center
Cleveland, Ohio 44135

PROGRAM OVERVIEW

- o FREPS SYSTEM
- o EARTH-TO-ORBIT PROGRAM
- o NASA LEWIS TEAM
- o EXTERNAL TEAM MEMBERS
- o FREPS PLANNED DEVELOPMENT

Turbomachinery
Blade Forced REsponse Prediction System

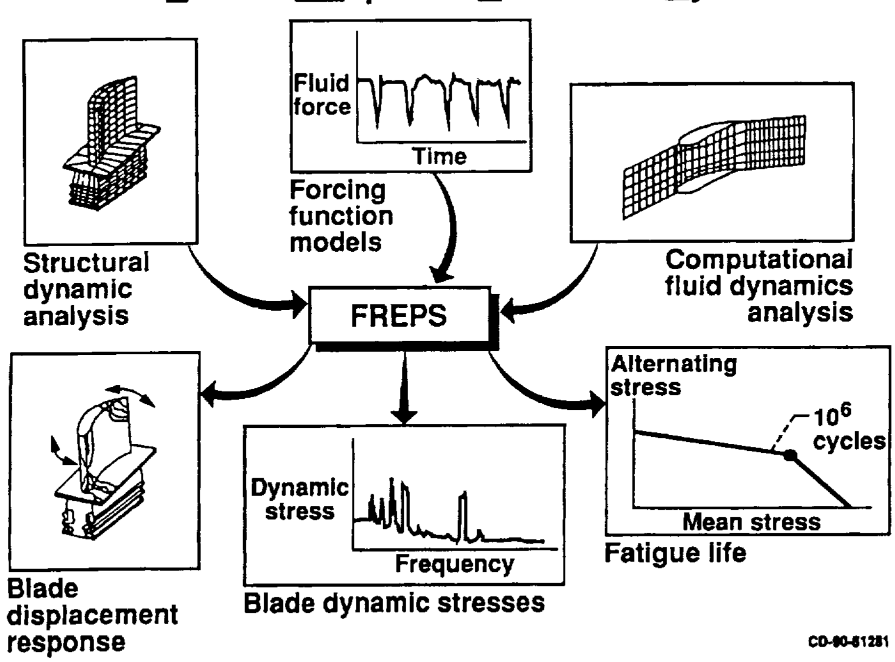

EARTH-TO-ORBIT PROPULSION
– TURBOMACHINERY SUBSYSTEMS –

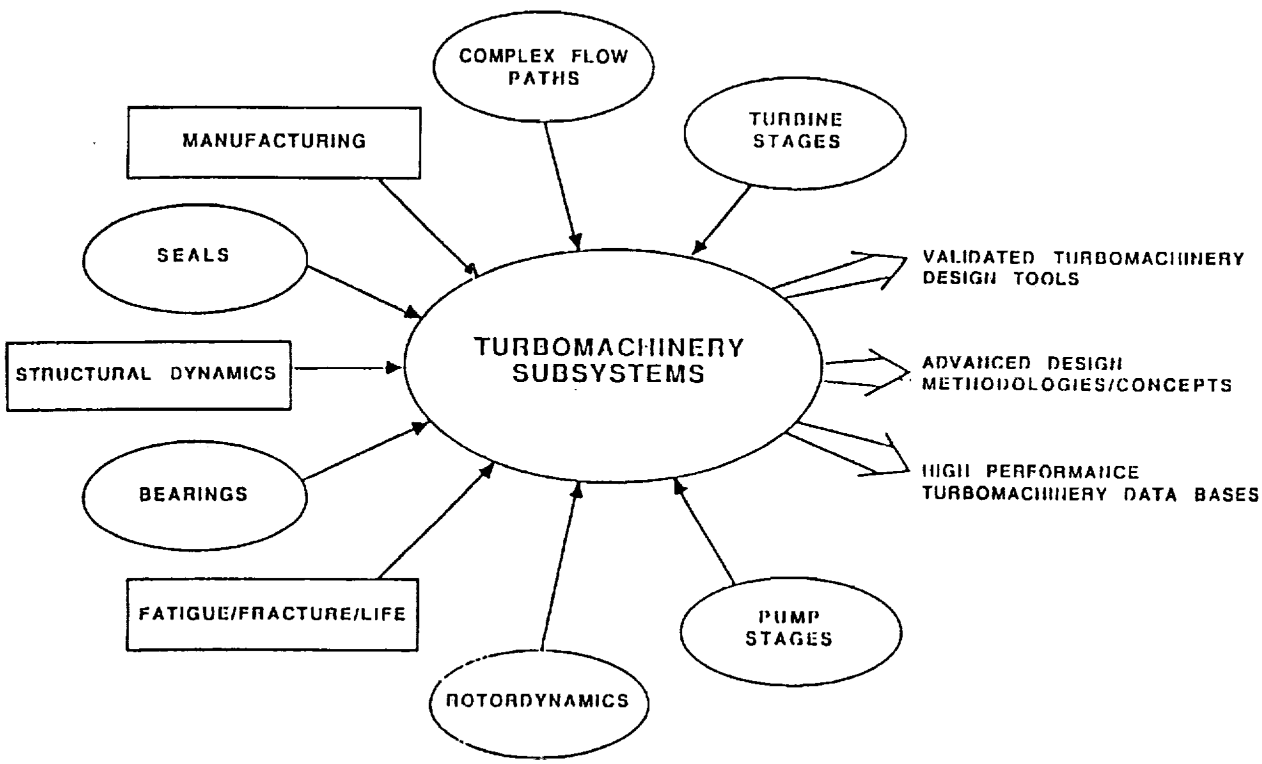

NASA LEWIS TEAMS

SPACE PROPULSION DIVISION		STRUCTURES DIVISION		PROPULSION SYSTEMS DIVISION	
DIV. CHIEF	L. DIEHL	DIV. CHIEF	L. PINSON	DIV. CHIEF	J. ZIEMIANSKI
BRANCH HEAD	S. GORLAND	BRANCH HEAD	G. STEFKO	BRANCH HEAD	L. BOBER
PRG MGRS	J. GAUNTNER A. LIANG	RESEARCHERS	D. MURTHY A. KURKOV M. MOREL	RESEARCHERS	D. HOYNIAK D. BUFFUM

EXTERNAL TEAM MEMBERS

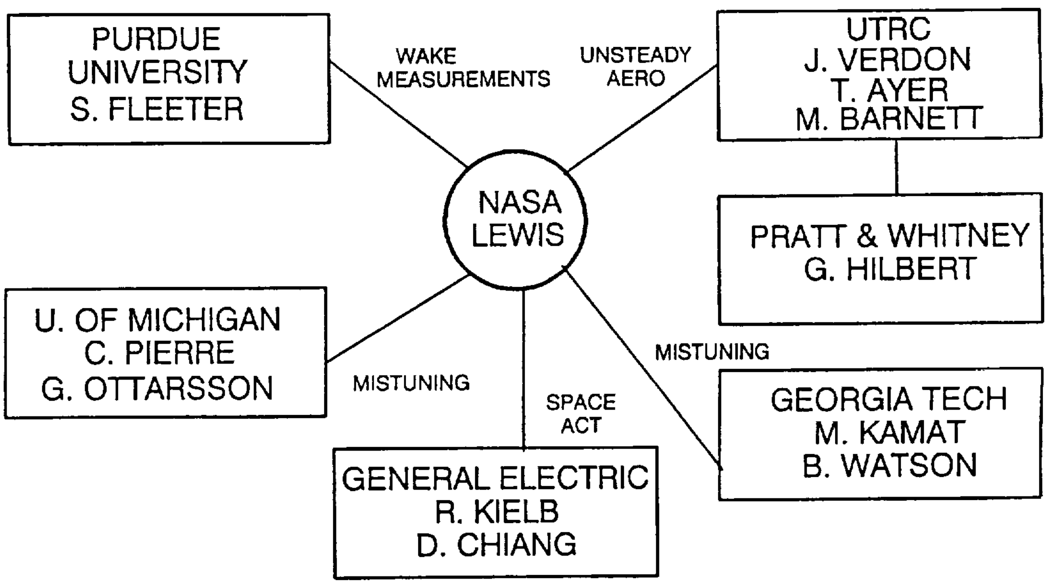

FREPS PLANNED DEVELOPMENT

93	94	95	96	97	98
o 2D FREPS	o 2D o WAKE MODEL o VALIDATION	o 2D o INVISCID/ VISCID AERO	o 3D FREPS	o 3D VALIDATION	o 3D VALIDATION

FREPS—OBJECTIVES AND OVERVIEW

D.V. Murthy*
NASA Lewis Research Center
Cleveland, Ohio 44135

Forced Vibratory Response in Turbomachinery

Consequences

- ▷ Decreases the Fatigue Life due to HCF Failures
- ▷ Increases Development and Maintenance Cost
- ▷ Imposes Operational Restrictions

Future Trends Point to Growing Problems

- ☞ *Higher Power-to-Weight Ratio Goals*
- ☞ *Lower Damping Designs (e.g. Blisks)*
- ☞ *Increased Exposure to Resonances (e.g. Low AR Blades)*

Rocket Engines vs Air Breathing Engines

	Rocket Engine Turbine	Air Breathing Engine Turbine
Turbine Inlet Temp, deg F	1540	2600
Blades Cooled?	No	Yes
Blade Metal Temp, deg F	1500	1500 Cruise
Rotor Tip Speed, fps	1850	1650 Take off
HP/Rotor Blade	500	600
Material	Super Alloy - MAR-M 246	Super Alloy - MAR-M 246
Useful Life, hours	0.1 to 7.5	8000

*NASA Resident Research Associate at Lewis Research Center.

Origins of Unsteady Aerodynamic Excitation

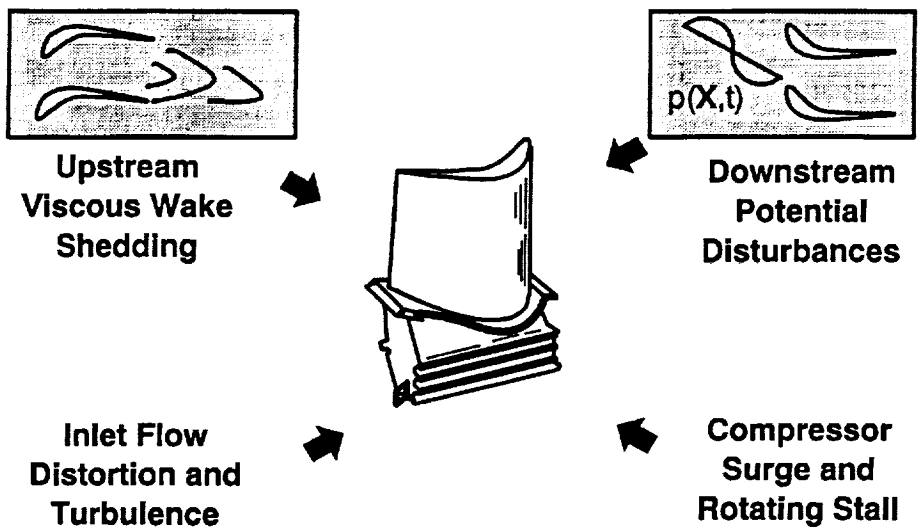

Origins of Unsteady Mechanical Excitation

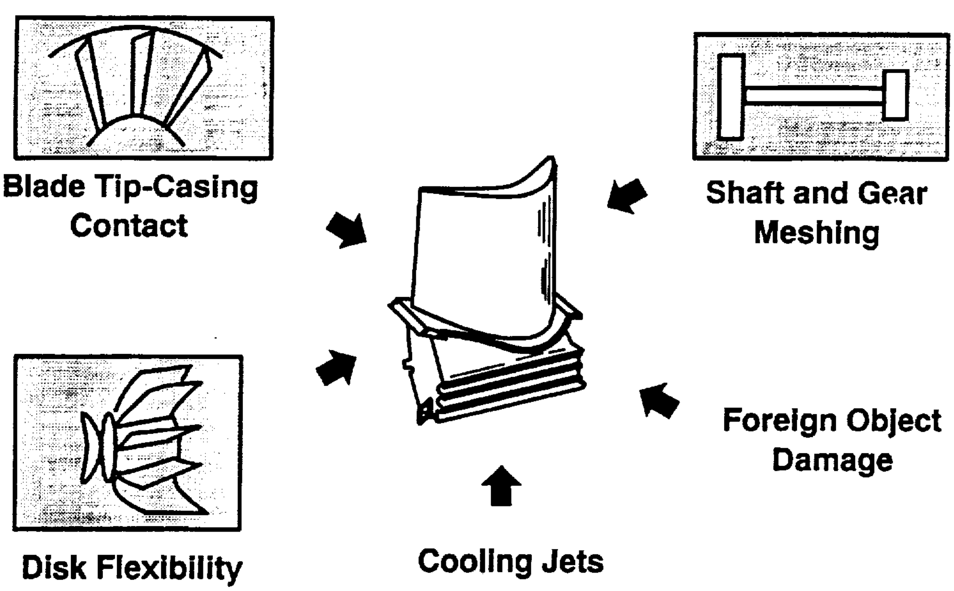

Campbell Diagram

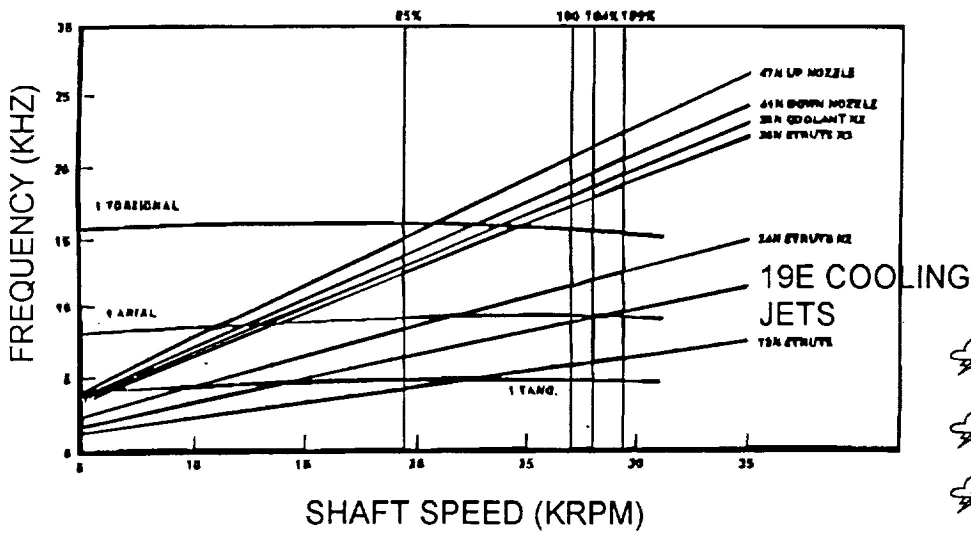

- No Quantitative Information
- Damping is Ignored
- No Accounting for Blade-to-Blade Variations

✔ FREPS Overcomes the Above Limitations and Provides an Efficient Tool for Design Environment

FREPS

Forced REsponse Prediction System

Objective

✓ To Develop a Design Tool for Predicting the Forced Vibratory Response of Turbomachinery Blades to Unsteady Excitations

✓ To Validate using Test/Experimental Data

Equations of Motion

Mechanical/Material Damping Forces from Damping Model

External Forcing Function from Mechanical Excitation Model

$$M\ddot{u} + C\dot{u} + Ku = F_A(u(t), \dot{u}(t), \ldots) + F_D(t) + F_M(t)$$

Elastic and Inertia Forces from Structural Model

Unsteady Aerodynamic Forces from Aerodynamic Model

Possible Models

ROTOR	BLADE	AERODYNAMIC	DAMPING
Tuned Identical Blades	**Typical Section** Lumped Parameter	**Fully Linear**	**Structural** Empirical
Mistuned Blade-to-Blade Variations	**Beam** 1d variation	**Linearized** Potential Euler	**Aerodynamic**
Rigid Disk	**Shell/Plate** 2d variation	**Nonlinear** Potential Euler	**Friction**
Flexible Disk	**Finite Element**		**Impact**

Goals

Accurate Predictions

Computational Efficiency

Detailed Models

Rotor	Steady Flow
Blade	Unsteady Flow

Rotor Structural Model: Tuned *or* Mistuned ?

Tuned Model is More Suitable to Design Procedures:

- ✓ **Model One Blade Only**
- ✓ **Smaller Problem Size**
- ✓ **Usually Designer's Preference**

Mistuned Model Difficult to Incorporate in Design Procedures:

- **Much Larger Problem Size**
- **Greater Complexity**
- **Mistuning Pattern / Strength Unknown at Design Time**
- **Mistuning Pattern / Strength Vary from Rotor to Rotor**
- **Monte Carlo Simulations are Very Expensive**

Blade Structural Model

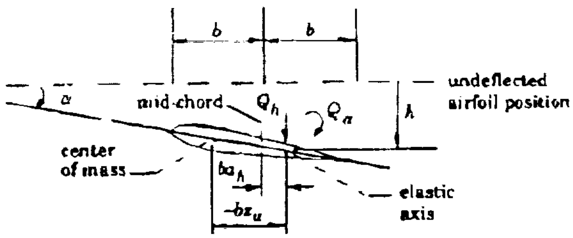

(a) typical section model

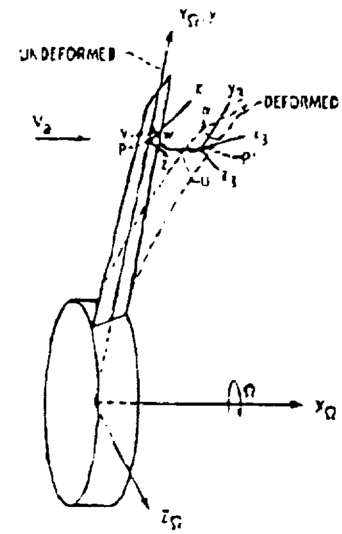

(b) beam model with rigid disk

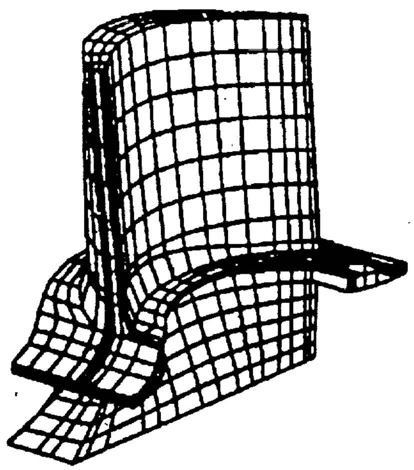

(c) finite element model

Aerodynamic Model

Steady Aerodynamic Model

2D Steady Nonlinear Potential
(SFLOW - Dr. Hoyniak, NASA Lewis)

Accounts for:
- *Incidence*
- *Camber*
- *Thickness*

Unsteady Aerodynamic Model

2D Unsteady Linearized Euler
(LINFLO - Dr. Verdon, UTRC)

- *Compressible*
- *Distorting gust*
- *Deforming Airfoil*
- *Vortical, Entropic and Acoustic Excitations*
- *Downstream Potential Disturbances*
- *Viscid / Inviscid Interaction*

Goals

Accurate Predictions

Computational Efficiency

Solution Methods

Linearized Dynamic Analysis

Modal Solution

Statistical Treatment of Mistuning

Goals

Accurate Predictions

Computational Efficiency

Solution Methods

Linearized Dynamic Analysis

Modal Solution

Statistical Treatment of Mistuning

FREQUENCY DOMAIN SOLUTION

NO TIME-MARCHING NEEDED

Goals

Accurate Predictions

Computational Efficiency

Solution Methods

Linearized Dynamic Analysis

Modal Solution

Statistical Treatment of Mistuning

FEWER DEGREES OF FREEDOM

LITTLE LOSS IN ACCURACY

Goals

Accurate Predictions

Computational Efficiency

Solution Methods

TUNED SYSTEM SIMPLICITY

USEFUL TREATMENT OF MISTUNING

Linearized Dynamic Analysis

Modal Solution

Statistical Treatment of Mistuning

N95- 19381

UNSTEADY AERODYNAMIC ANALYSES FOR TURBOMACHINERY AEROELASTIC PREDICTIONS

S1-07
37011
24P

J.M. Verdon, M. Barnett, and T.C. Ayer
United Technologies Research Center
East Hartford, Connecticut 06108

UNSTEADY AERODYNAMIC ANALYSES

- Applications
  - Aeroelastic: blade flutter and forced vibration
  - Aeroacoustic: noise generation
  - Vibration and noise control
  - Effects of unsteadiness on performance
- Requirements
  - Accuracy/efficiency
    - Realistic operating conditions
    - Arbitrary modes of unsteady excitation
- Approaches
  - Numerical simulation/analytical modeling

ASSUMPTIONS

- Turbulence and transition can be modeled

  $\Longrightarrow$ Reynolds averaged, Navier-Stokes equations
- High Reynolds number, "attached" flow

  $\Longrightarrow$ Thin-layer Navier-Stokes equations, or
  Inviscid/viscid interaction analyses
- Small-amplitude unsteady excitations

  $\Longrightarrow$ Nonlinear steady + linearized unsteady analyses
- $Re \to \infty \Longrightarrow$ inviscid flow
  - Potential steady background flow $\Longrightarrow$ LINFLO
  - Uniform steady background flow $\Longrightarrow$ CLT

CONTRACT NAS3-25425

NASA Program Managers: J. Gauntner, G. Stefko

- Linearized inviscid unsteady aerodynamic analysis: LINFLO
- Unsteady viscous layer analysis: UNSVIS
- Steady, inviscid/viscid interaction analysis: SFLOW-IVI
- Coupled SFLOW-IVI/LINFLO analysis

EXAMPLE CONFIGURATION

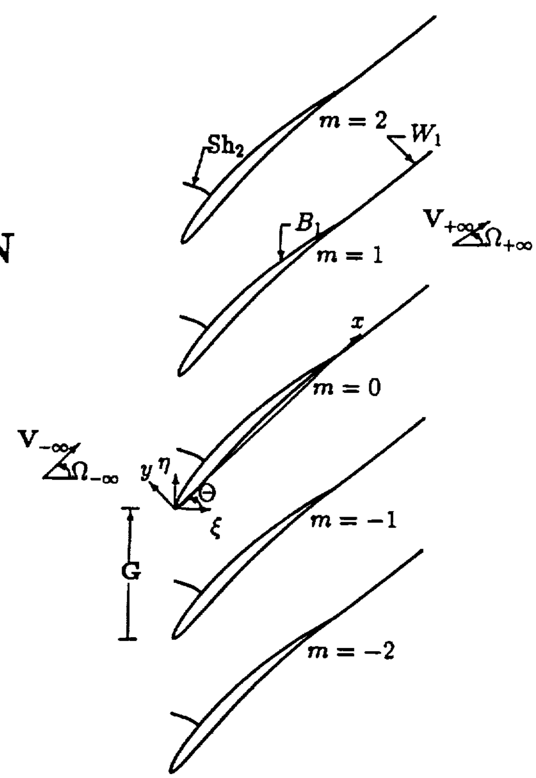

UNSTEADY EXCITATIONS

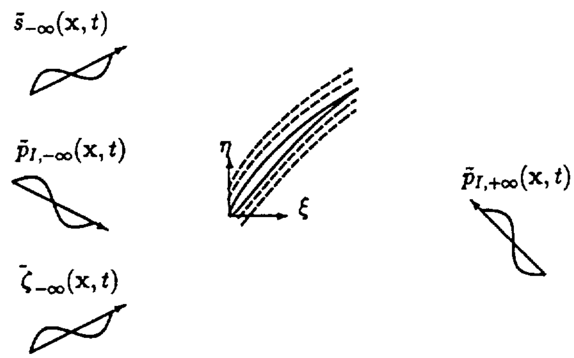

- **Far-field conditions (uniform mean flow)**

$$\bar{s}(\mathbf{x}, t) = Re\{s_{-\infty} \exp[i(\boldsymbol{\kappa}_{-\infty} \cdot \mathbf{x} + \omega t)]\}, \quad \xi < \xi_-$$

$$\bar{\zeta}(\mathbf{x}, t) = \mathrm{Re}\{\boldsymbol{\zeta}_{-\infty} \exp[i(\boldsymbol{\kappa}_{-\infty} \cdot \mathbf{x} + \omega t)]\}, \quad \xi < \xi_-$$

$$\bar{p}_{I,\mp\infty}(\mathbf{x}, t) = \mathrm{Re}\{p_{I,\mp\infty} \exp[-\beta_{\mp\infty}\xi + i(\boldsymbol{\kappa}_{\mp\infty} \cdot \mathbf{x} + \omega t)]\}, \quad \xi \lessgtr \xi_{\mp}$$

LINEARIZED INVISCID ANALYSES

- **Linearization**

$$\bar{P}(\mathbf{x}, t) = P(\mathbf{x}) + \mathrm{Re}\{p(\mathbf{x}) \exp(i\omega t)\} + \dots$$

$\Longrightarrow$

- **Nonlinear BVP for steady background flow**
- **Linear variable-coefficient problem for each Fourier component of first-order unsteady flow**
  - **Time independent**
  - **Surface conditions imposed at mean surfaces**
  - **Analytic far-field solutions for** s, ζ, and p
  - **Single extended blade-passage solution domain**

$$\bar{P}(\mathbf{x} + m\mathbf{G}, t) = P(\mathbf{x}) + \mathrm{Re}\{p(\mathbf{x}) \exp[i(\omega t + m\sigma)]\} + \dots$$

- **Prescribed quantities:**

$$\omega,\ \sigma,\ \mathbf{r}_{\mathrm{B}},\ s_{-\infty}\ \zeta_{-\infty},\ \text{and}\ \ p_{I,\mp\infty}$$

LINFLO

- Unsteady perturbation of a potential mean flow
- Steady flow: $\nabla \cdot (\bar{\rho} \nabla \Phi) = 0$
- Unsteady velocity decomposition: $\mathbf{v} = \nabla(\phi + \phi_*) + \mathbf{v}_R$
  - $p = -\bar{\rho} \bar{D}\phi / Dt$
  - $\nabla \cdot \mathbf{v}_R = 0$ far upstream
  - $\bar{D}\phi_* / Dt \equiv 0$; $(\nabla \phi_* + \mathbf{v}_R) \cdot \mathbf{n} \equiv 0$ on B_m & W_m
- Entropy & rotational velocity: $\mathbf{X} = \Delta \mathbf{e}_T + \Psi \mathbf{e}_N \rightarrow \mathbf{x}$ as $\xi \rightarrow -\infty$

$$s(\mathbf{x}) = s_{-\infty} \exp(i \boldsymbol{\kappa}_{-\infty} \cdot \mathbf{X})$$

$$\mathbf{v}_R(\mathbf{x}) = [\nabla(\mathbf{X} \cdot \boldsymbol{\mathcal{A}}_{-\infty}) + s_{-\infty} \nabla \Phi / 2] \times \exp(i \boldsymbol{\kappa}_{-\infty} \cdot \mathbf{X})$$

- Unsteady velocity potential

$$\bar{D}(A^{-2} \bar{D}\phi / Dt) / Dt - \bar{\rho}^{\,-1} \nabla \cdot (\bar{\rho} \nabla \phi) = \bar{\rho}^{\,-1} \nabla \cdot [\bar{\rho} \nabla \phi_*]$$

where $\phi_* = F(\boldsymbol{\mathcal{A}}_{-\infty}, \Psi) \exp(i \boldsymbol{\kappa}_{-\infty} \cdot \mathbf{X})$

- Surface conditions:
  - Blades: $\nabla \phi \cdot \mathbf{n} = f(\mathbf{r}_B)$
  - Wakes: $[\![\bar{D}\phi / Dt]\!] = 0$ and $[\![\nabla \phi]\!] \cdot \mathbf{n} = 0$
  - Shocks: $[\![\bar{\rho} \nabla \phi + \rho \nabla \Phi]\!] \cdot \mathbf{n} = f(\mathbf{r}_{Sh} \cdot \mathbf{n}, \nabla \Phi); \mathbf{r}_{Sh} \cdot \mathbf{n} = -[\![\phi]\!] / [\![\Phi_n]\!]$
- Far field conditions:
  - $\phi_{I, \mp\infty}$ prescribed; $\phi_{R, \mp\infty}$ must be determined
  - Analytic far-field solutions for $\phi = \phi_I + \phi_R$

NUMERICAL SOLUTION DOMAIN

- Extended blade-passage region of finite extent in axial-flow direction

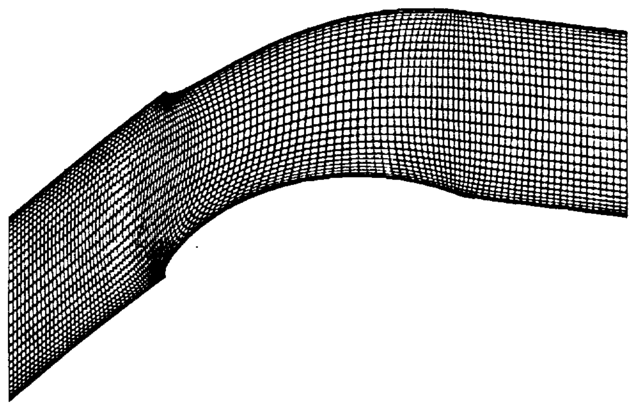

NUMERICAL APPROXIMATION

- Implicit, least-squares, finite-difference model

$$(\mathcal{L}\phi)_o \approx (L\phi)_o = q^o\phi_o + \sum_{m=1}^{m} \beta_m(\phi_m - \phi_o)$$

- Transonic differencing strategies
- Cascade, local and composite mesh solutions
- Direct solution procedure
  - Block tridiagonal system of algebraic equations for subsonic flow
  - Block pentadiagonal system for transonic flow with fitted shocks

AERODYNAMIC RESPONSE AT A BLADE SURFACE

- **Surface pressure (transonic flow):**

$$\tilde{P}(\tau_B, t) = P(\tau_B) + \mathrm{Re}\{p_B(\tau_B)\exp(i\omega t)\} + \sum_n \tilde{P}_{Sh_n}(\tau_B, t) + \ldots$$

- **Blade motion:** $\mathbf{r}_B(\mathbf{x}) = \sum_{i=1}^{I} \delta_i \mathbf{R}_i(\mathbf{x})$
- **Unsteady airloads:**

$$q_i = \oint q_{i,\tau} d\tau = -\oint_B [P\frac{\partial \mathbf{r}_B}{\partial \tau} \times \mathbf{e}_z + p_B\mathbf{n} - \sum_n r_{Sh_n}[P]\mathbf{n}] \cdot \mathbf{R}_i d\tau$$

- **Work per cycle/pressure-displacement function**

$$W_C = \oint \frac{d\tilde{W}}{dt} dt = \oint_B w(\tau) d\tau = \pi \oint \mathrm{Im}\{\delta_i^* q_{i,\tau}\} d\tau = \pi \mathrm{Im}\{\sum_{i=1}^{I} \delta_i^* q_i\}$$

EXAMPLE RESPONSE PREDICTIONS

- **Compressor exit guide vane (EGV):** $\Theta = 15\,\mathrm{deg},\ G = 0.6$
  - Thick, highly-cambered NACA 0012 airfoils
  - Subsonic flow: $M_{-\infty} = 0.3,\ \Omega_{-\infty} = 40\,\mathrm{deg}$
  - Vortical excitation: $\omega = 10,\ \sigma = -2\pi$
  - Acoustic excitation from downstream: $\omega = 10,\ \sigma = 0$
- **High speed compressor cascade:** $\Theta = 45\,\mathrm{deg},\ G = 1$
  - Cambered NACA 0006 airfoils
  - Subsonic flow: $M_{-\infty} = 0.7,\ \Omega_{-\infty} = 58\,\mathrm{deg}$
  - Transonic flow: $M_{-\infty} = 0.8,\ \Omega_{-\infty} = 55\,\mathrm{deg}$
  - SDOF blade motions: $\delta_i = (1,0),\ \omega = 1$
- **Linear/nonlinear result comparisons**
  - NGUST analysis (Navier-Stokes)
  - NPHASE analysis (Euler)

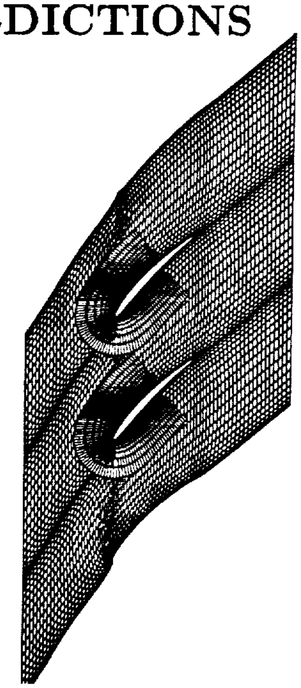

COMPRESSOR EXIT GUIDE VANE

NGUST Computational Grid

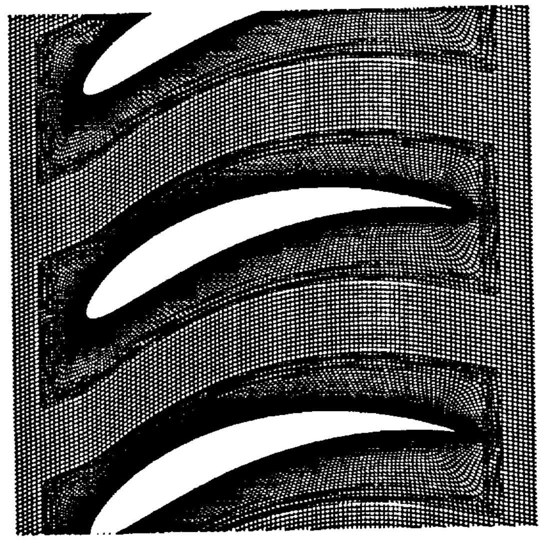

COMPRESSOR EXIT GUIDE VANE

Steady surface pressure coefficient

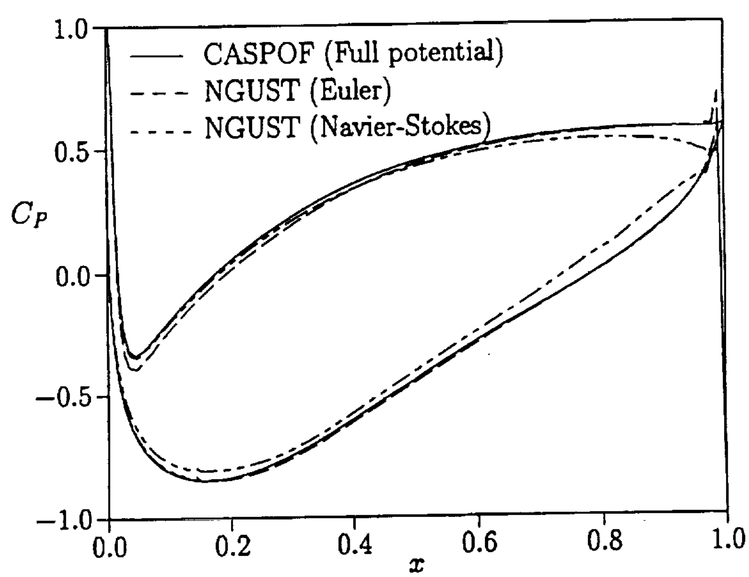

VORTICITY WAVE IN AN EGV CASCADE

Unsteady vorticity, $\vec{v}_{R,-\infty} = (0.05\bar{q}, 0)$, $\sigma = -2\pi$, $\omega = 10.0$

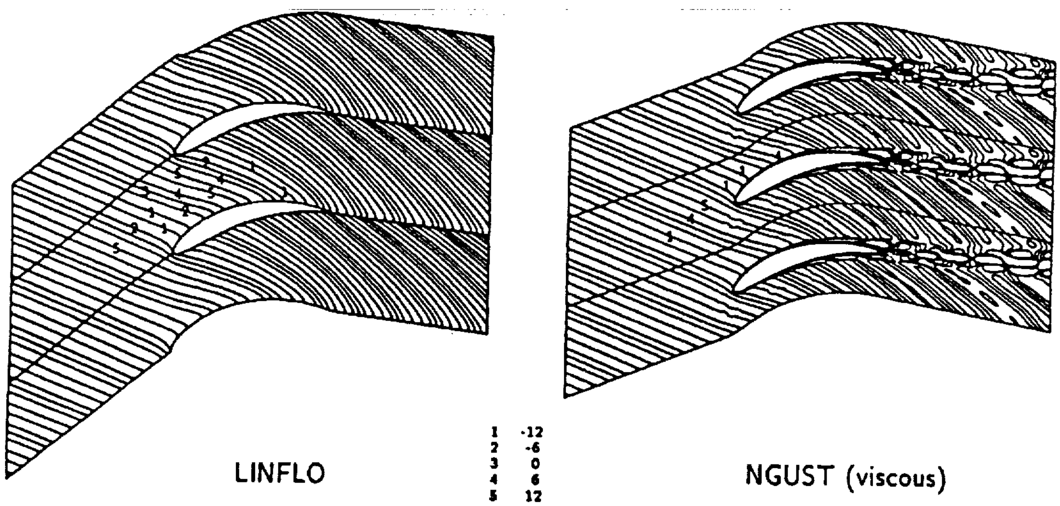

VORTICITY WAVE IN AN EGV CASCADE

Unsteady pressure, $\vec{v}_{R,-\infty} = (0.05\bar{q}, 0)$, $\sigma = -2\pi$, $\omega = 10.0$

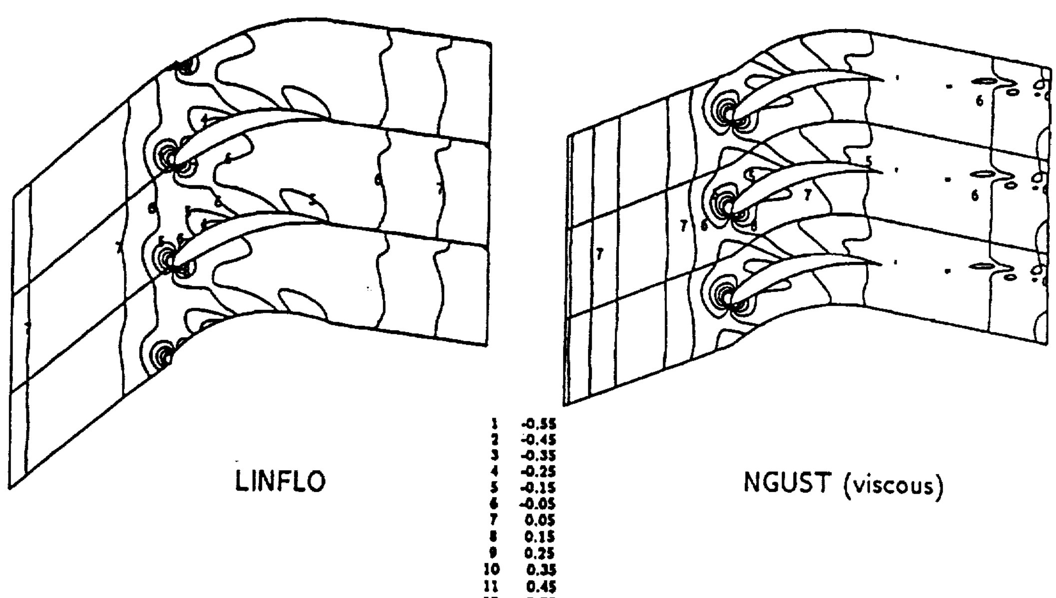

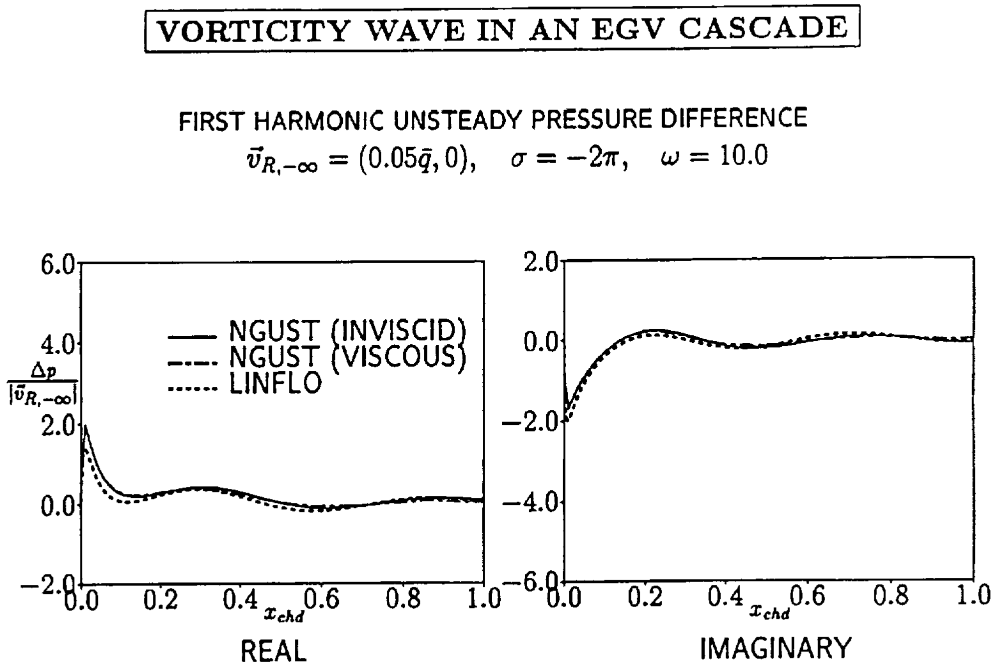

VORTICITY WAVE IN AN EGV CASCADE
FIRST HARMONIC UNSTEADY PRESSURE DIFFERENCE
$\vec{v}_{R,-\infty} = (0.05\bar{q}, 0)$, $\sigma = -2\pi$, $\omega = 10.0$
NGUST (INVISCID)
NGUST (VISCOUS)
LINFLO
$\frac{\Delta p}{|\vec{v}_{R,-\infty}|}$
x_{chd}
REAL
IMAGINARY

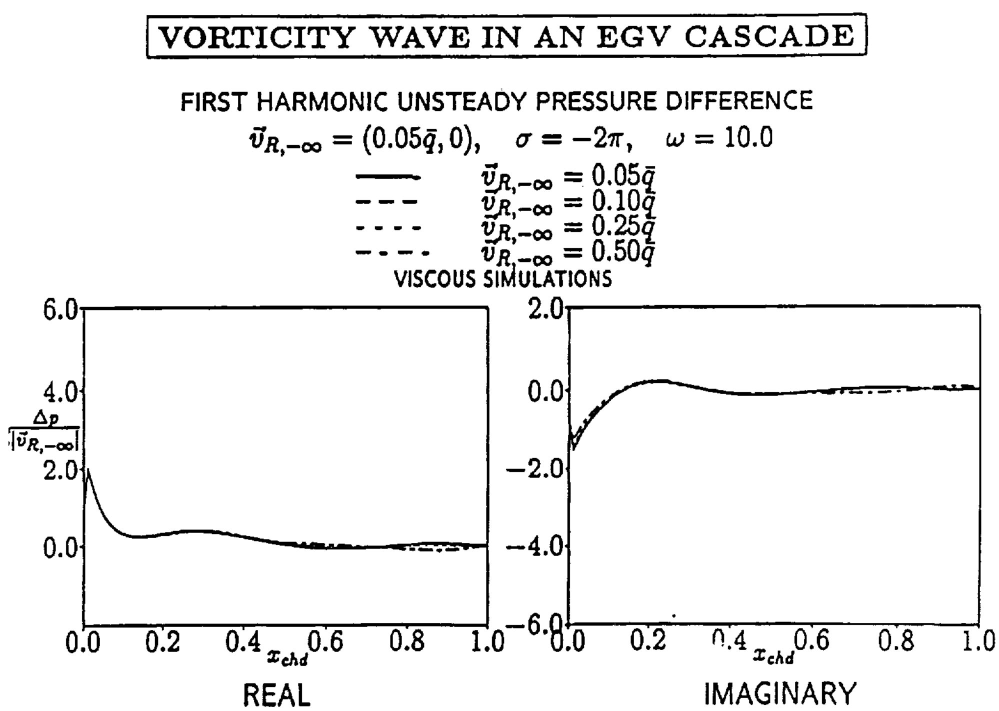

VORTICITY WAVE IN AN EGV CASCADE
FIRST HARMONIC UNSTEADY PRESSURE DIFFERENCE
$\vec{v}_{R,-\infty} = (0.05\bar{q}, 0)$, $\sigma = -2\pi$, $\omega = 10.0$
$\vec{v}_{R,-\infty} = 0.05\bar{q}$
$\vec{v}_{R,-\infty} = 0.10\bar{q}$
$\vec{v}_{R,-\infty} = 0.25\bar{q}$
$\vec{v}_{R,-\infty} = 0.50\bar{q}$
VISCOUS SIMULATIONS
$\frac{\Delta p}{|\vec{v}_{R,-\infty}|}$
x_{chd}
REAL
IMAGINARY

COMPRESSOR EXIT GUIDE VANE

Unsteady Pressure Response

$p_{+\infty} = (0.04, 0)$, $\omega = 10.0$, $\sigma = 0.0$

Linearized Inviscid (LINFLO) Navier-Stokes (NGUST)

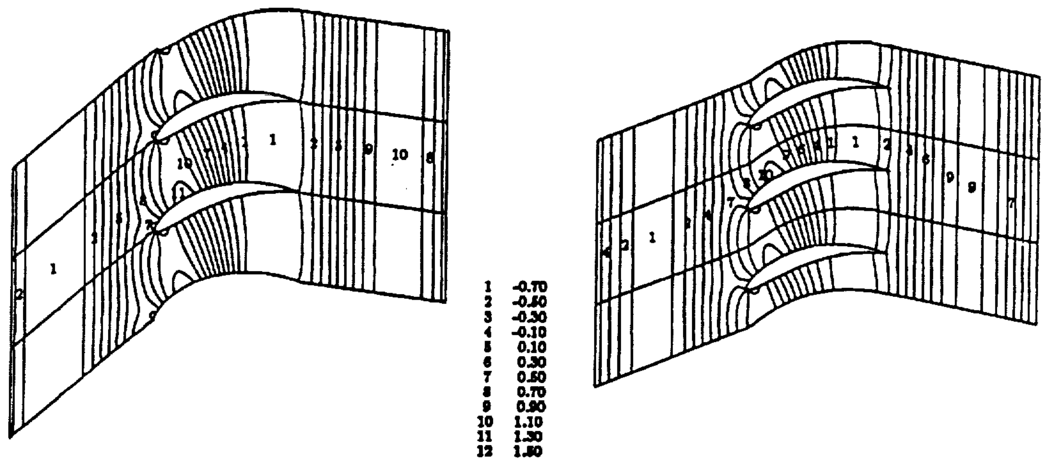

EXIT ACOUSTIC WAVE IN AN EGV CASCADE

FIRST HARMONIC UNSTEADY PRESSURE DIFFERENCE

$p_{I,+\infty} = (0.04\bar{P}, 0)$, $\sigma = 0$, $\omega = 10.0$

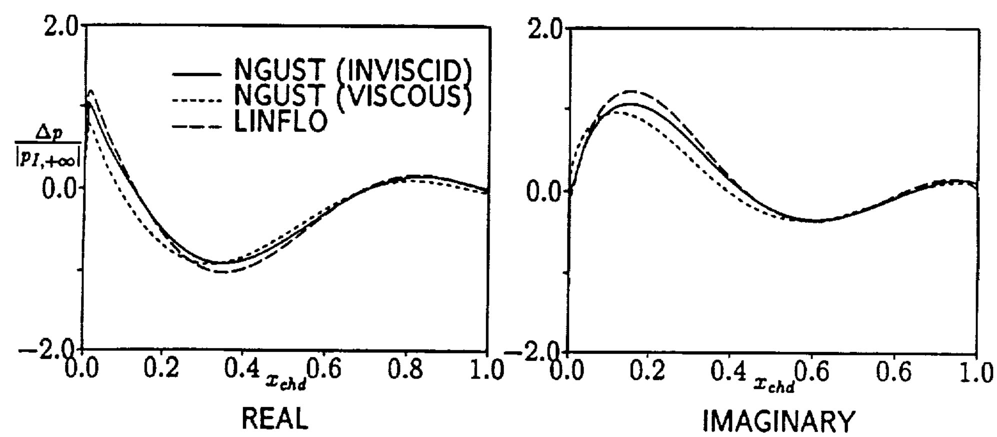

EXIT ACOUSTIC WAVE IN AN EGV CASCADE

FIRST HARMONIC UNSTEADY PRESSURE DIFFERENCE

$p_{I,+\infty} = (0.04\bar{P}, 0), \quad \sigma = 0, \quad \omega = 10.0$

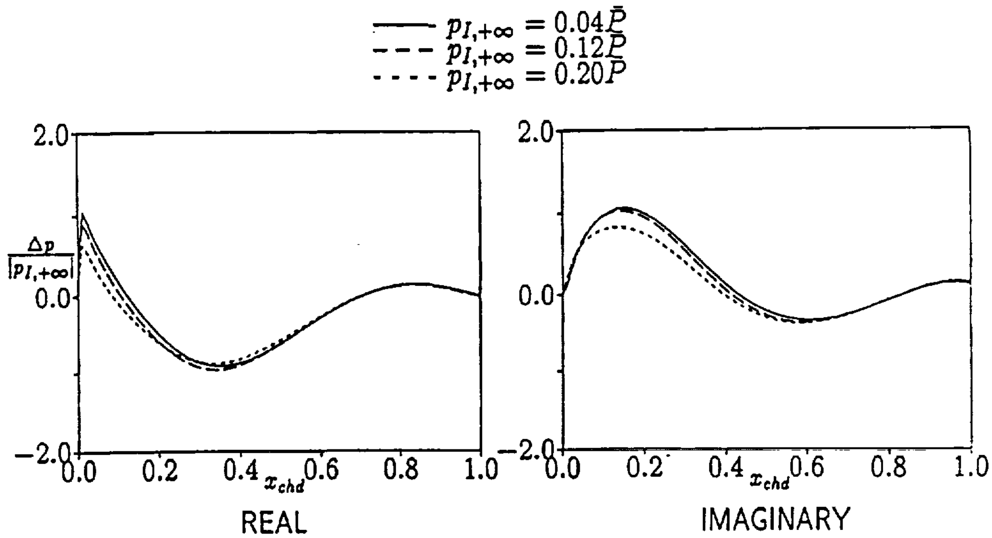

NACA 0006 CASCADE

NPHASE Computational Grid

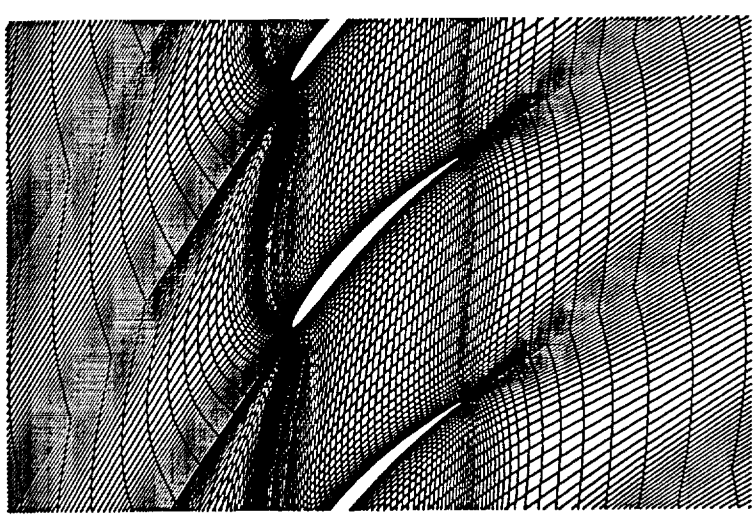

HIGH SPEED COMPRESSOR CASCADE

Surface Mach Number Distributions
—— Potential, – – – – Euler

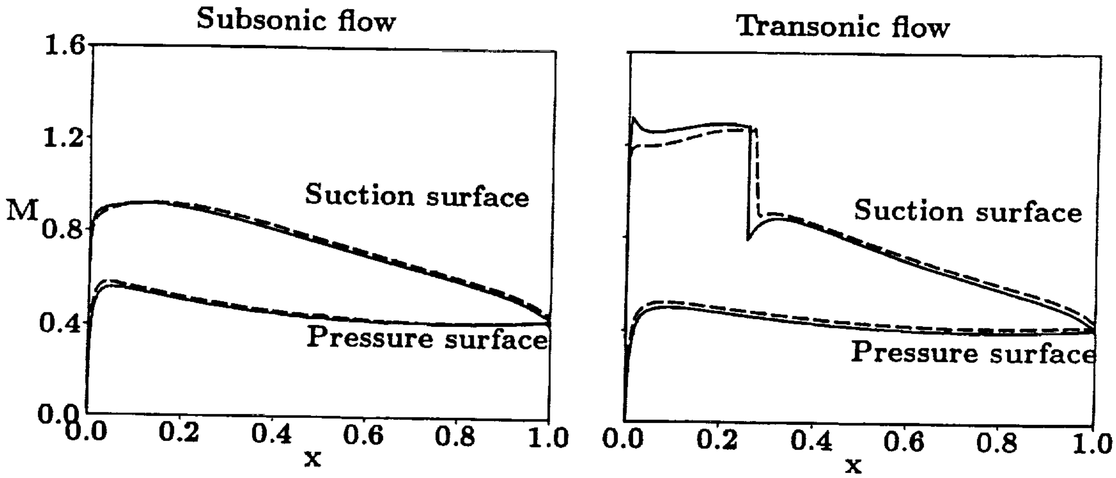

HIGH SPEED COMPRESSOR CASCADE

Pressure Displacement Function Distributions for
Torsional Blade Vibrations at $\alpha = 2\ deg$, $\omega = 1$

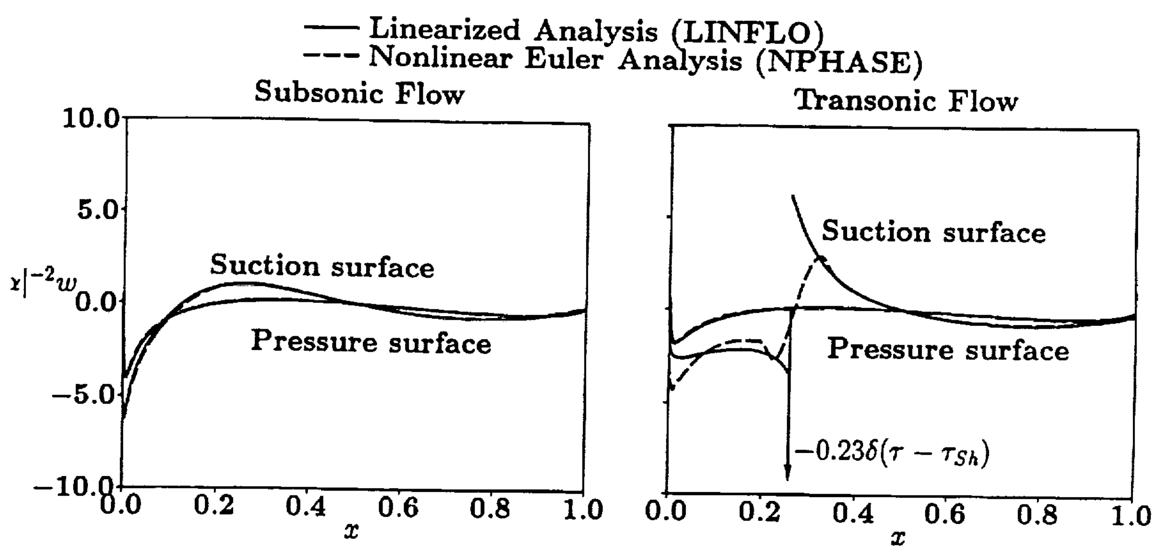

HIGH SPEED COMPRESSOR CASCADE

Work per Cycle versus Interblade Phase Angle for
Torsional Blade Vibrations at $\alpha = 2\ deg$, $\omega = 1$

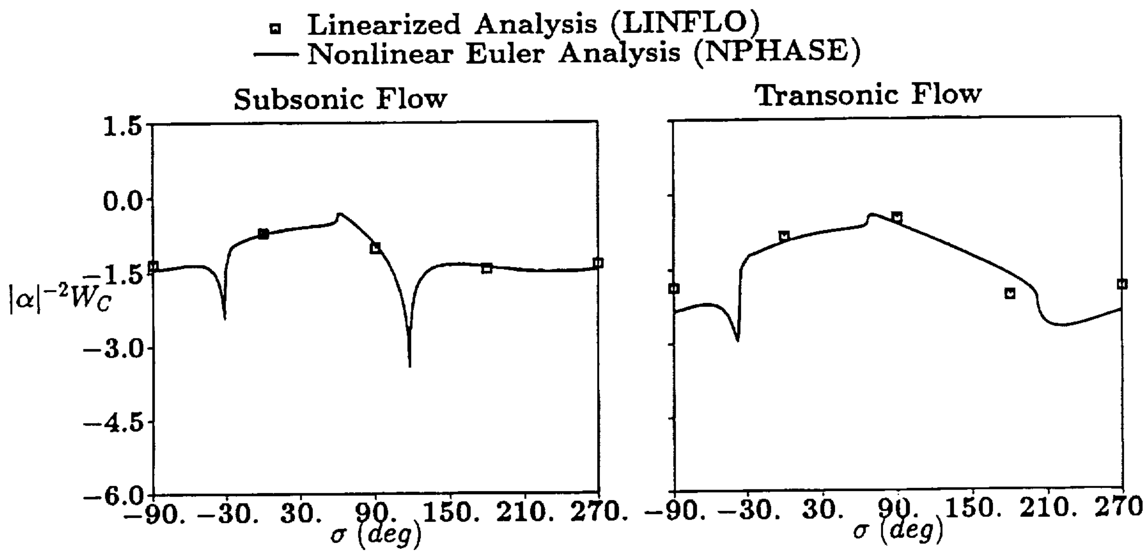

INVISCID/VISCID INTERACTION ANALYSES

- High Reynolds Number Flow
- Inviscid region: Euler or potential flow equations
  - Surface conditions modified to account for viscous displacement effects
- Viscous region: Prandtl's equations
  - Direct solution: $P \rightarrow \bar{\delta}$
  - Inverse solution: $\bar{\delta} \rightarrow P$
- Inviscid viscid interaction law
  - Weak interaction $\Rightarrow$ sequential solution, pressure determined by inviscid flow
  - Strong interaction $\Rightarrow$ simultaneous solution, pressure determined by inviscid and viscous flows

CASCADE FLOW WITH LOCAL REGIONS OF STRONG INTERACTION

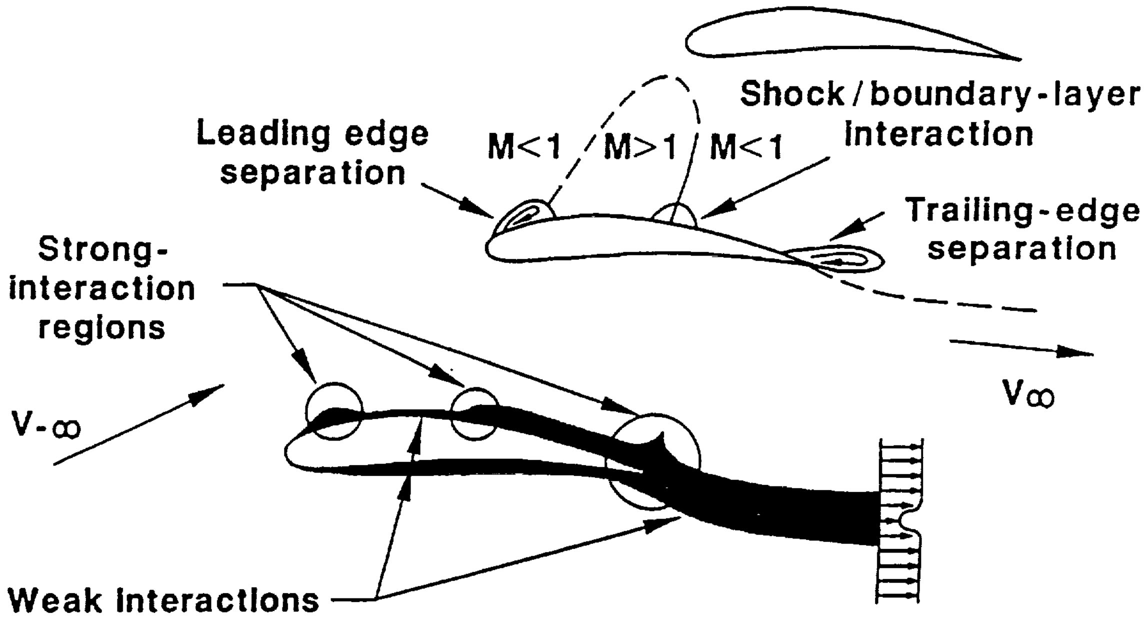

SFLOW-IVI: INVISCID REGION

- Field equation
  - $\bar{\rho}\nabla\Phi = 0$ or $A^2\nabla^2\Phi = \nabla\Phi \cdot \nabla(\nabla\Phi)^2/2$
- Surface b.c.'s account for viscous displacement effects; i.e.,
  - Blades: $\nabla\Phi \cdot \vec{n}|_S = \rho_e^{-1} d(\rho_e u_e \delta)/ds$
  - Wakes: $[\nabla\Phi] \cdot \vec{n}_+|_W = \rho_e^{-1} d(\rho_e u_e \delta_W)/ds$
- Inlet flow conditions prescribed
- Exit flow conditions determined by Kutta cond. & global mass conservation

SFLOW-IVI: VISCOUS REGION

- Classical Viscous-Layer Eqs. (Boundary layers & Wakes)
  - Weak interaction:
    specify $du_e/ds \rightarrow$ calc. δ^* (direct)
  - Strong interaction:
    specify $\overline{m} = \rho_e u_e \delta^* \rightarrow$ calc. u_e (inverse)
- Turbulence and transition
  - Algebraic eddy-viscosity model
    - Blade: Cebeci-Smith w/separation modification
    - Wake: Chang, et al
  - Instantaneous transition
- Solutions in terms of Levy Lees variables

SFLOW-IVI: COUPLING PROCEDURE

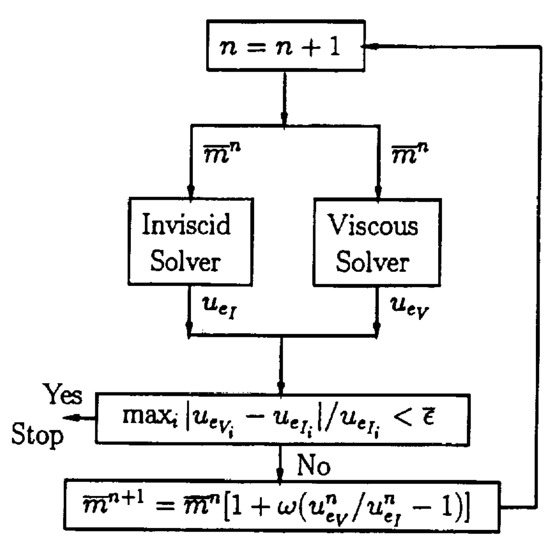

NUMERICAL RESULTS

- Two Cascade Configurations
  - Compressor exit guide vane (EGV)
  - High-speed compressor cascade
- Effect of Varying Re
- Comparison with Navier-Stokes solutions
- Incidence Angle Study (EGV)

COMPRESSOR EXIT GUIDE VANE

Effect of Varying *Re*: — — — $Re = 10^5$
- - - - $Re = 10^6$
——— Inviscid

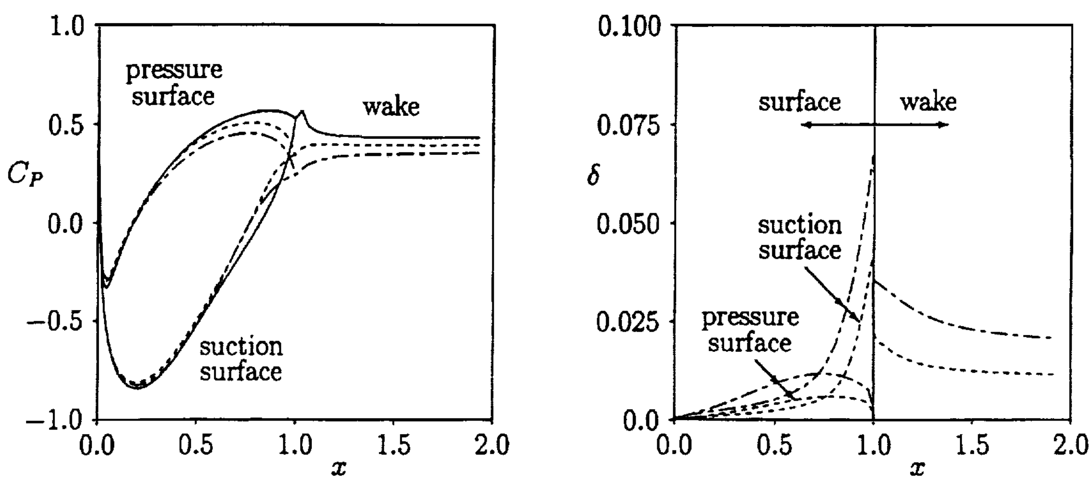

COMPRESSOR EXIT GUIDE VANE

Comparison with Navier-Stokes Solution: $Re = 10^6$

—— IVI
– – – N-S

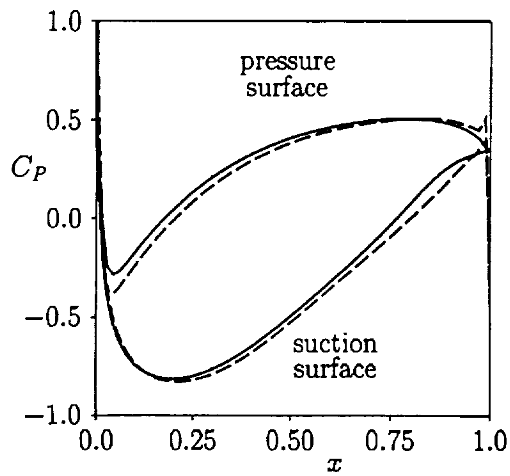

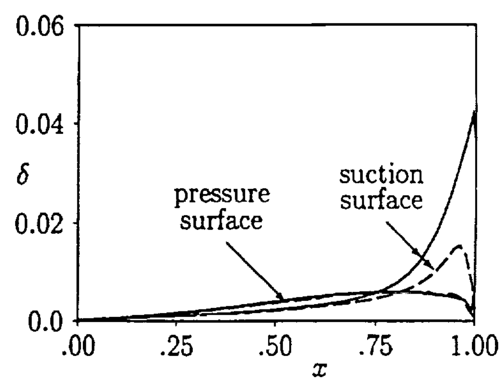

COMPRESSOR EXIT GUIDE VANE

Comparison with Navier-Stokes Solution: $Re = 10^6$

—— IVI
– – – N-S

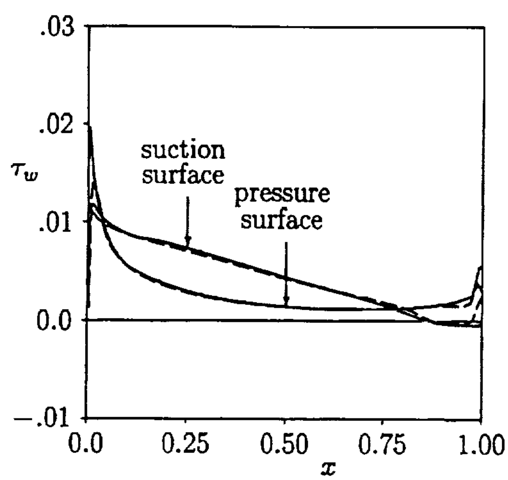

COMPRESSOR EXIT GUIDE VANE

Loss Parameter, $\bar{\omega}$, & separation point location, x_{sep}, versus Inlet Flow Angle:

$Re = 10^6$, $M_{-\infty} = 0.3$

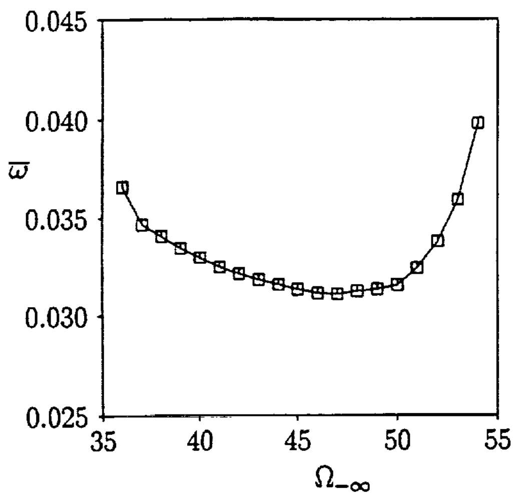

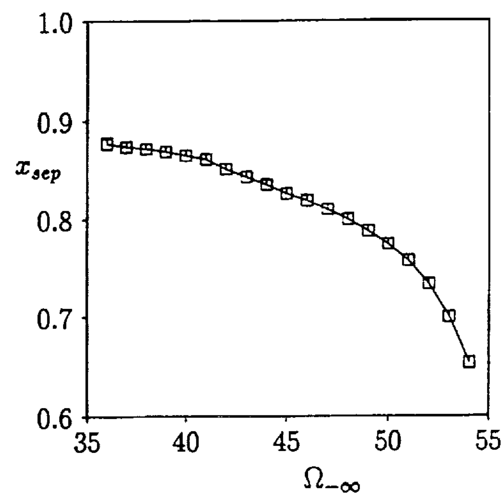

COMPRESSOR EXIT GUIDE VANE

Streamlines in Trailing-Edge Region: $Re = 10^6$

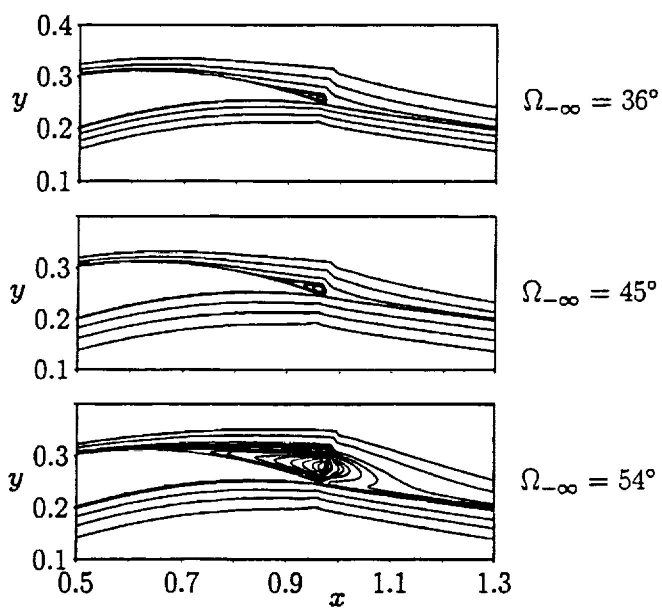

HIGH SPEED COMPRESSOR CASCADE

Comparison with Navier-Stokes Solution: $Re = 10^6$

——— IVI
– – – – N-S

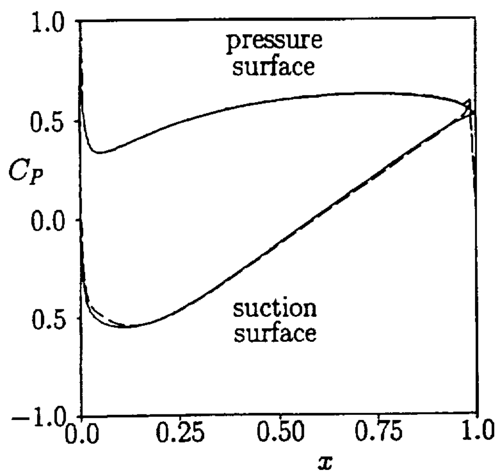

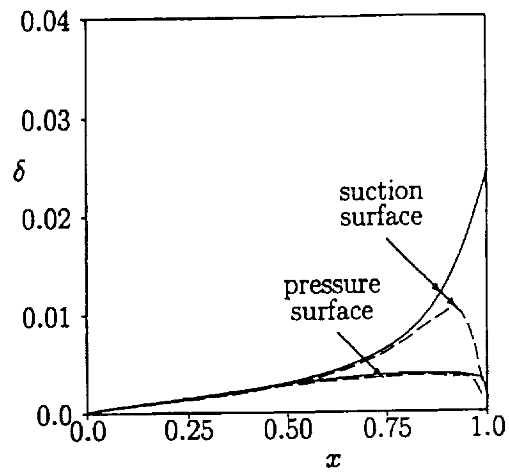

HIGH SPEED COMPRESSOR CASCADE

Comparison with Navier-Stokes Solution: $Re = 10^6$

——— IVI
– – – – N-S

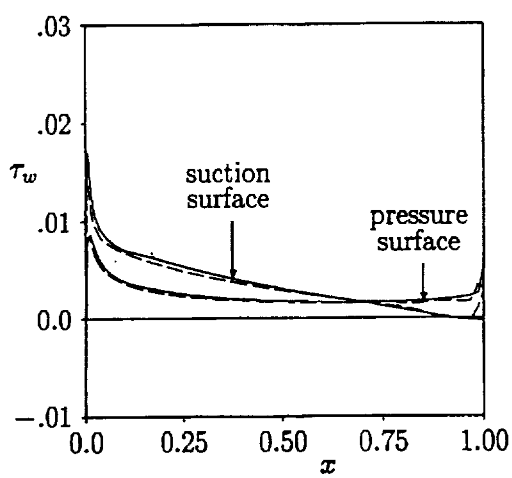

GOAL: UNSTEADY IVI ANALYSIS FOR AEROELASTIC APPLICATIONS

- High Re unsteady cascade flows
- Inviscid region
  - Nonlinear steady (SFLOW) $\Rightarrow \Phi$
  - Linearized unsteady (LINFLO) $\Rightarrow s, \mathbf{v}_R, \phi$
    note: $\tilde{\mathbf{V}} = \nabla\Phi + Re\{[\nabla(\phi + \phi^*) + \mathbf{v}_R]\exp(i\omega t)\}$
  - Surface conditions
    - Blades: $(\tilde{\mathbf{V}} - \dot{\mathcal{R}}) \cdot \mathbf{n} = f_B\{\bar{\tilde{\delta}}\}$
    - Wakes: $[\![\tilde{\mathbf{V}}]\!] \cdot \mathbf{n} = f_W\{\bar{\tilde{\delta}}\}$
- Viscous region
  - Unsteady viscous layer analysis UNSVIS
  - UNSVIS is a direct, time marching solution procedure
- Inviscid/viscid coupling
  - Procedure must be developed for unsteady flows
- Issues
  - Must modify UNSVIS to deal with moving blades
  - Matching of inviscid and viscid solutions for s and $\mathbf{v}_R$ excitations
  - Need inverse unsteady viscous layer calculation
  - Inviscid/viscid coupling $\Rightarrow$ long computer run times; unless
    - $\tilde{\delta} \approx \bar{\delta} + \delta\exp(i\omega t)$, i.e., linearization, or
    - Integral boundary layer calculation

INTERMEDIATE STEP: COUPLED SFLOW-IVI/LINFLO

- **Effects of strong steady interactions on unsteady pressure response**
- **Assumptions**
  - $\bar{\bar{\delta}}(\mathbf{x}, t) = \bar{\delta}(\mathbf{x}) + \tilde{\delta}(\mathbf{x}, t)$
  - **Strong steady inviscid/viscid interaction**
  - **Weak unsteady interaction**
- **SFLOW-IVI will provide steady background flow information for LINFLO calculation**
  - **Unsteady surface pressure determined by linearized inviscid calculation**
  - **Unsteady viscous layer determined by direct solution procedure**

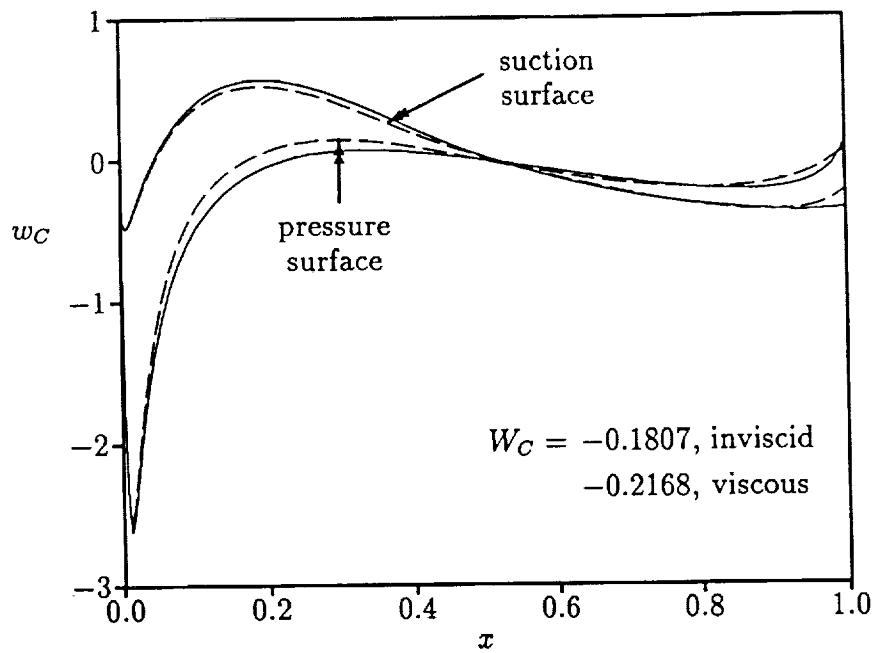

Figure 1: LINFLO results for EGV cascade undergoing torsional vibration ($\alpha = (1,0)$, $\sigma = 0$ deg, $\omega = 1$); $\Omega_{-\infty} = 40$ deg, $M_{-\infty} = 0.30$: (— — — —) inviscid; (———) viscous, $Re = 10^6$.

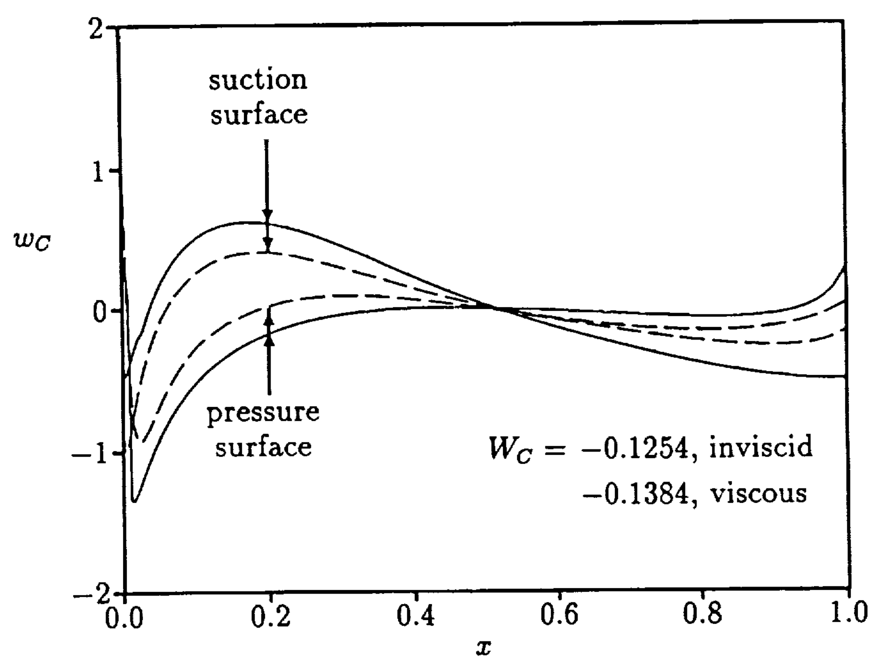

Figure 2: LINFLO results for EGV cascade undergoing torsional vibration ($\alpha = (1,0)$, $\sigma = 0$ deg, $\omega = 1$); $\Omega_{-\infty} = 54$ deg, $M_{-\infty} = 0.30$: (— — — —) inviscid; (———) viscous, $Re = 10^6$.

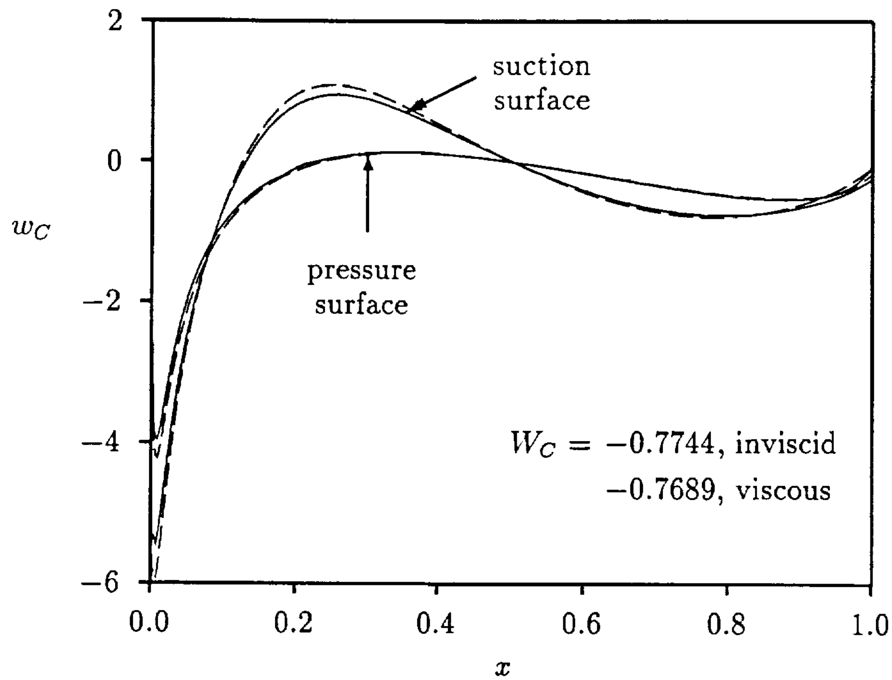

Figure 1: LINFLO results for HSC cascade undergoing torsional vibration [$\alpha = (1, 0)$, $\sigma = 0$ deg, $\omega = 1$]; $\Omega_{-\infty} = 55$ deg, $M_{-\infty} = 0.70$: (— — — —) inviscid; (———) viscous, $Re = 10^6$.

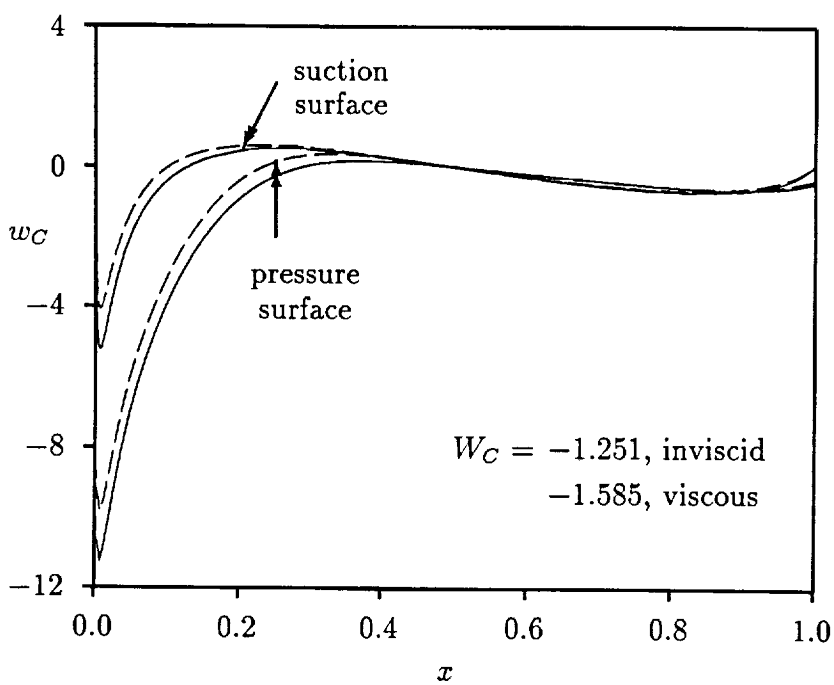

Figure 2: LINFLO results for HSC cascade undergoing torsional vibration [$\alpha = (1, 0)$, $\sigma = 180$ deg, $\omega = 1$]; $\Omega_{-\infty} = 55$ deg, $M_{-\infty} = 0.70$: (— — — —) inviscid; (———) viscous, $Re = 10^6$.

CONCLUDING REMARKS

- Linearized unsteady aerodynamic analysis: LINFLO
  - Realistic 2D flow configurations
  - Arbitrary modes and frequencies of excitation
  - Efficient prediction of unsteady pressure response
- Steady inviscid/viscid interaction analysis: SFLOW-IVI
  - 2D cascade flows
  - Local strong inviscid/viscid interactions
  - Efficient: CPU < 5 min
  - Robust: wide range of operating conditions
- Future work
  - Transonic/supersonic gust response analysis
  - SFLOW-IVI/LINFLO coupling
  - Unsteady IVI analysis

N95- 19382

STEADY POTENTIAL SOLVER FOR UNSTEADY AERODYNAMIC ANALYSES

D. Hoyniak
NASA Lewis Research Center
Cleveland, Ohio 44135

S2-07
37012
13P

Presentation Outline

- Description of flow solver, SFLOW
- Subsonic Calculations (Steady & Unsteady)
  - Compressor Cascade (10th Standard Configuration)
  - Turbine Cascade (4th Standard Configuration)
  - GE Low Speed Research Compressor
  - GE Low Speed Research Turbine
- Transonic Calculations (Steady)
  - Compressor Cascade (10th Standard Configuration)

Objective

Develop steady flow solver for use with LINFLO

- Compatible with LINFLO
- Composite Mesh
- Transonic Capability

Approach

- Steady flow potential equation written in nonconservative form
- Newton's Method
- Implicit, Least-Squares, Interpolation Method used to obtain finite difference expressions
- Matrix inversion routines from LINFLO

Differential Equations

Steady Flow

$$A^2\nabla^2\phi - (\gamma-1)\nabla^2\Phi\frac{\bar{D}\phi}{Dt} - \frac{\bar{D}^2\phi}{Dt^2} - \nabla\phi\cdot\frac{\nabla(\nabla\Phi)^2}{2}$$
$$= -A^2\nabla^2\Phi + \nabla\Phi\cdot\frac{\nabla(\nabla\Phi)^2}{2}$$

$$\frac{\bar{D}}{Dt} = \nabla\Phi\cdot\nabla$$

Unsteady Flow

$$A^2\nabla^2\phi - (\gamma-1)\nabla^2\Phi\frac{\bar{D}\phi}{Dt} - \frac{\bar{D}^2\phi}{Dt^2} - \nabla\phi\cdot\frac{\dot{\nabla}(\nabla\Phi)^2}{2} = 0$$

$$\frac{\bar{D}}{Dt} = i\omega + \nabla\Phi\cdot\nabla$$

Newton' Method

$$[A(\Phi)]\{\phi\} = \{b(\Phi)\}$$

$$\Phi(\bar{x})^{n+1} = \Phi(\bar{x})^n + \phi(\bar{x})^n$$

Convergence Criterion

$$|\phi(\bar{x})^n| < \varepsilon$$

Cascade Geometry

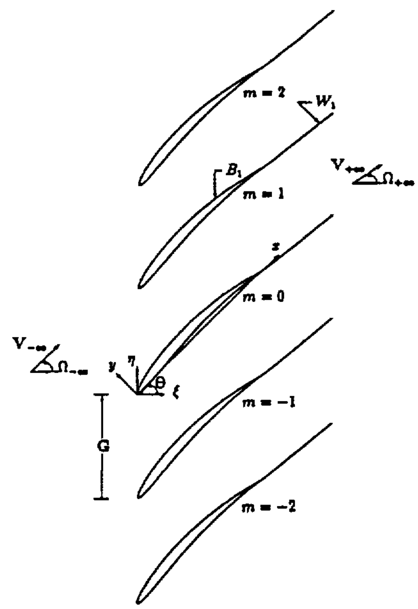

Composite Mesh

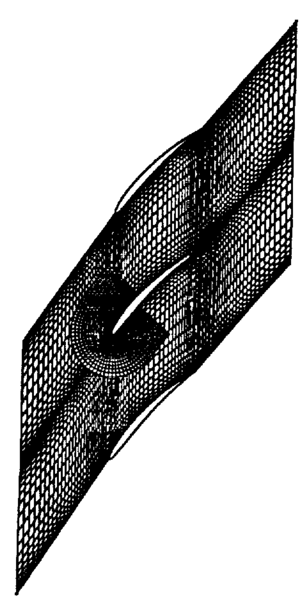

10th Standard Configuration, Subsonic Flow Conditions
Steady Mach Number Distribution
$M_{-\infty} = 0.7$, $\Omega_{-\infty} = 55$ deg

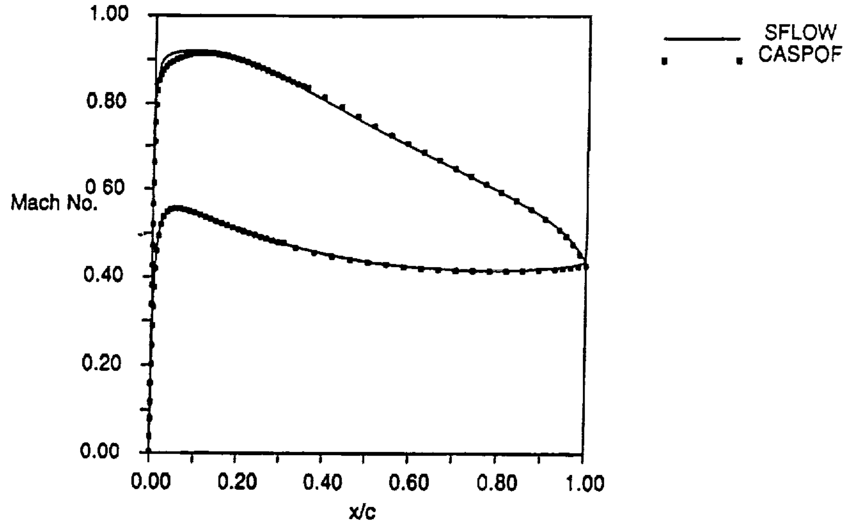

10th Standard Configuration, Subsonic Flow Conditions
Unsteady Torsion Mode Response

$\alpha = 1.0$, $\omega = 0.24$ $\sigma = 30$ deg

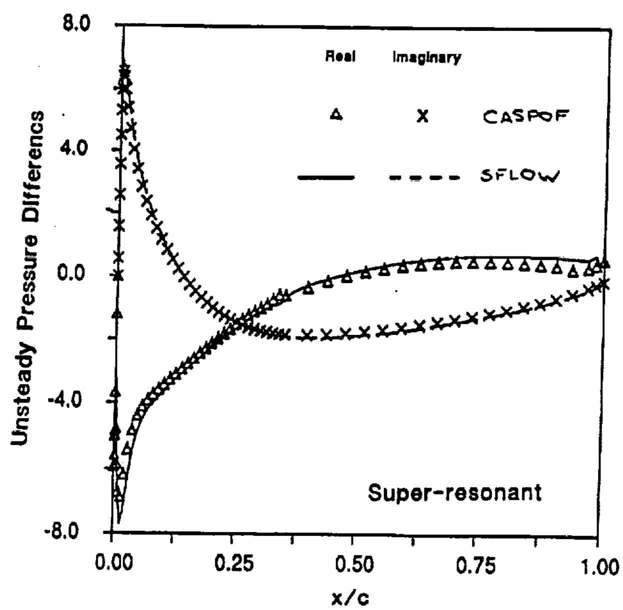

10^{th} Standard Configuration, Subsonic Flow Conditions
Unsteady Torsion Mode Response

$\alpha = 1.0, \quad \omega = 0.24 \quad \sigma = 180$ deg

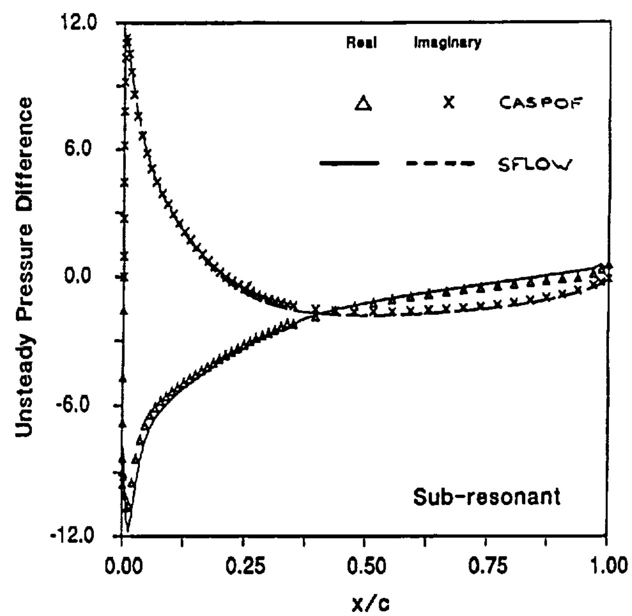

Standard Configuration Number 4
Turbine Cascade Composite Mesh

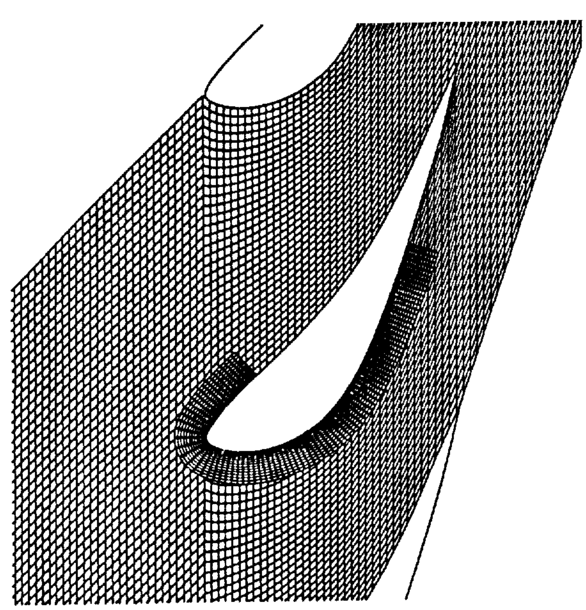

Standard Configuration Number 4
Steady Surface Mach Number Distribution

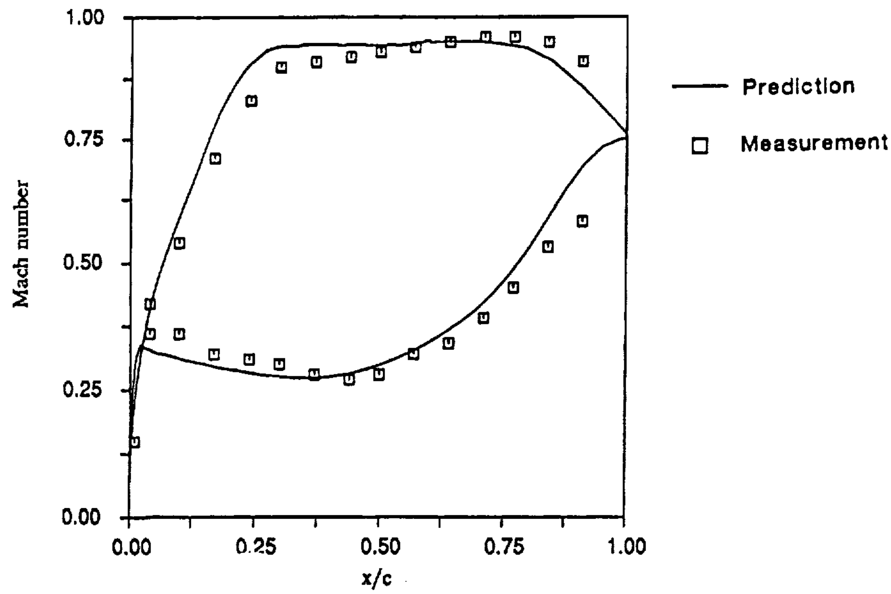

Standard Configuration Number 4
Unsteady Aerodynamic Response

h = (0.0016,0.0029), ω = 0.24, σ = -90 Deg

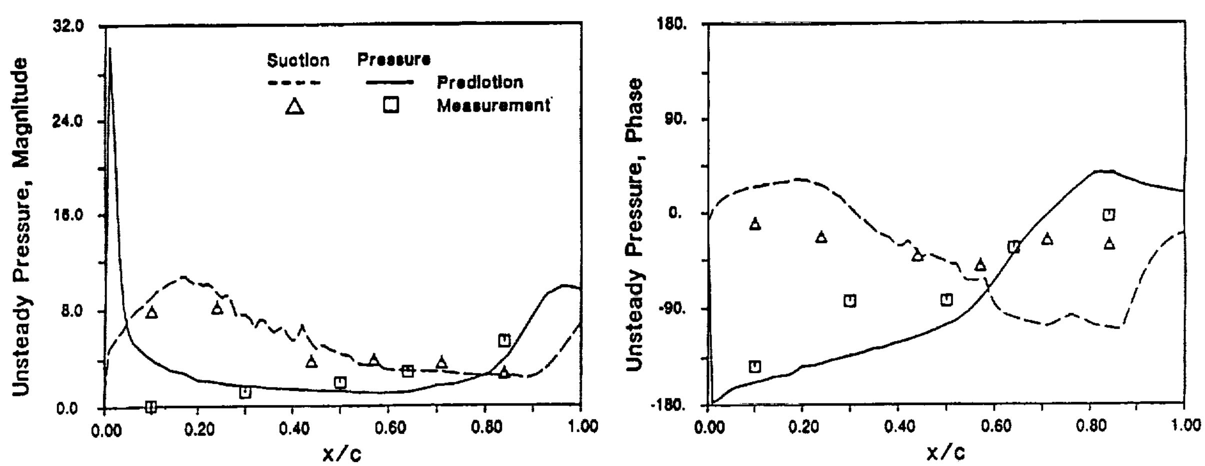

Standard Configuration Number 4
Unsteady Aerodynamic Response

h = (0.0016,0.0029), ω = 0.24, σ = 90 Deg

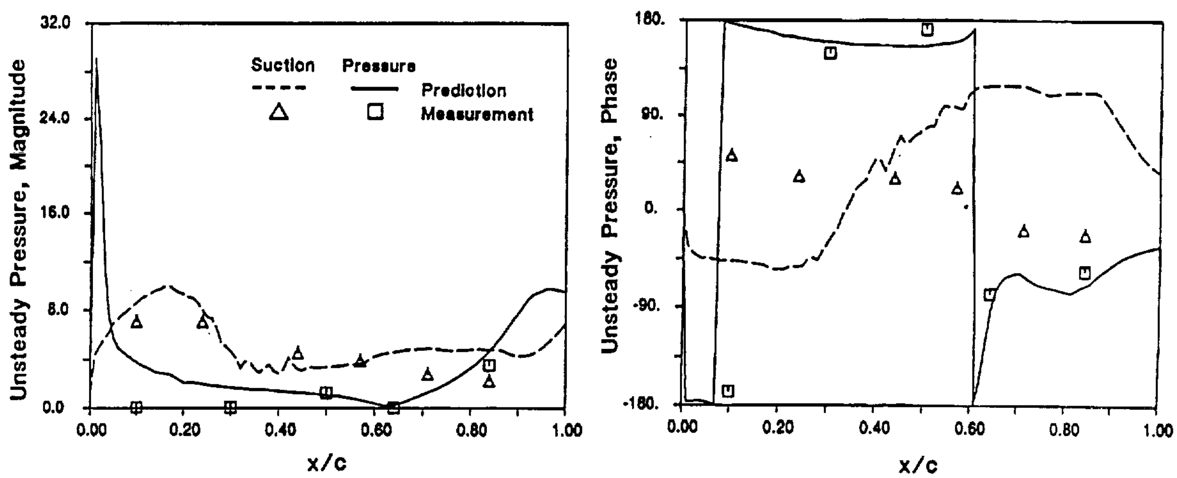

GE Low Speed Research Compressor & Turbine Configurations

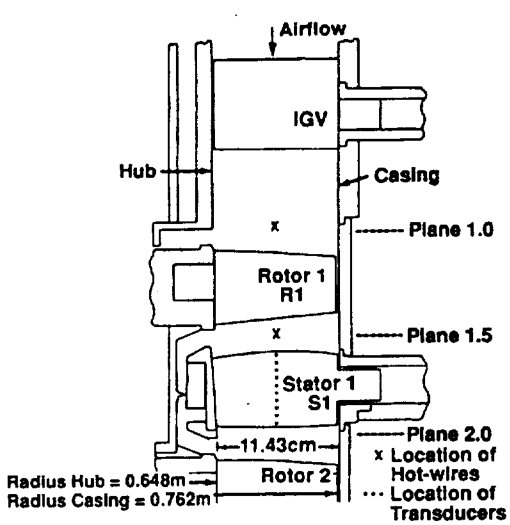

Compressor Test Rig

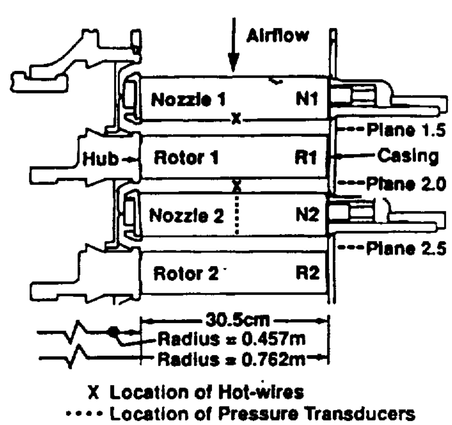

Turbine Test Rig

GE Low Speed Research Compressor
Steady Blade Loading

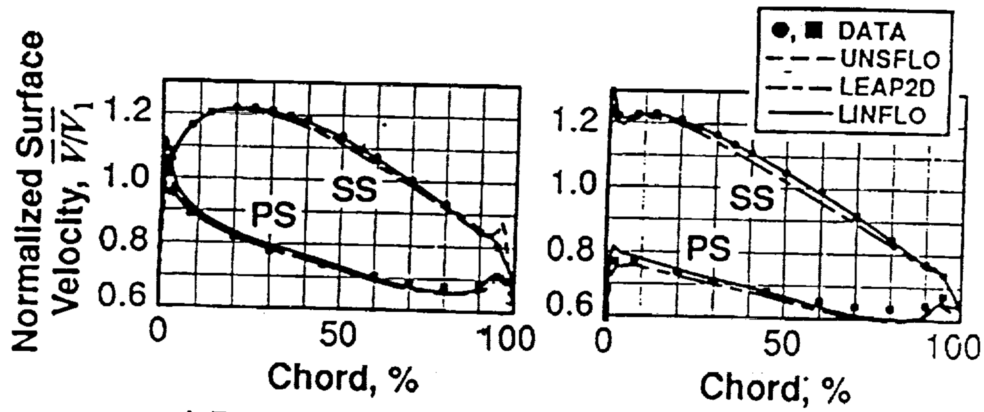

a) Design Point (DP) b) High Loading (HL)

GE Low Speed Research Compressor
Design Point, Suction Surface

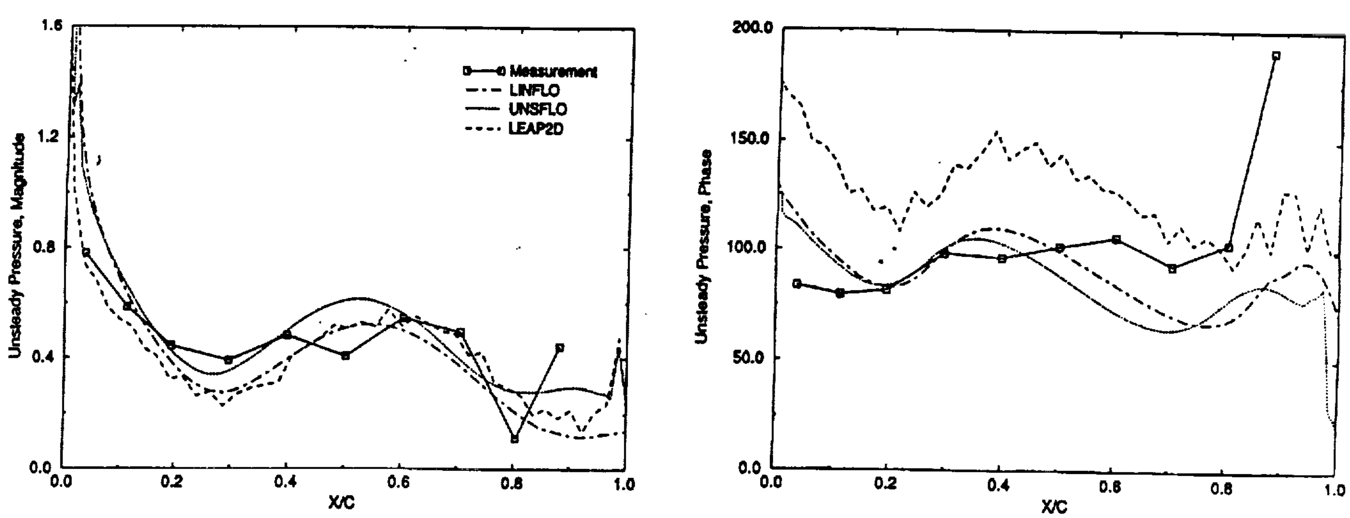

GE Low Speed Research Compressor
Design Piont, Pressure Surface

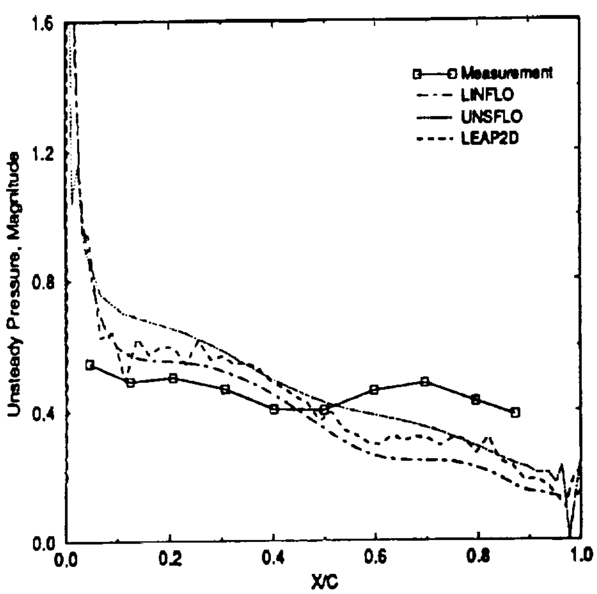

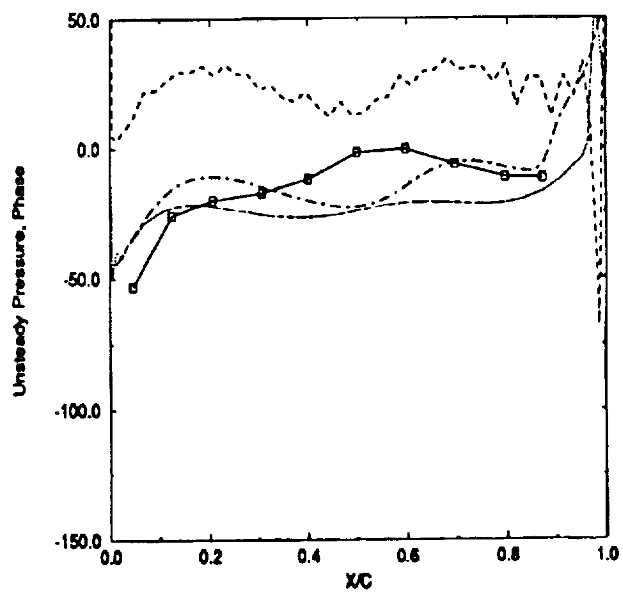

GE Low Speed Research Turbine
Steady Blade Loading

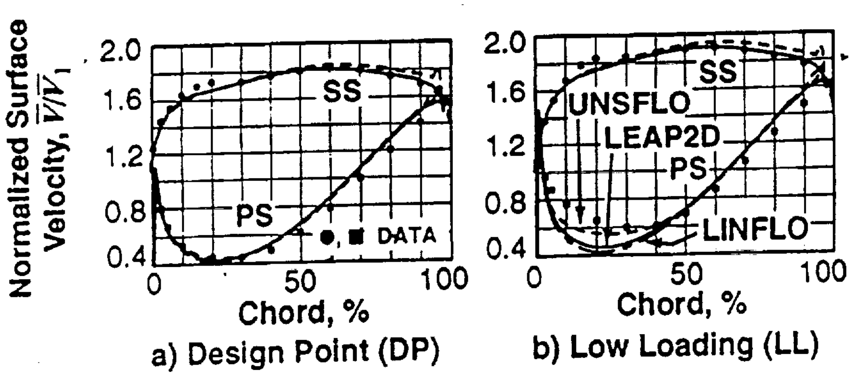

GE Low Speed Research Turbine
Design Point, Pressure Surface

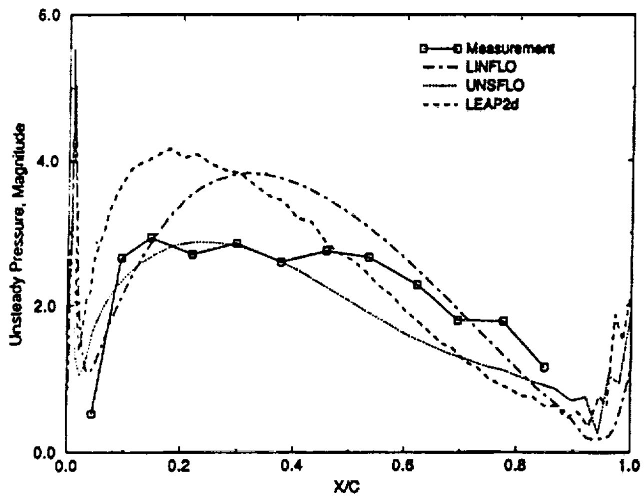

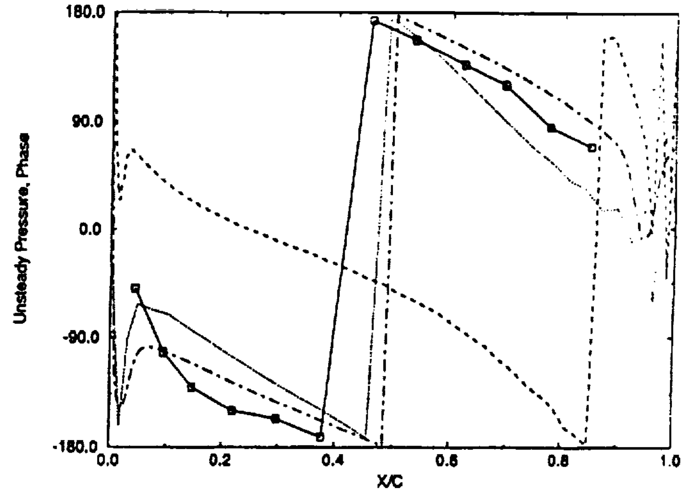

GE Low Speed Research Turbine
Design Point, Suction Surface

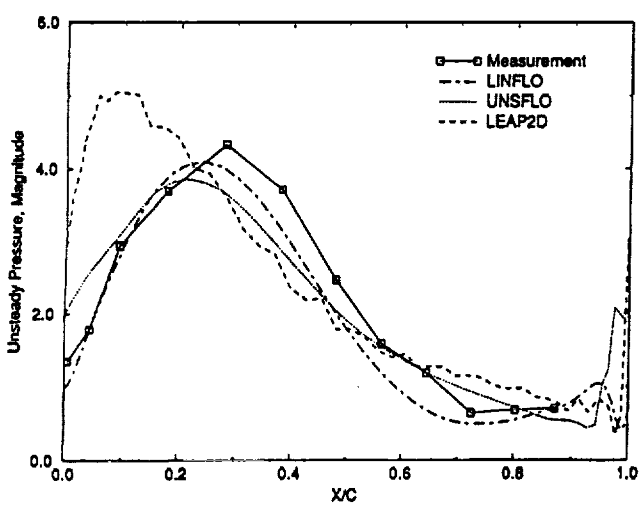

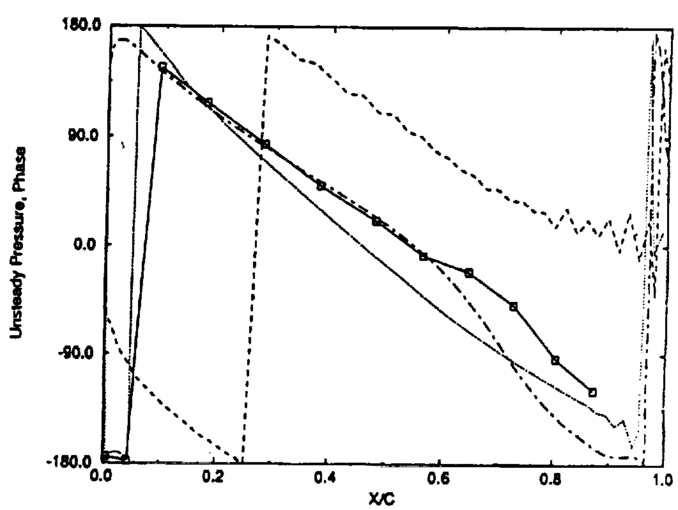

Transonic Flow Calculations

- Artificial viscosity added using rotated difference scheme of Jameson
- Dissipation coefficient based on local Mach number
- Modified Newton's method used to solve resulting equations

Modified Newton' Method for Transonic Flow Calculations

$$[A(\Phi)]\{\phi\} = \{b(\Phi)\}$$

$$\Phi(\vec{x})^{n+1} = \Phi(\vec{x})^{n} + \omega\phi(\vec{x})^{n}$$

Convergence Criterion

$$|\phi(\vec{x})^{n}| < \varepsilon$$

10th Standard Configuration, Transonic Flow Conditions
$M_{-\infty}= 0.8, \Omega_{-\infty}=58$ deg.

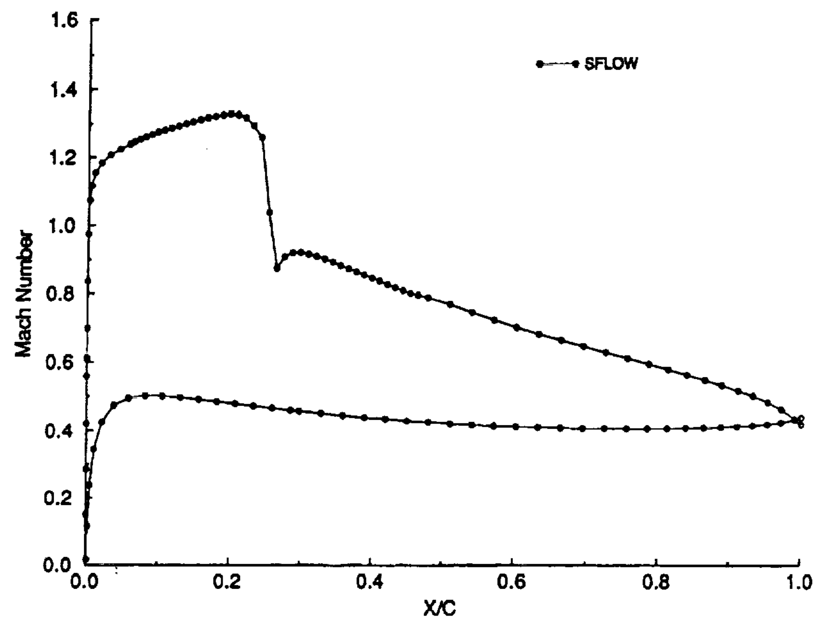

10th Standard Configuration, Transonic Flow Conditions
Comparison with NPHASE & CASPOF Results
$M_{-\infty}= 0.8, \Omega_{-\infty}=58$ deg.

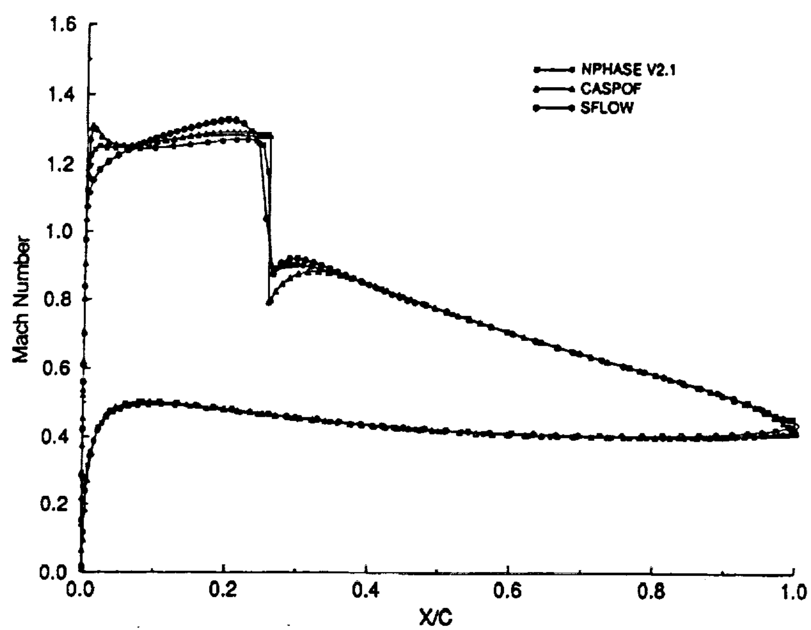

Summary

- 10^{th} standard configuration predictions show good agreement with other flow solvers
- 4^{th} standard configuration turbine predictions show good agreement with the magnitude of measured data, however there are some problems with phase near trailing edge on suction surface
- GE low speed research compressor and turbine predictions show reasonable agreement with magnitude and phase measurements
- Transonic solution progressing, needs better model for artificial viscosity near shock, and mesh clustering capability

omit
5P

FREPS—IMPLEMENTATION

D.V. Murthy*
NASA Lewis Research Center
Cleveland, Ohio 44135

Coupling Among Disciplines

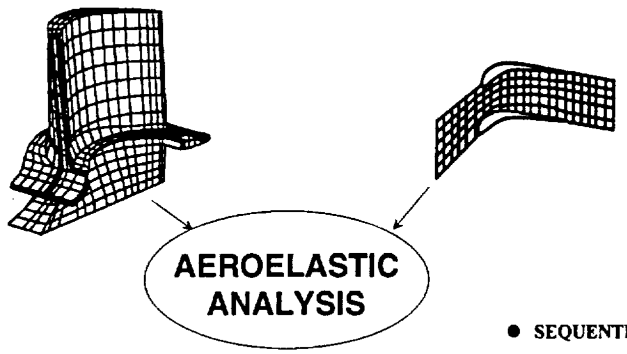

- SEQUENTIAL COUPLING
- STRIP THEORY
- INTERPOLATION/ EXTRAPOLATION
- COORDINATE TRANSFORMATIONS

Sequential Coupling

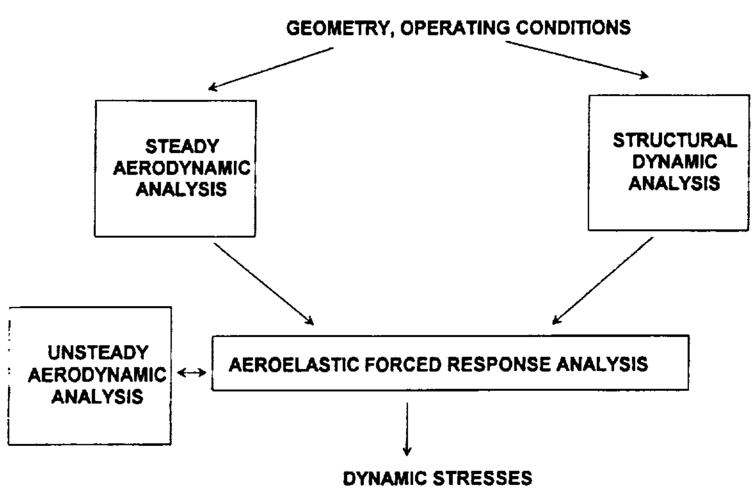

*NASA Resident Research Associate at Lewis Research Center.

Equations of Motion

Mechanical/Material Damping Forces from Damping Model

External Forcing Function from Mechanical Excitation Model

$$M\ddot{u} + C\dot{u} + Ku = F_A(u(t),\dot{u}(t),t) + F_A(t) + F_M(t)$$

Elastic and Inertia Forces from Structural Model

Unsteady Aerodynamic Forces from Aerodynamic Model

Tuned System Assumption

CONSTANT INTERBLADE PHASE ANGLE MODES - UNCOUPLE THE EQUATIONS OF MOTION

$$u_j(t) = \sum_{r=1}^{n} u^r(t)\ e^{i\beta_r j} \qquad . \qquad \beta_r = \frac{2\pi r}{n}$$

LEADS TO

$$M\ddot{u}^r + C\dot{u}^r + Ku^r = F_A^u(u^r(t),\dot{u}^r(t),t) + F_A^r(t) + F_M^r(t)$$

VALID FOR MOTION IN THE INTERBLADE PHASE ANGLE β_r

Modal Transformation

$$q(t) = \phi^T u(t)$$

$$\boxed{M_G\ddot{q} + C_G\dot{q} + K_G q = Q_A^u(q(t),\dot{q}(t),t) + Q_A(t) + Q_M(t)}$$

$$Q_A(t) = \bar{Q}_A e^{i\omega t}$$
$$Q_M(t) = \bar{Q}_M e^{i\omega t}$$
$$q(t) = \bar{q} e^{i\omega t}$$

$$Q_A^u(q(t), \dot{q}(t), t) = A(\omega)\, \bar{q}\, e^{i\omega t}$$

$$\boxed{\left[-\omega^2 \mathbf{I} + (1+i2\zeta_j)\left[\ddots\ \omega_j^2\ \ddots\right] - A(\omega)\right]\bar{q} = 0}$$

Discipline Communication through Databases

F. E. DATABASE

GRID POINT COORDINATES, ELEMENT CONNECTIVITIES,
NATURAL FREQUENCIES, NATURAL MODE SHAPES, NATURAL MODAL STRESSES

STEADY AERODYNAMIC DATABASE

AIRFOIL DEFINITION, STEADY MESH, STEADY POTENTIAL FIELD

UNSTEADY AERODYNAMIC DATABASE

UNSTEADY MESH

Input Interface

FINITE ELEMENT ANALYSIS	USER-SELECTED
STEADY AERODYNAMIC ANALYSIS	QN/ANS
UNSTEADY AERODYNAMIC MESH GENERATION	QN/ANS
FREPS AEROELASTIC ANALYSIS	KEYWORDS NASTRAN-LIKE

EXAMPLES

STRIP 1 235,236,237,238,239,240,241,242,243,244,245,246,247,248,250,

SFLUID 100,1520.0,4635.0, 0.0000, 5618.0,1.367

ROTOR 78 29000.0 4.790 5.290

Output Interface

INPUT ECHO

GEOMETRY ECHO

STEADY FLOW RESULTS ECHO

FINITE ELEMENT ANALYSIS RESULTS ECHO

UNSTEADY FLOW RESULTS FOR EACH STRIP

GENERALIZED FORCES

AEROELASTIC EIGENVALUES, DAMPING RATIOS, EIGENVECTORS

FORCED DISPLACEMENT AMPLITUDES

FORCED STRESS AMPLITUDES

PRINTER PLOTS

PATRAN NEUTRAL FILE

Current Capabilities

- INCIDENCE, CAMBER AND THICKNESS EFFECTS
- SOLID/SHELL ELEMENTS
- AERODYNAMIC DAMPING
- DISTORTING GUST
- VORTICAL, ENTROPIC, ACOUSTIC EXCITATIONS
- SUBSONIC FLOW
- MISTUNING SENSITIVITY MEASURE
- MSC/NASTRAN INTERFACE
- PRINTER PLOTS
- PATRAN POST-PROCESSING

Features in Coming Versions

- TIGHTER INTEGRATION OF AERODYNAMIC/AEROELASTIC MODULES
- TRANSONIC FLOW CAPABILITY
- DISK FLEXIBILITY / CYCLIC SYMMETRY MODEL SUPPORT
- OTHER FEA PROGRAM SUPPORT
- WAKE MODELING
- VISCOUS EFFECTS (INVISCID/VISCID INTERACTIONS)
- IMPROVED MISTUNING SENSITIVITY MEASURE
- GRAPHICAL USER INTERFACE
-
-

MEASUREMENT OF GUST RESPONSE ON A TURBINE ANNULAR CASCADE

A.P. Kurkov and B.L. Lucci
NASA Lewis Research Center
Cleveland, Ohio 44135

omit
16P

OUTLINE

- Test facility
- Instrumentation
- Wake measurements
- Steady-state blade-surface-pressure measurements
- Unsteady blade-surface-pressure measurements
- Concluding Remarks

INSTRUMENTATION

UNSTEADY PRESSURE BLADE

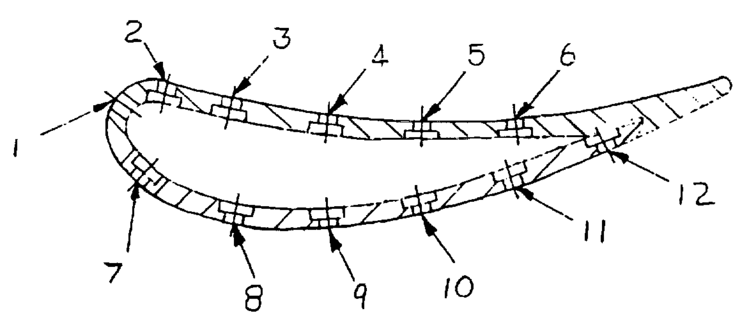

PRECEDING PAGE BLANK NOT FILMED

HOT-WIRE MEASUREMENTS

U Component, M=0.27, Far Wake

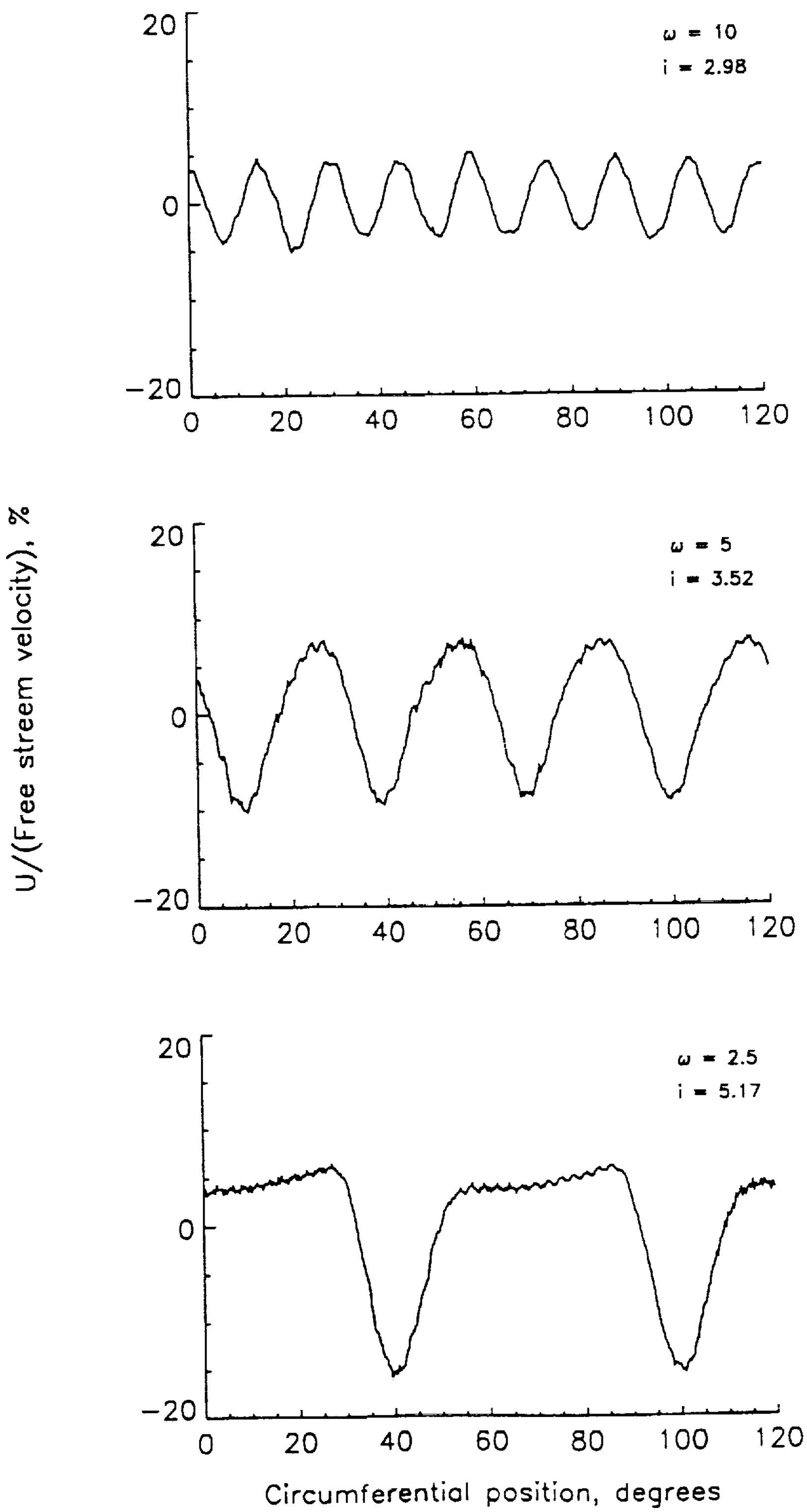

V Component, M=0.27, Far Wake

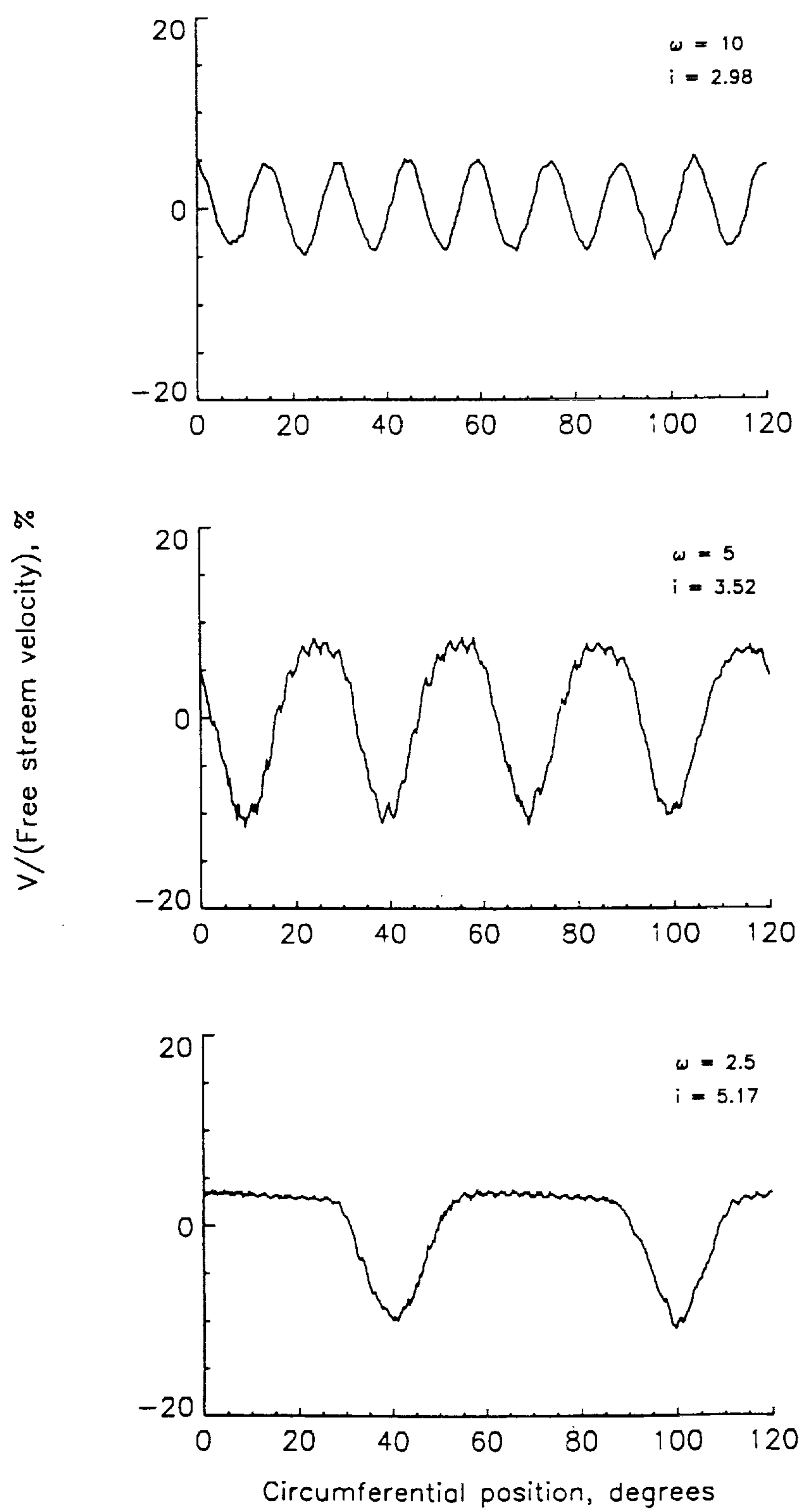

U Component, M=0.27, Far Wake

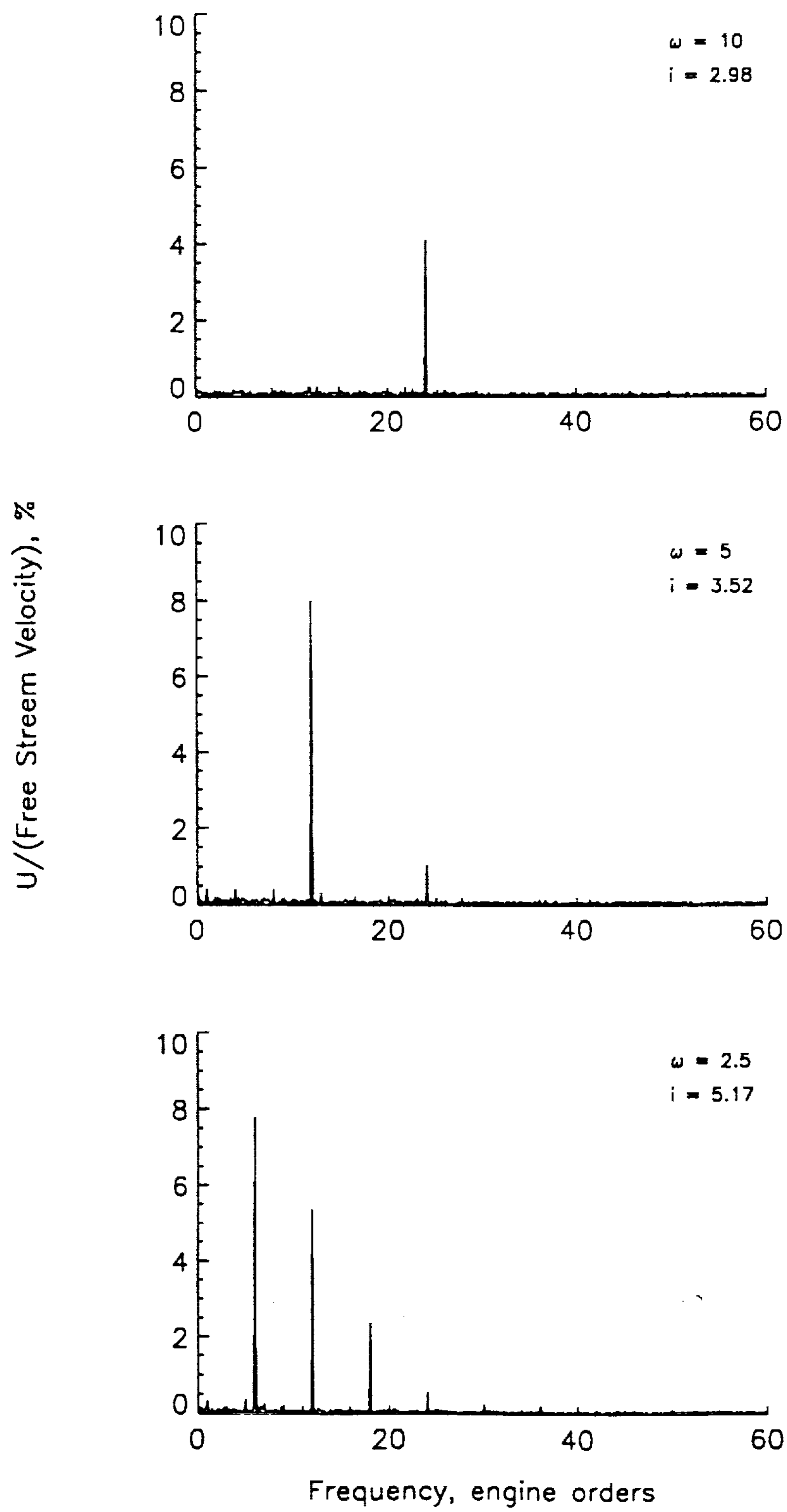

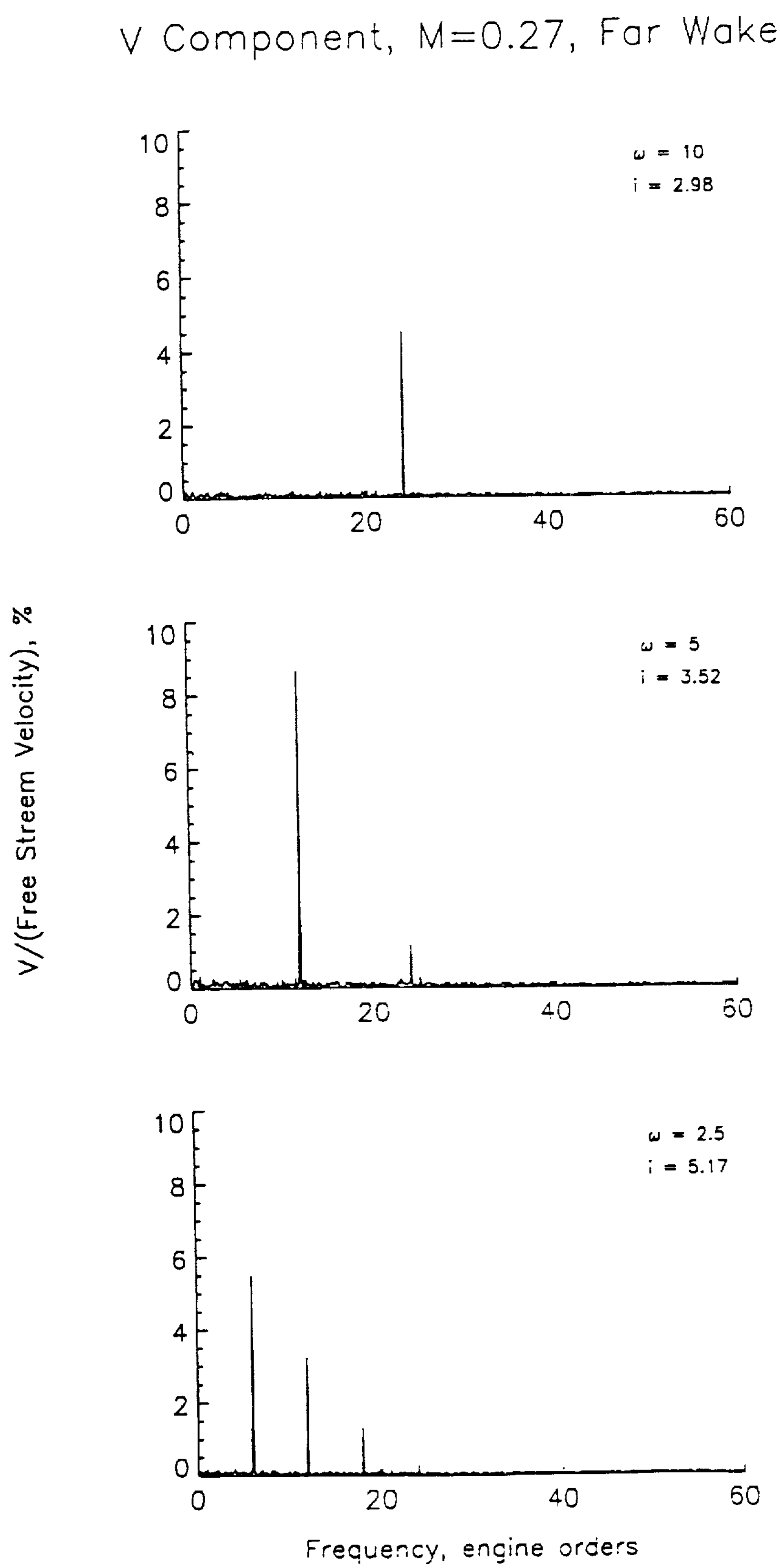
V Component, M=0.27, Far Wake
ω = 10
i = 2.98
ω = 5
i = 3.52
ω = 2.5
i = 5.17
V/(Free Streem Velocity), %
Frequency, engine orders
0
2
4
6
8
10
0
20
40
60

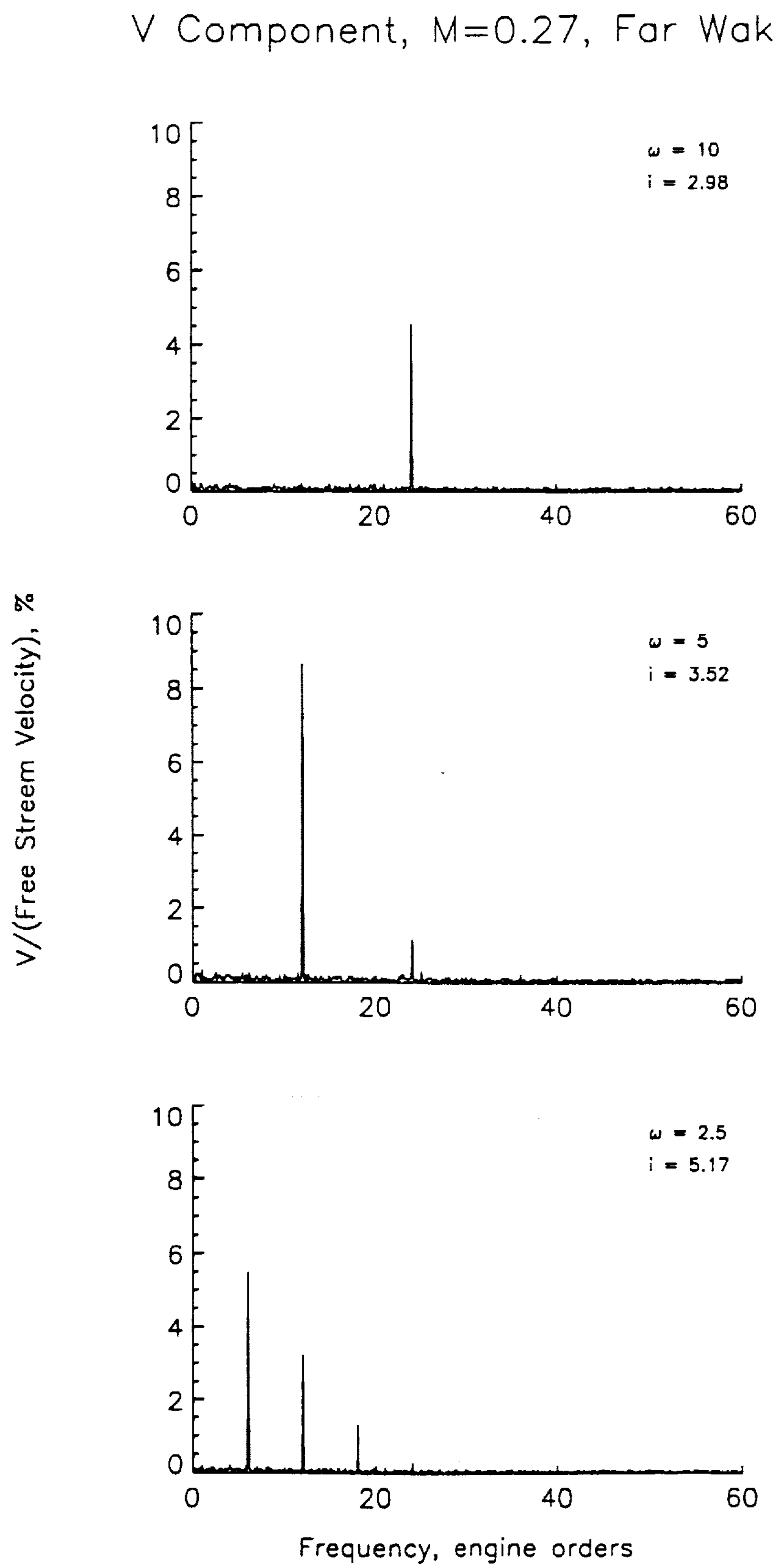
V Component, M=0.27, Far Wake
V/(Free Streem Velocity), %
ω = 10
i = 2.98
ω = 5
i = 3.52
ω = 2.5
i = 5.17
Frequency, engine orders

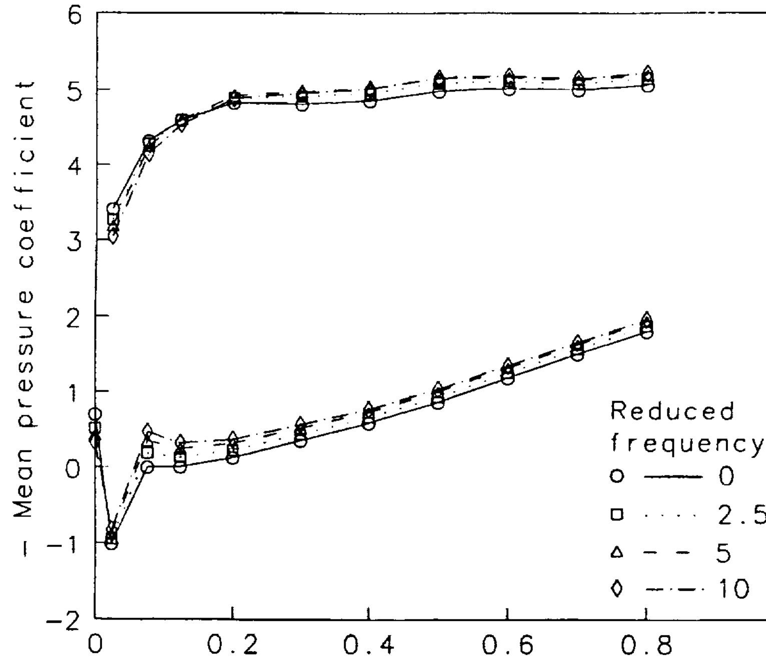

M = 0.2, Positive incidence

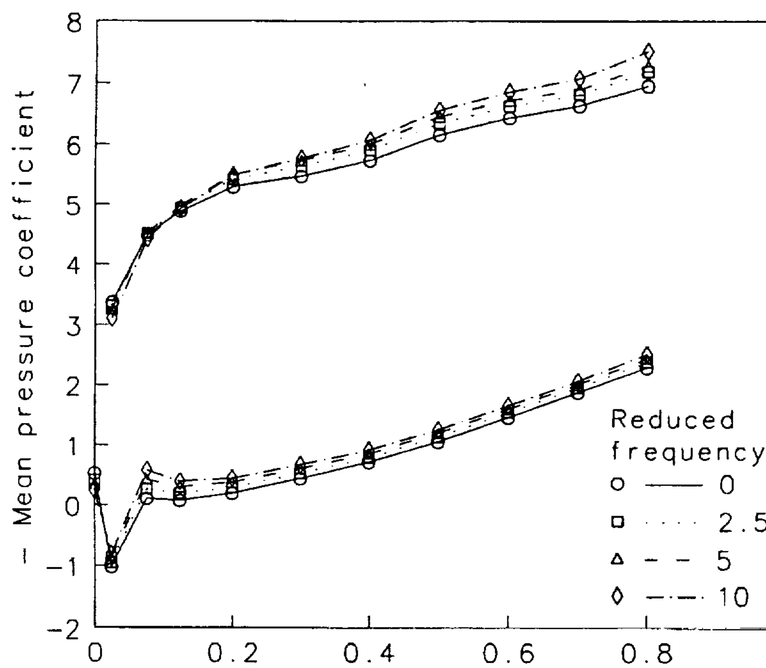

M = 0.27, Positive incidence

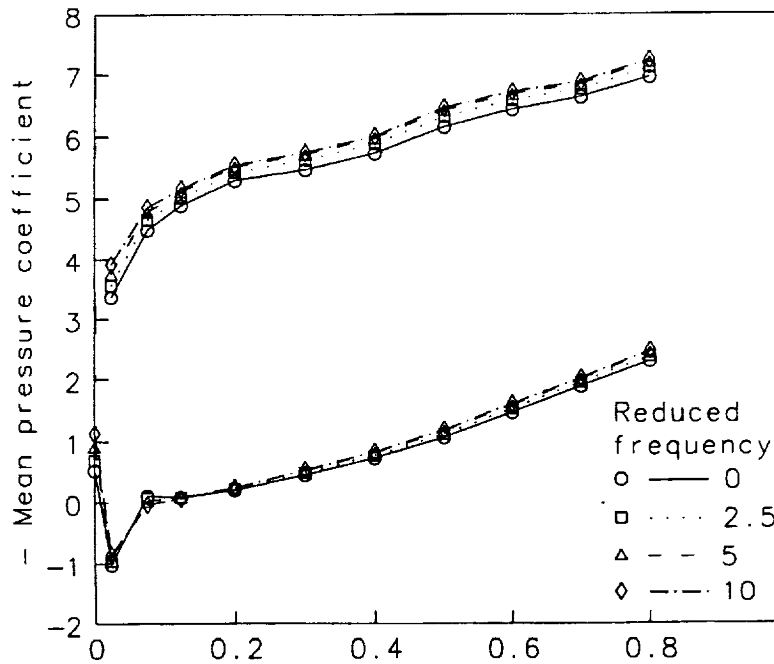

M = 0.27, Negative incidence

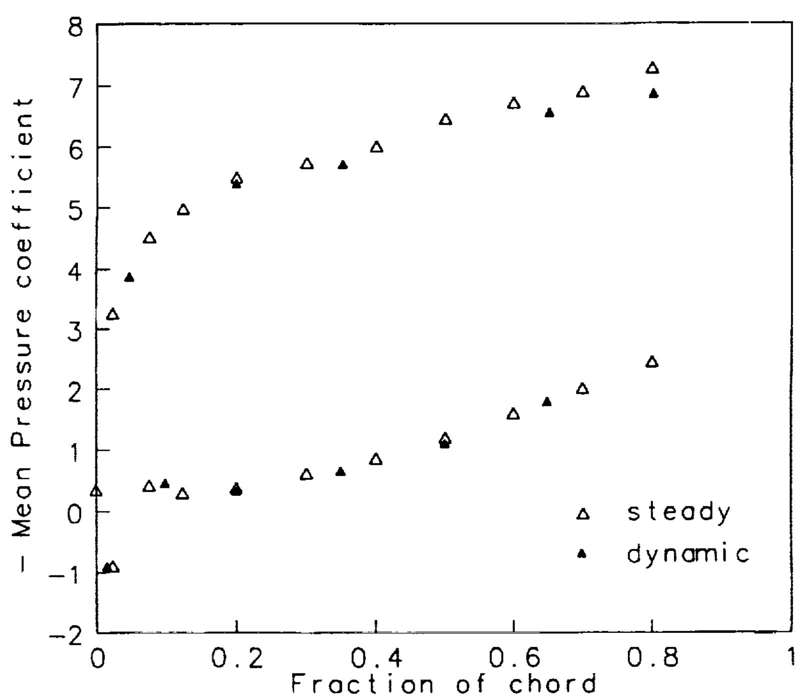

M=0.27 Positive incidence, Reduced frequency 5

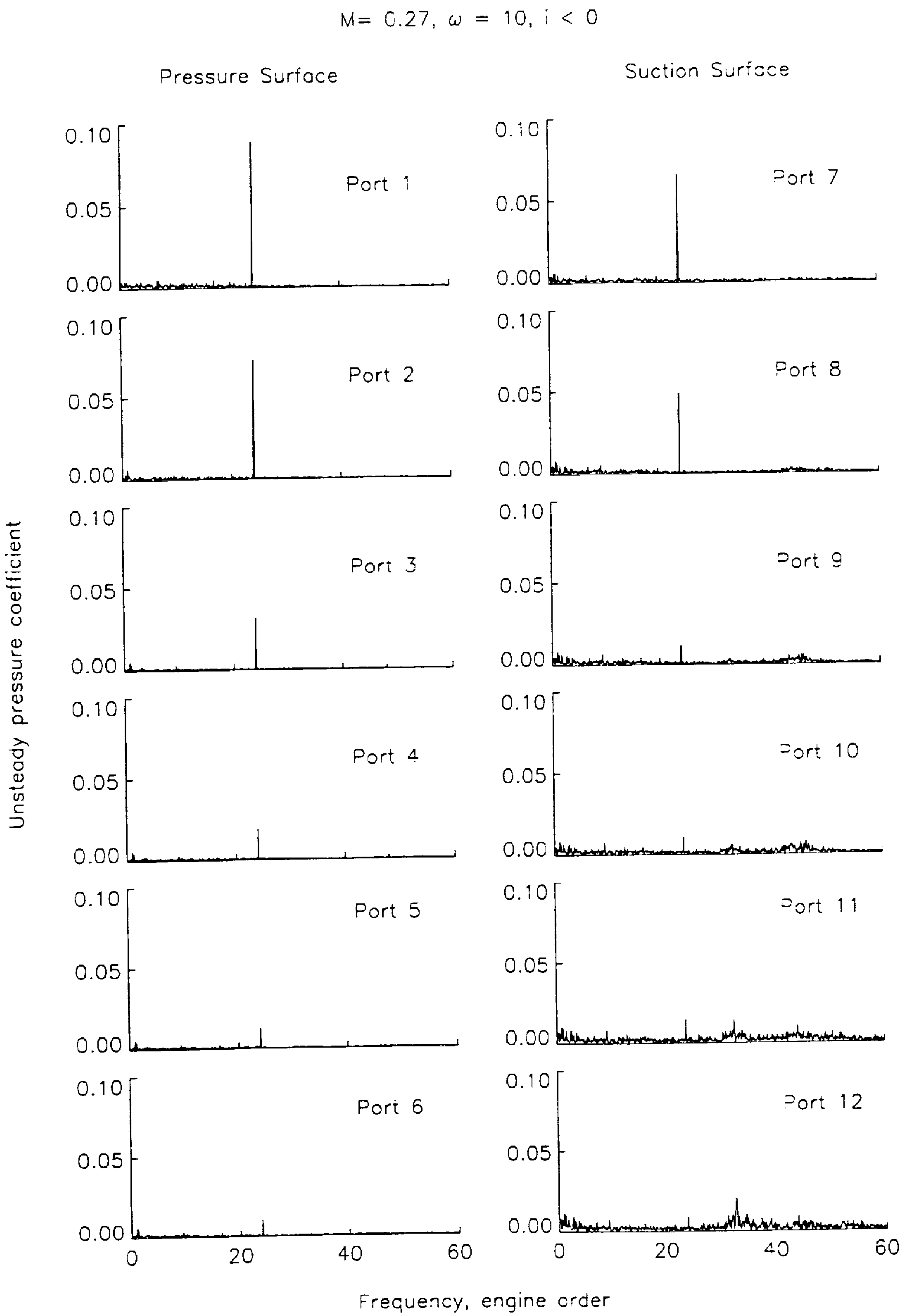
M= 0.27, ω = 10, i < 0
Pressure Surface
Suction Surface
Port 1
Port 2
Port 3
Port 4
Port 5
Port 6
Port 7
Port 8
Port 9
Port 10
Port 11
Port 12
0.10
0.05
0.00
0
20
40
60
Unsteady pressure coefficient
Frequency, engine order

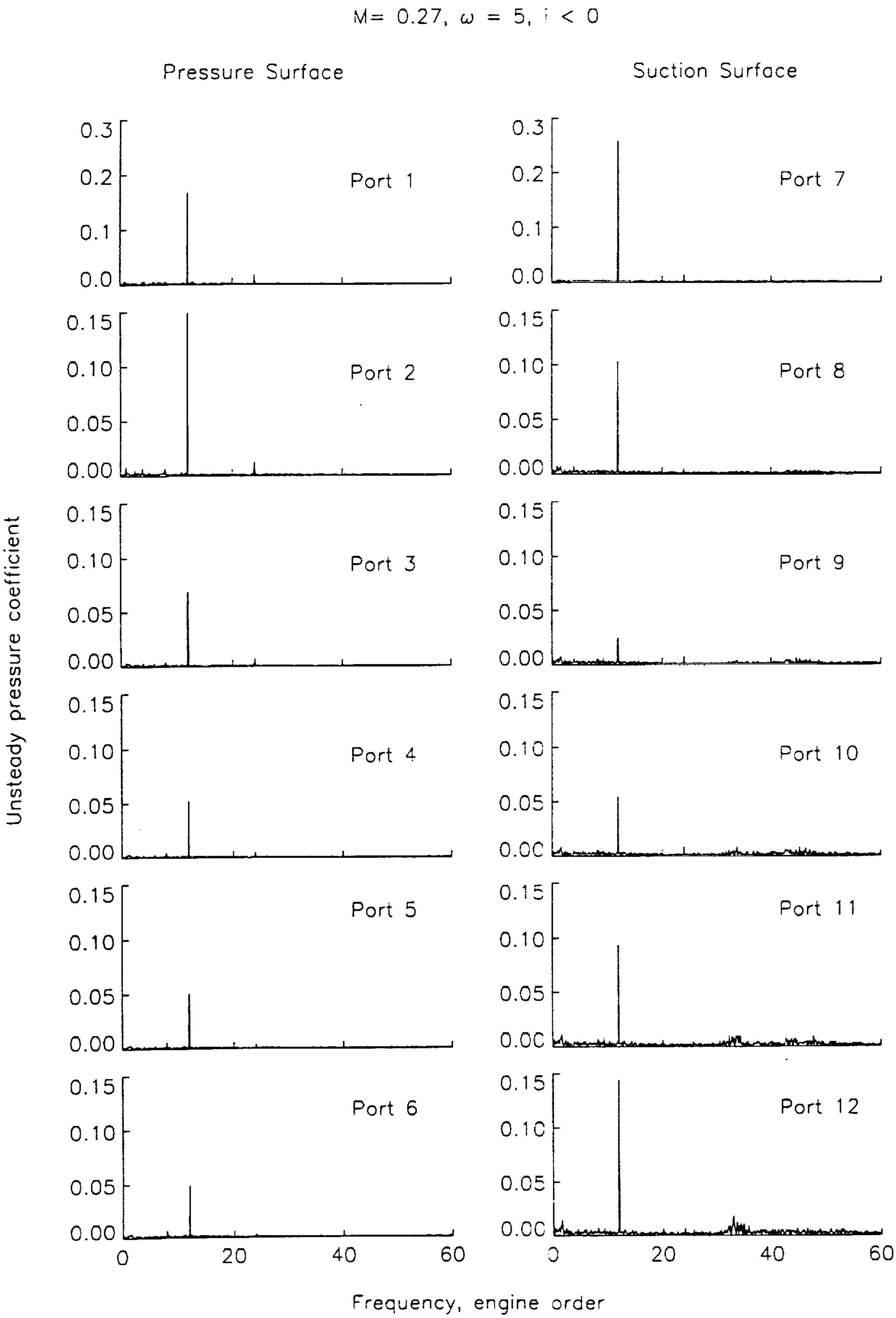
M= 0.27, ω = 5, i < 0
Pressure Surface
Suction Surface
Port 1
Port 2
Port 3
Port 4
Port 5
Port 6
Port 7
Port 8
Port 9
Port 10
Port 11
Port 12
Unsteady pressure coefficient
Frequency, engine order
0.3
0.2
0.1
0.0
0.15
0.10
0.05
0.00
0
20
40
60

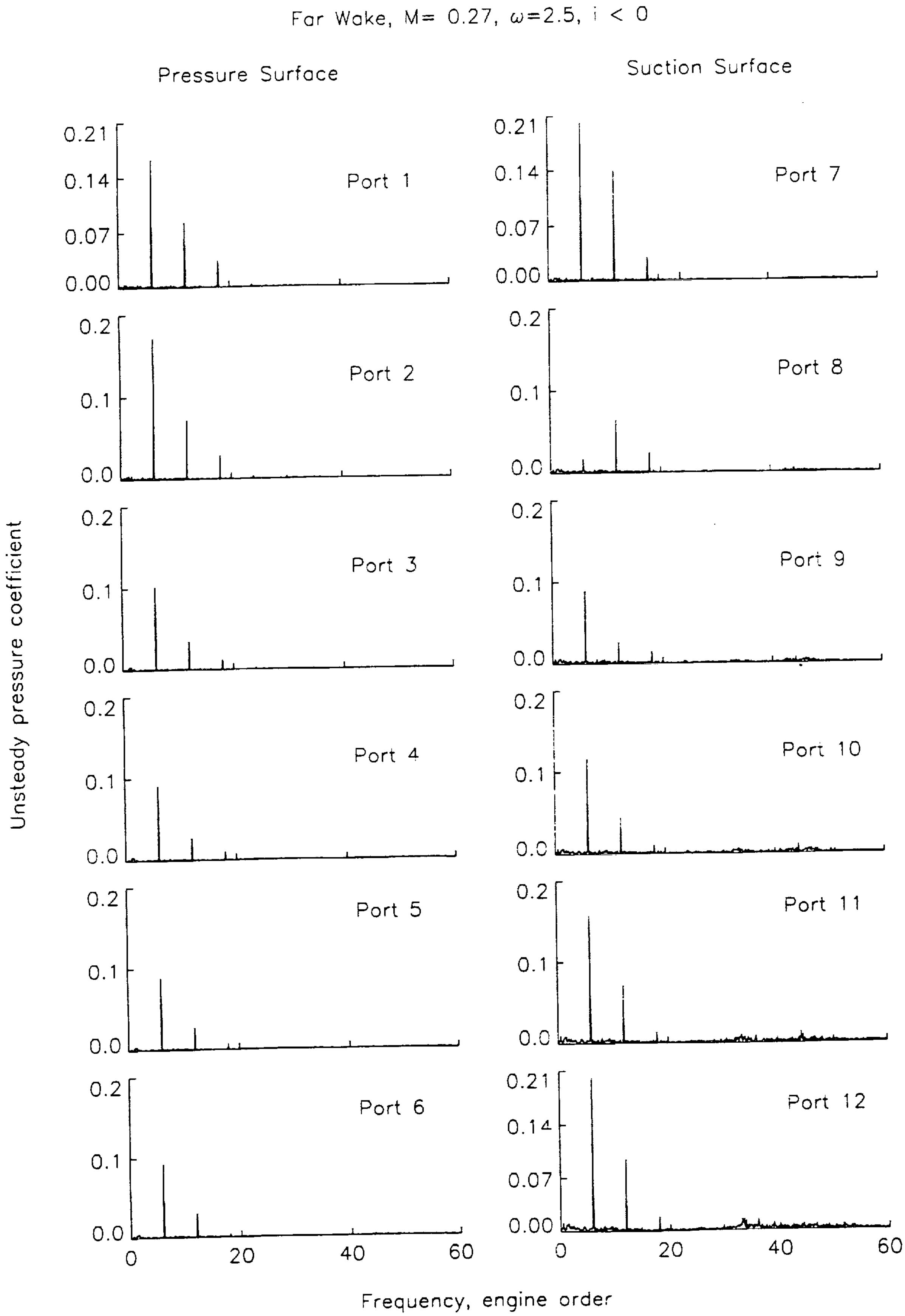
Far Wake, M= 0.27, ω=2.5, i < 0
Pressure Surface
Suction Surface
Port 1
Port 2
Port 3
Port 4
Port 5
Port 6
Port 7
Port 8
Port 9
Port 10
Port 11
Port 12
0.21
0.14
0.07
0.00
0.2
0.1
0.0
0
20
40
60
Unsteady pressure coefficient
Frequency, engine order

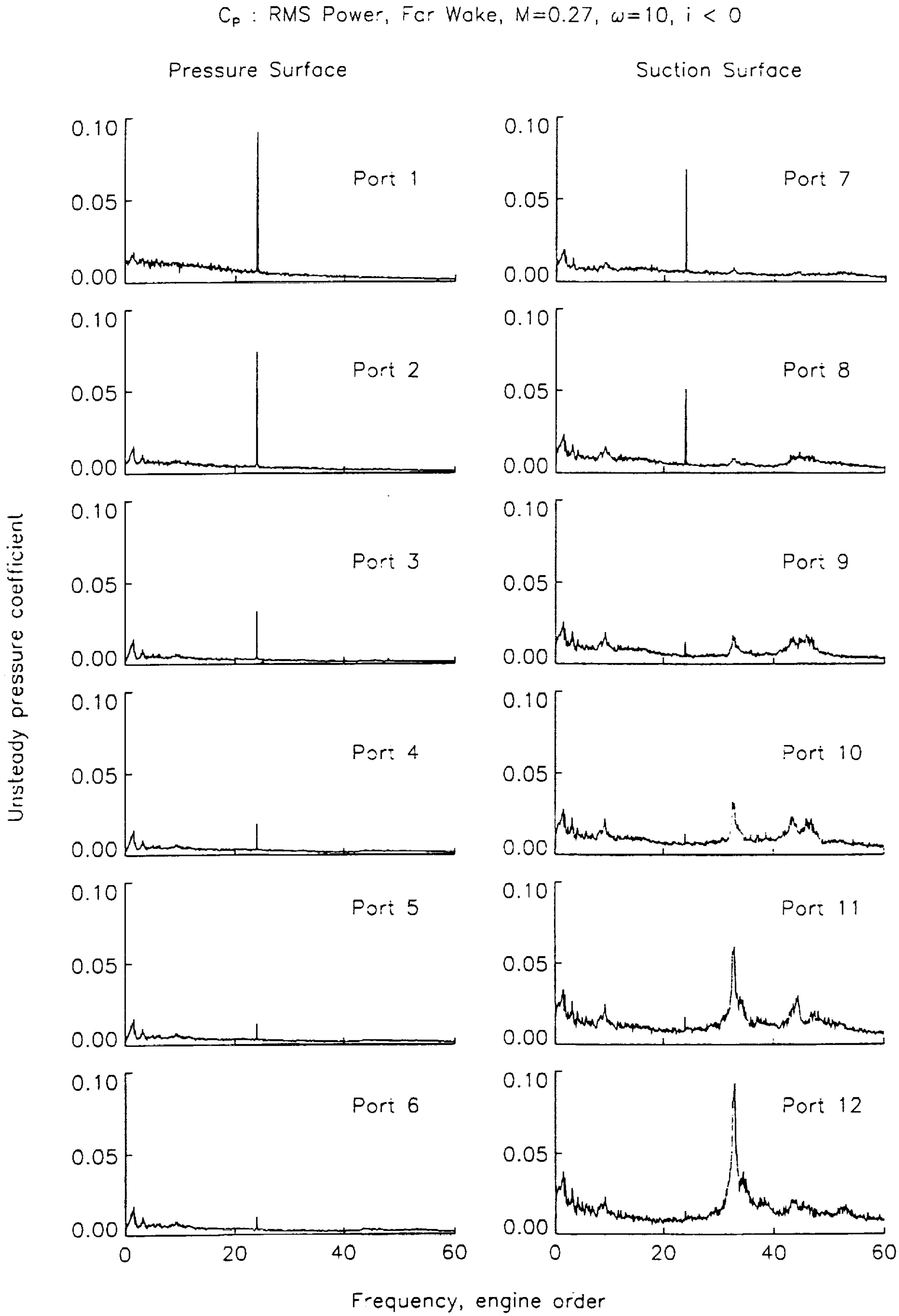

C_p : RMS Power, Far Wake, M=0.27, ω=10, i < 0
Pressure Surface
Suction Surface
Port 1
Port 2
Port 3
Port 4
Port 5
Port 6
Port 7
Port 8
Port 9
Port 10
Port 11
Port 12
0.10
0.05
0.00
0
20
40
60
Unsteady pressure coefficient
Frequency, engine order

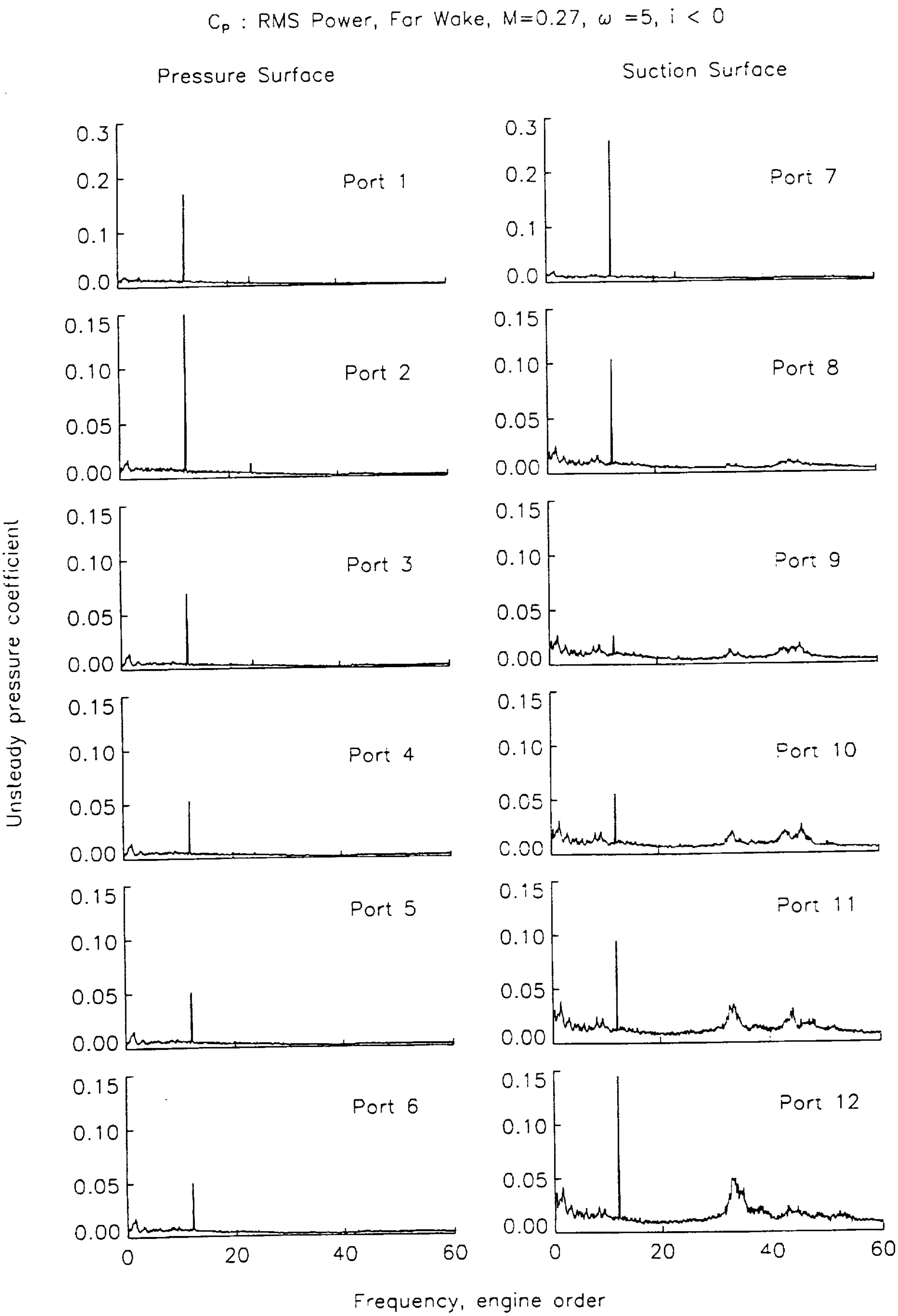

Cp : RMS Power, Far Wake, M=0.27, ω =5, i < 0
Pressure Surface
Suction Surface
Port 1
Port 2
Port 3
Port 4
Port 5
Port 6
Port 7
Port 8
Port 9
Port 10
Port 11
Port 12
0.3
0.2
0.1
0.0
0.15
0.10
0.05
0.00
0
20
40
60
Unsteady pressure coefficient
Frequency, engine order

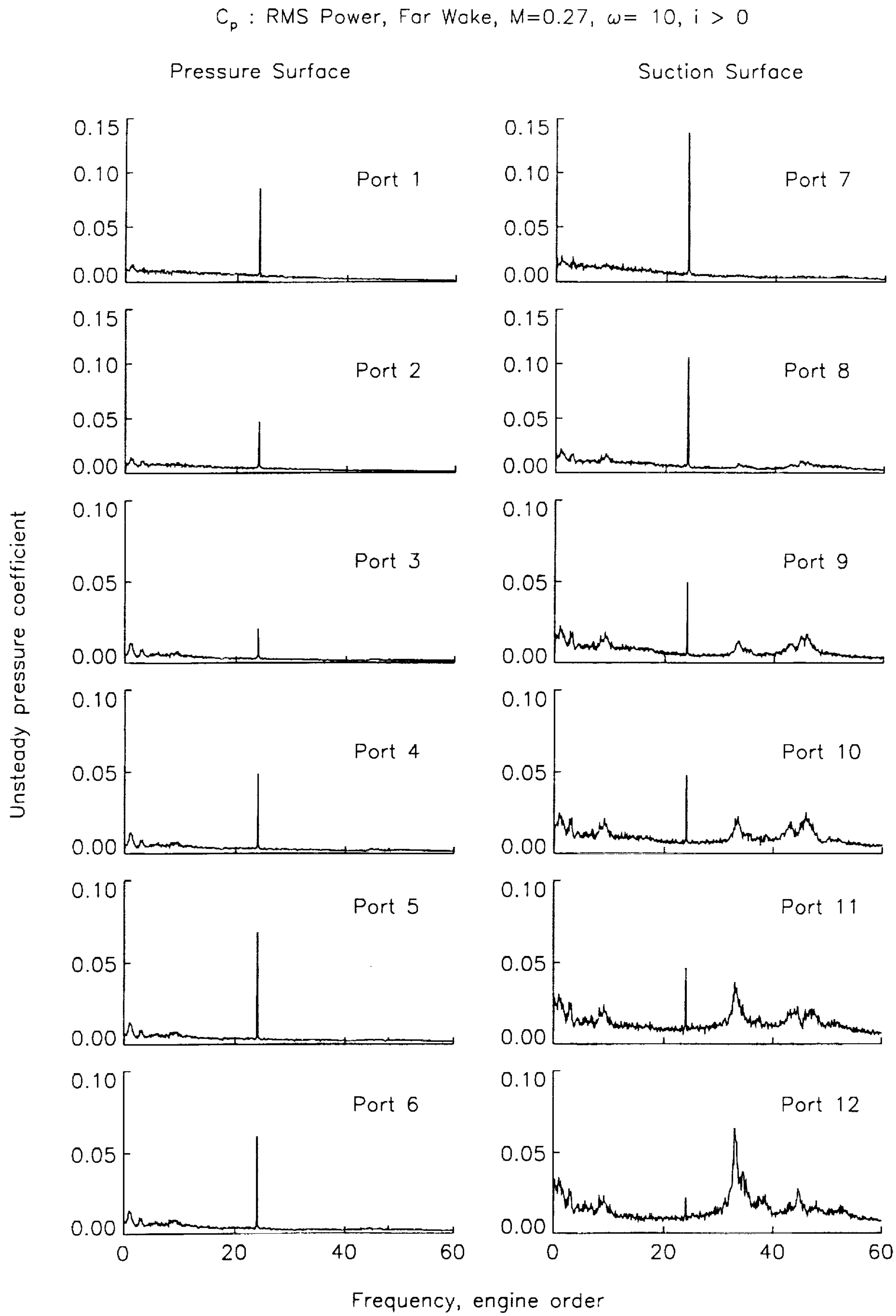
C_p : RMS Power, Far Wake, M=0.27, ω= 10, i > 0
Pressure Surface
Suction Surface
Port 1
Port 2
Port 3
Port 4
Port 5
Port 6
Port 7
Port 8
Port 9
Port 10
Port 11
Port 12
Unsteady pressure coefficient
Frequency, engine order

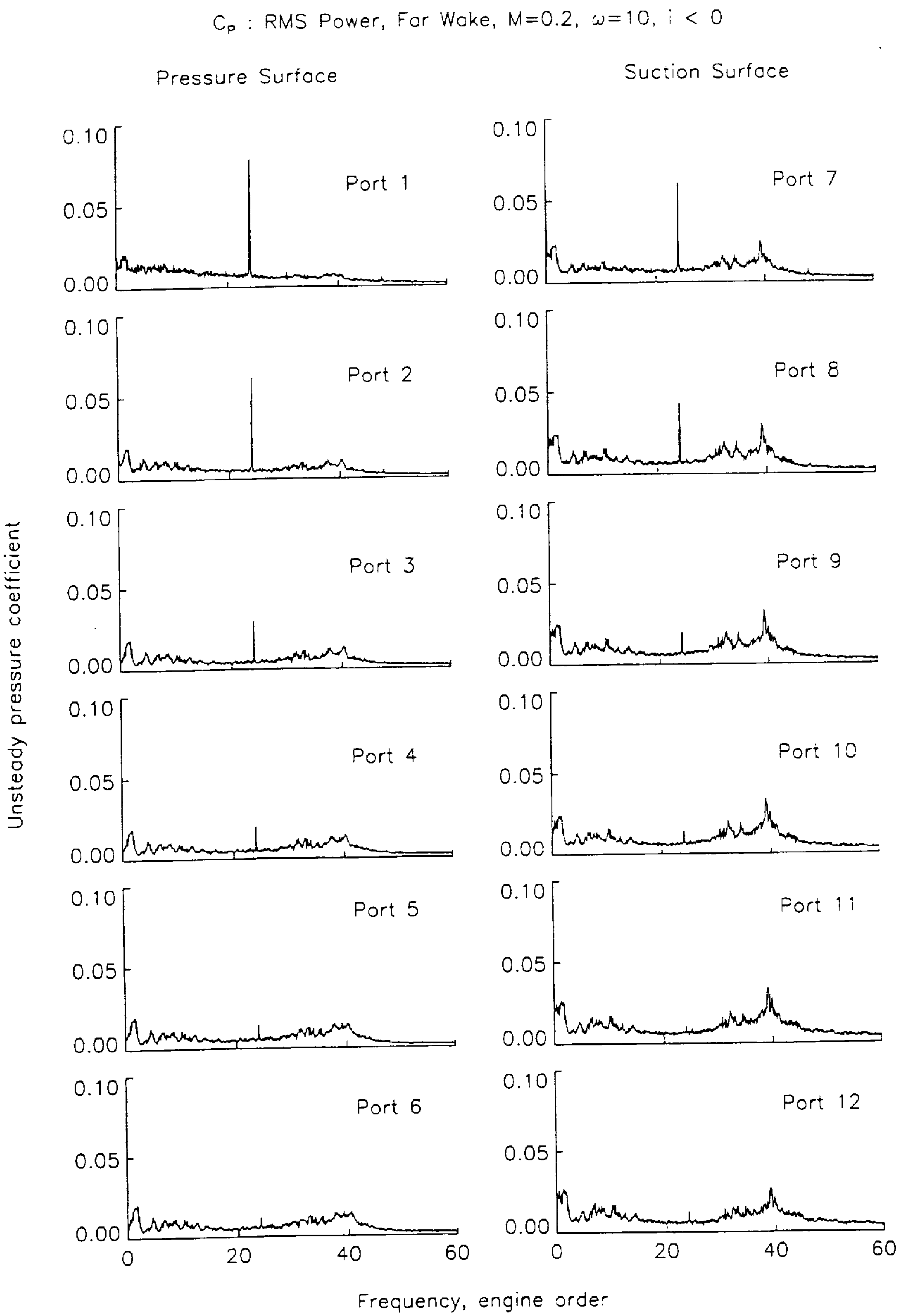

Cp : RMS Power, Far Wake, M=0.2, ω=10, i < 0
Pressure Surface
Suction Surface
Port 1
Port 2
Port 3
Port 4
Port 5
Port 6
Port 7
Port 8
Port 9
Port 10
Port 11
Port 12
0.10
0.05
0.00
0
20
40
60
Unsteady pressure coefficient
Frequency, engine order

CONCLUDING REMARKS

- At the higher Mach number, steady-state blade pressure distribution is to some extent dependent on the reduced frequency of the gust.

- Unsteady blade pressures are strongly dependent on reduced frequency and incidence. Mach number dependence is weaker.

- Strong pressure variation was noticed on the suction side of the forward part of the blade at lower reduced frequencies and negative incidence.

- At the higher Mach number, a high-frequency narrow-band excitation on the suction surface near the trailing edge was observed.

EXPERIMENTAL INVESTIGATION OF AIRFOIL-GENERATED GUST FORCING FUNCTION

S. Fleeter
Purdue University
West Lafayette, Indiana 47907

omit
22 p

Forcing Function Modeling For Flow Induced Vibration

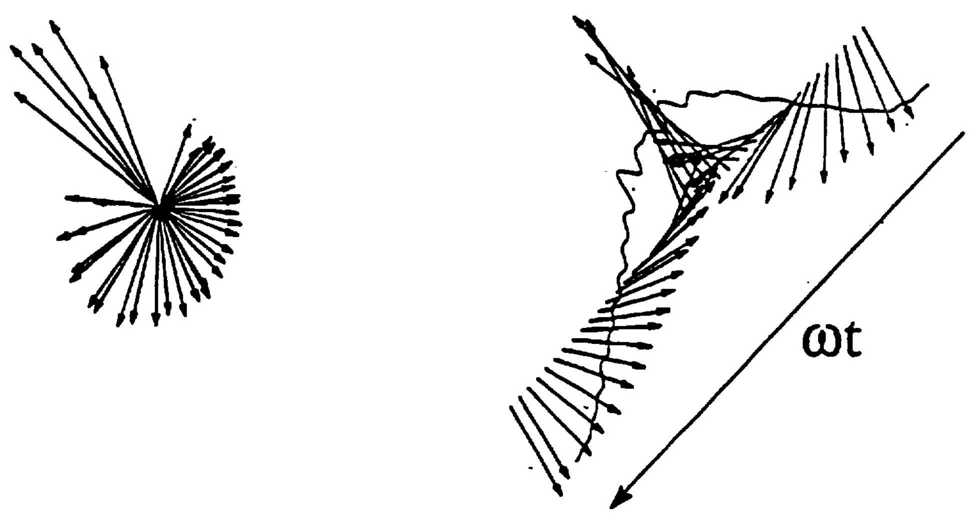

INTRODUCTION

* Blade Row-Wake Interactions - Most Common Unsteady Aerodynamic Excitation Causing High-Cycle Blade Fatigue

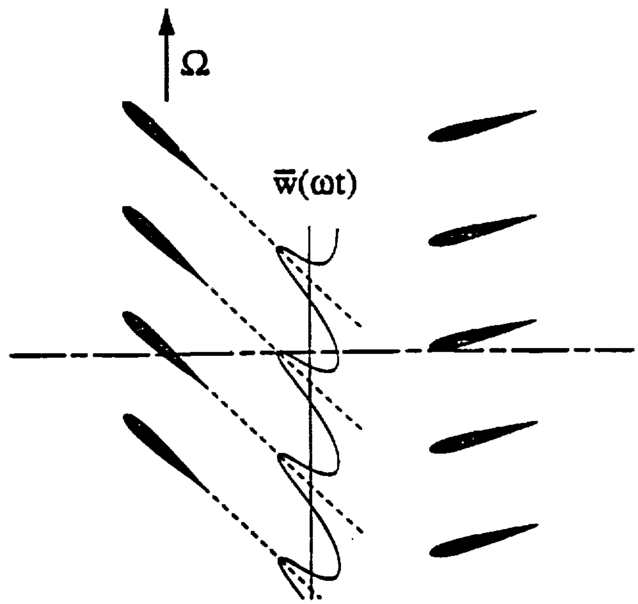

* Forced Response Design Systems Require Valid Wake Forcing Function Model

    * Based on Steady Performance Wake Data

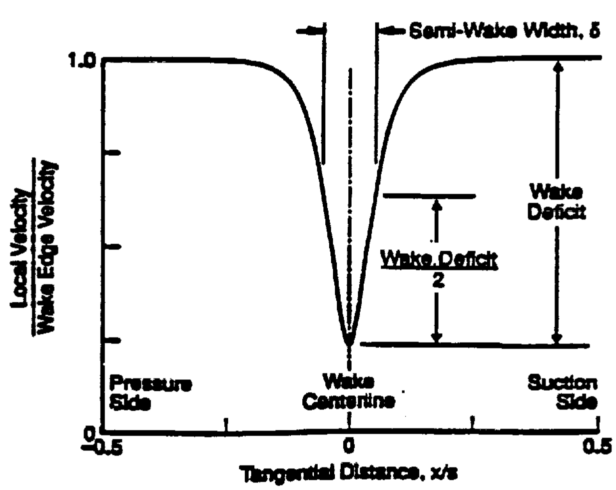

FORCED RESPONSE DESIGN SYSTEMS

* Wake - Unsteady Aerodynamic Forcing Function

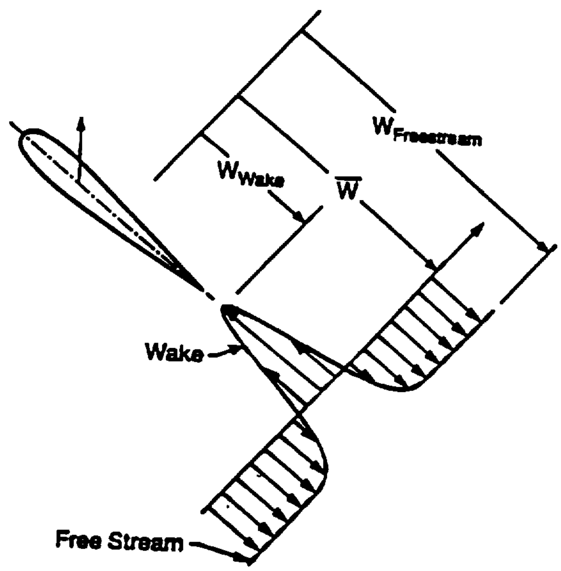

* Harmonic Wake - Gust Response

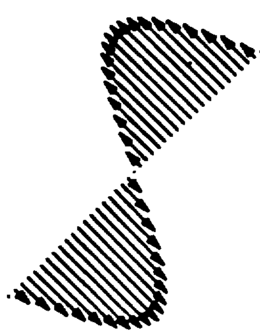

1st Harmonic Vortical Gust

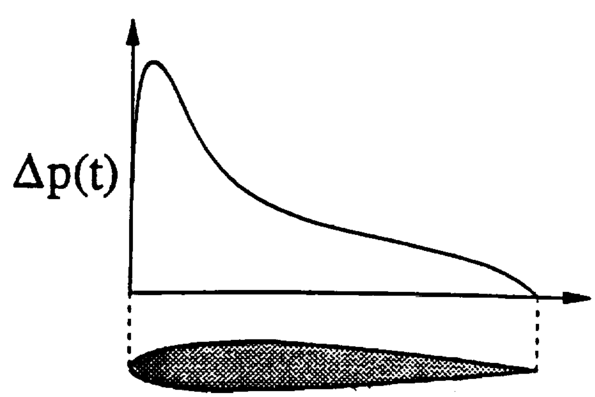

Downstream Airfoil Response

PROBLEM

* Unique Requirements of Forced Response Design Systems
    * Vortical & Potential Gust Forcing Functions

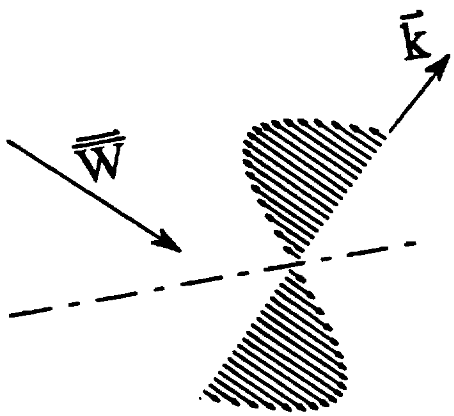

Vortical Gust

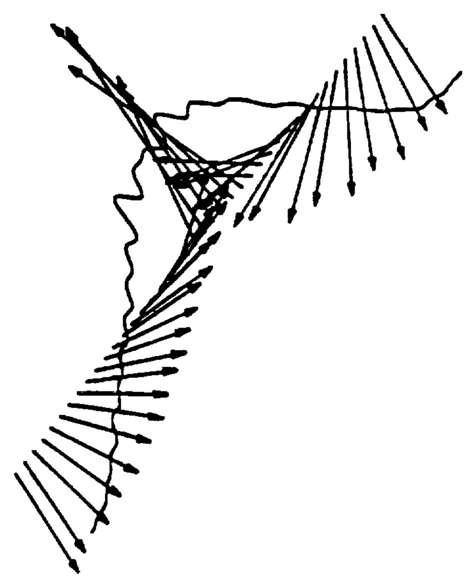

Airfoil Wake-Gust

RESEARCH OBJECTIVE

* Develop Complete Model of Unsteady Aerodynamic Forcing Functions Within Linear Theory Framework

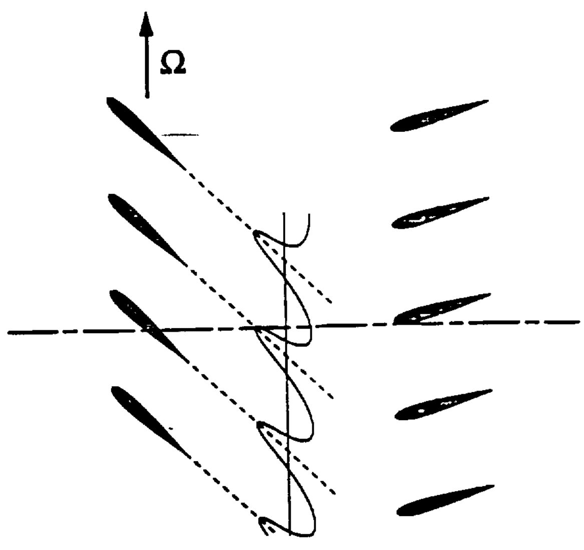

TECHNICAL APPROACH

* Perform Series of Fundamental Experiments to Investigate Unsteady Aerodynamic Forcing Functions
    * Vortical and Potential Gusts

TURBOMACHINE FLOW FIELD

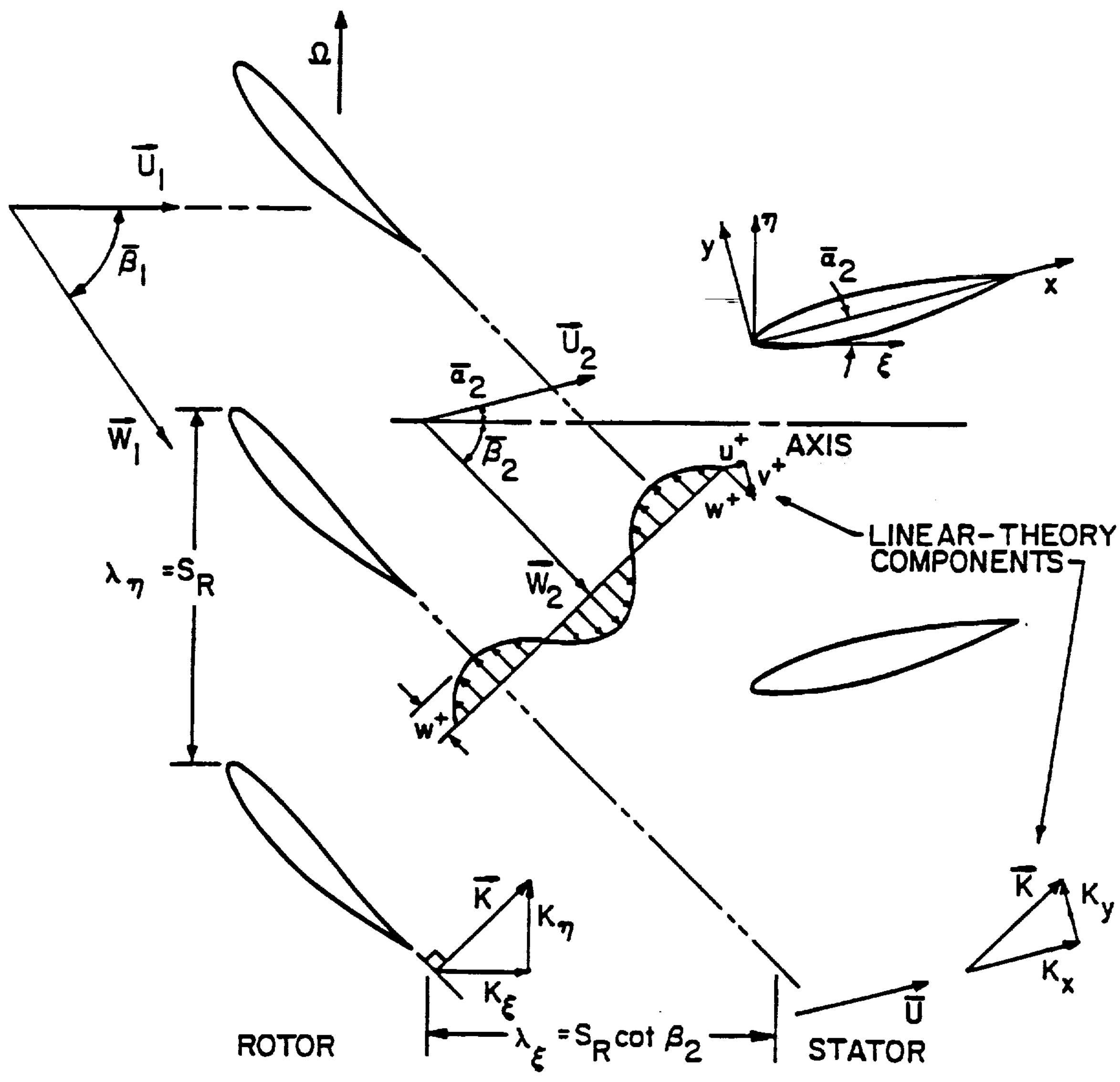

* **Periodicity in Axial-Tangential Coordinate System $\overline{W}_2 \perp \vec{k}$**

LINEAR THEORY GUST MODEL

$$\frac{1}{c_0^2}\frac{\overline{D}p}{Dt} + \overline{\rho}\nabla\cdot\overline{w} = 0 \qquad \text{(Continuity)}$$

$$\overline{\rho}\frac{\overline{D}\vec{w}}{Dt} + \nabla p = 0 \qquad \text{(Momentum)}$$

Vortical & Potential Splitting

$$\vec{w} = \vec{w}_v + \vec{w}_p$$

Vortical Gust $\vec{w}_v$

$$\nabla\cdot\vec{w}_v = 0$$

$$\frac{\overline{D}\vec{w}_v}{Dt} = 0$$

Potential Gust $\vec{w}_p$

$$\vec{w}_p = \nabla\phi_p$$

$$p = -\overline{\rho}\,\frac{\overline{D}\phi_p}{Dt}$$

Vortical Gust Propagation

$$\vec{w}_v = \vec{w}_v^{+}\exp\left[-i\vec{k}\cdot\left(\vec{x} - \vec{\vec{W}}t\right)\right]$$

$$\vec{k}\cdot\vec{\vec{W}} = 0$$

$$\vec{k}\cdot\vec{w}_v^{+} = 0 \qquad\qquad \vec{w}_v \perp \vec{k}$$

$$\vec{w}_v^{+} \parallel \vec{\vec{W}}$$

$$\vec{w}_v = D\vec{\vec{W}}\exp\left(-i\vec{k}\cdot\vec{x}\right)$$

- 2 Constraints
  - $\phi_w = 0°$ or $180°$
  - $\beta_w = \bar{\beta}_2$

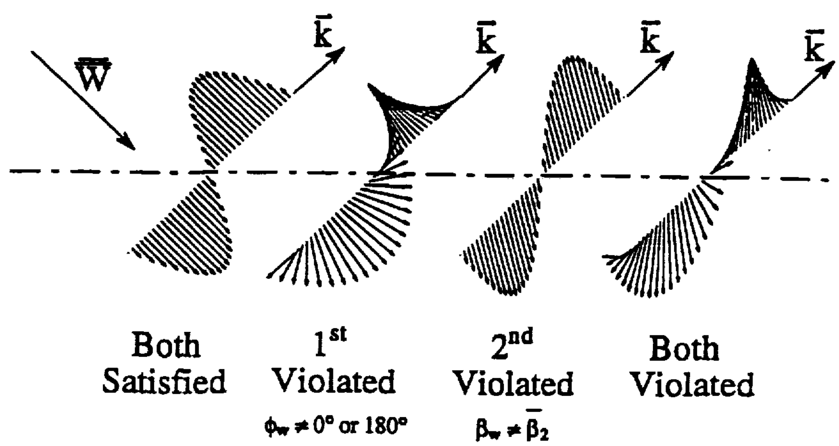

Potential Gust Propagation

$$\overline{w}_p = \nabla\phi_p$$

$$\left(1\text{-}M^2\right)\frac{\partial^2\phi_p}{\partial x^2} + \frac{\partial^2\phi_p}{\partial y^2} = 0$$

$$\phi_p = A\ \exp\left[-ik_\eta\eta + \chi\xi\right]$$

$$\chi = \frac{iM_\xi M_\eta k_\eta - \sqrt{\left(1\text{-}M^2\right)k_\eta^2}}{1\text{-}M_\xi^2}$$

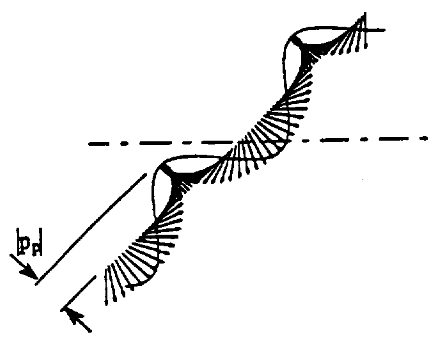

Combined Vortical and Potential Gust

$$\bar{w}_v = \sum_n D_n \overline{\overline{W}} \exp\left[-i\left(k_{\eta n}\eta + k_{\xi n}\xi\right)\right]$$

$$\phi_p = \sum_n A_n \exp\left[-ik_{\eta n}\eta + \chi_n \xi\right]$$

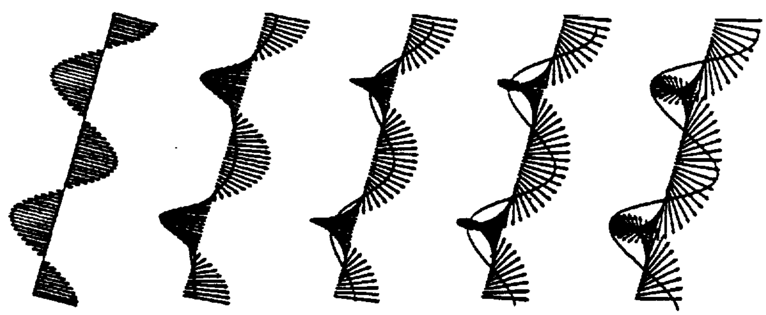

Vortical Combined Potential

Relating Measurements to Theory

- 2 Unknowns - A & D
- Experimentally Measure 3 Quantities
  - u, v, p
- Solution:
  Weighted Least Squares Approach

System of Equations

$$\begin{bmatrix} \chi & \overline{W}_\xi \\ -ik_\eta & \overline{W}_\eta \\ \overline{\rho}\left(-\overline{W}_\xi\chi+\overline{W}_\eta ik_\eta\right) & 0 \end{bmatrix} \begin{Bmatrix} A \\ D \end{Bmatrix} = \begin{Bmatrix} u \\ v \\ p \end{Bmatrix}$$

$$[T]\{c\} = \{b\}$$

Weighted Least Squares

$$[T]^T[W][T]\{c\} = [T]^T[W]\{b\}$$

where

$$[W] = \begin{bmatrix} W_v & 0 & 0 \\ 0 & W_v & 0 \\ 0 & 0 & W_p \end{bmatrix}$$

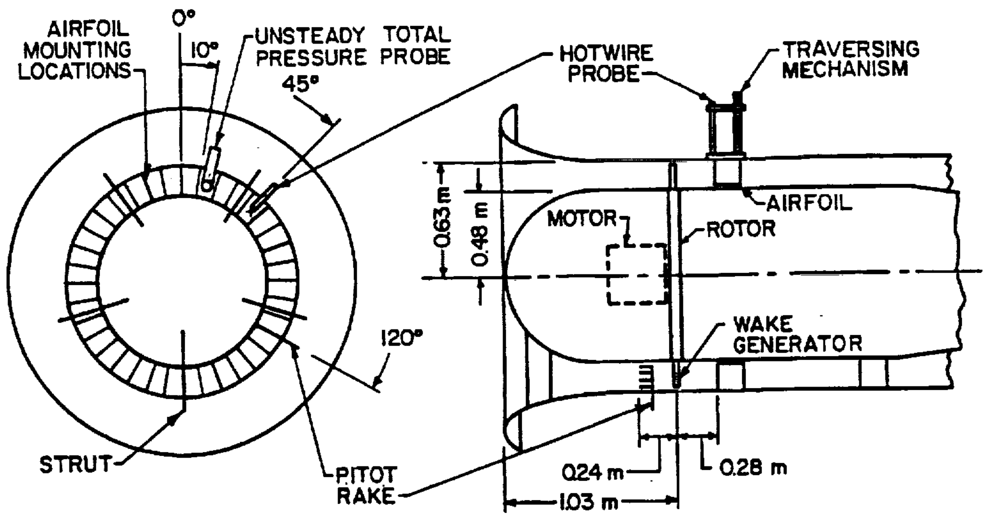
AIRFOIL MOUNTING LOCATIONS
0°
10°
UNSTEADY TOTAL PRESSURE PROBE
45°
HOTWIRE PROBE
TRAVERSING MECHANISM
120°
STRUT
PITOT RAKE
0.63 m
0.48 m
MOTOR
ROTOR
AIRFOIL
WAKE GENERATOR
0.24 m
0.28 m
1.03 m

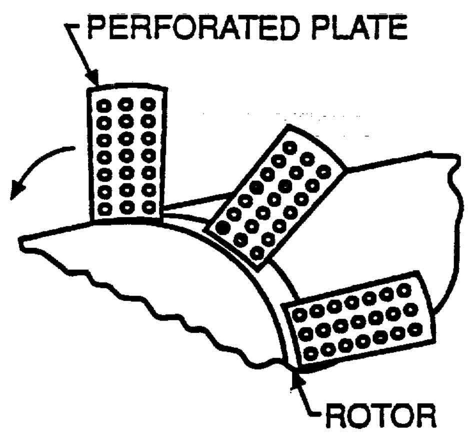
PERFORATED PLATE
ROTOR

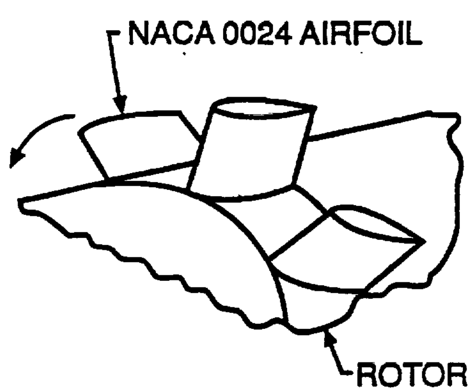
NACA 0024 AIRFOIL
ROTOR

Perforated Plate Gust

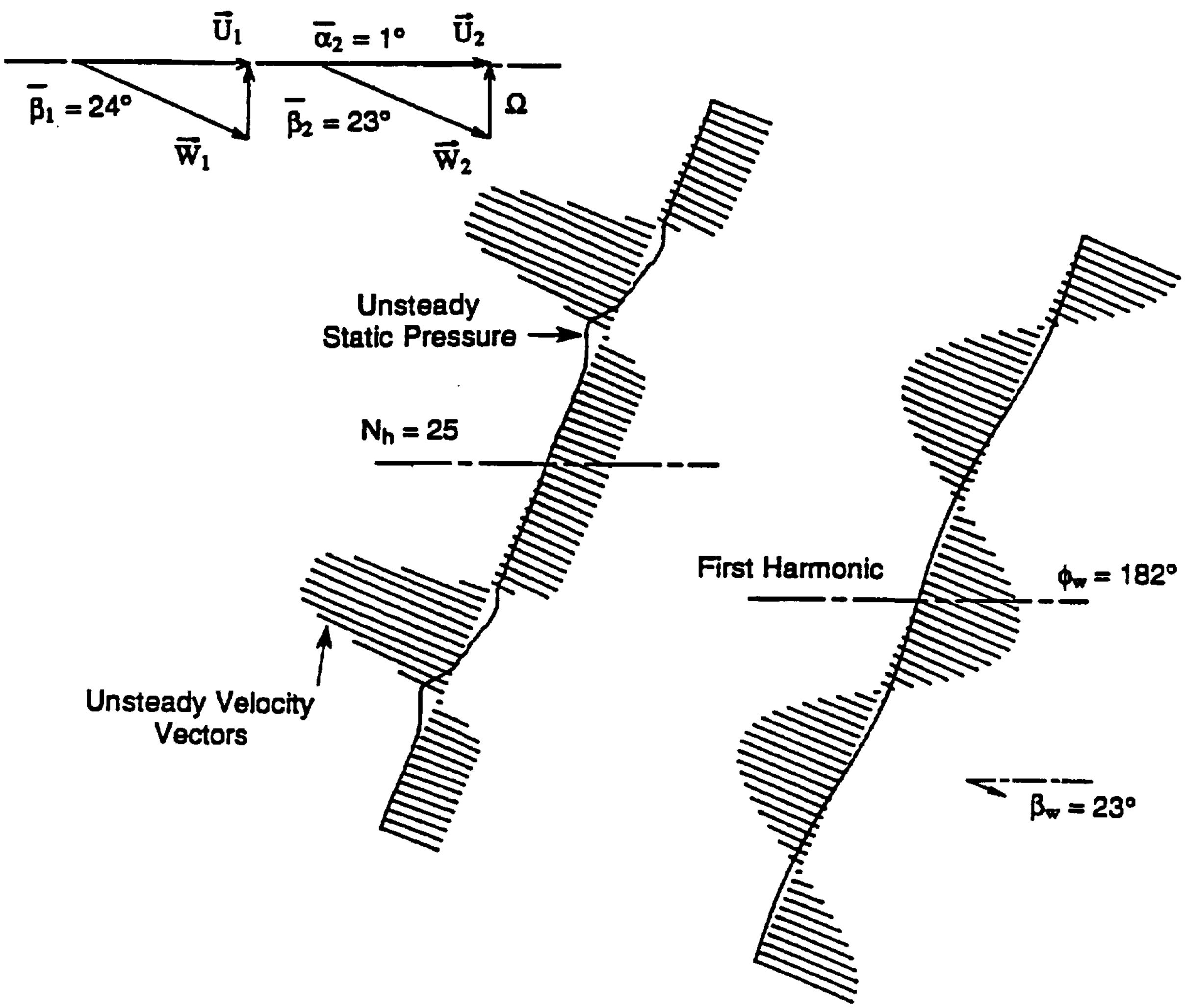

Perforated Plate

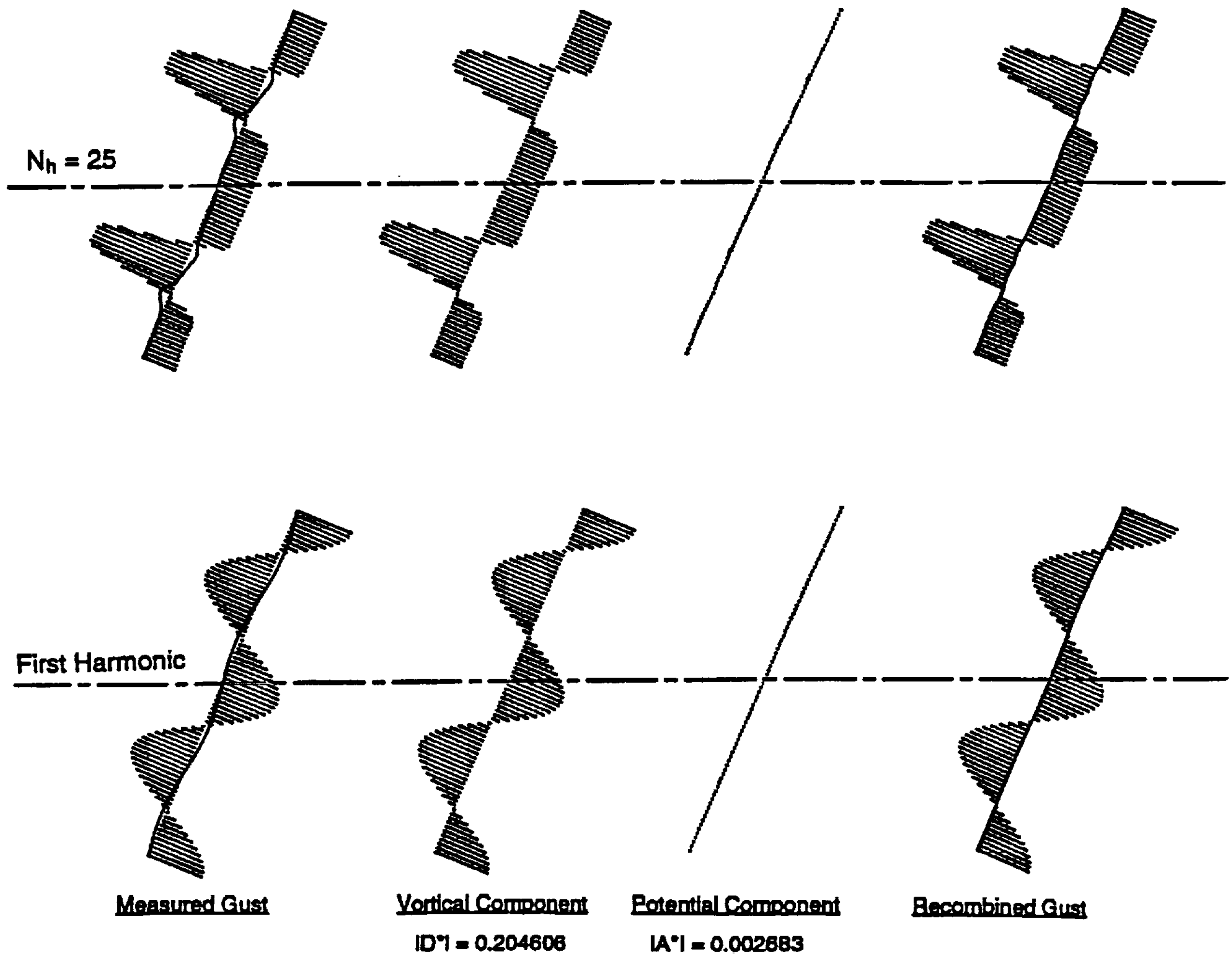

Neutrally Loaded Airfoil
Method V

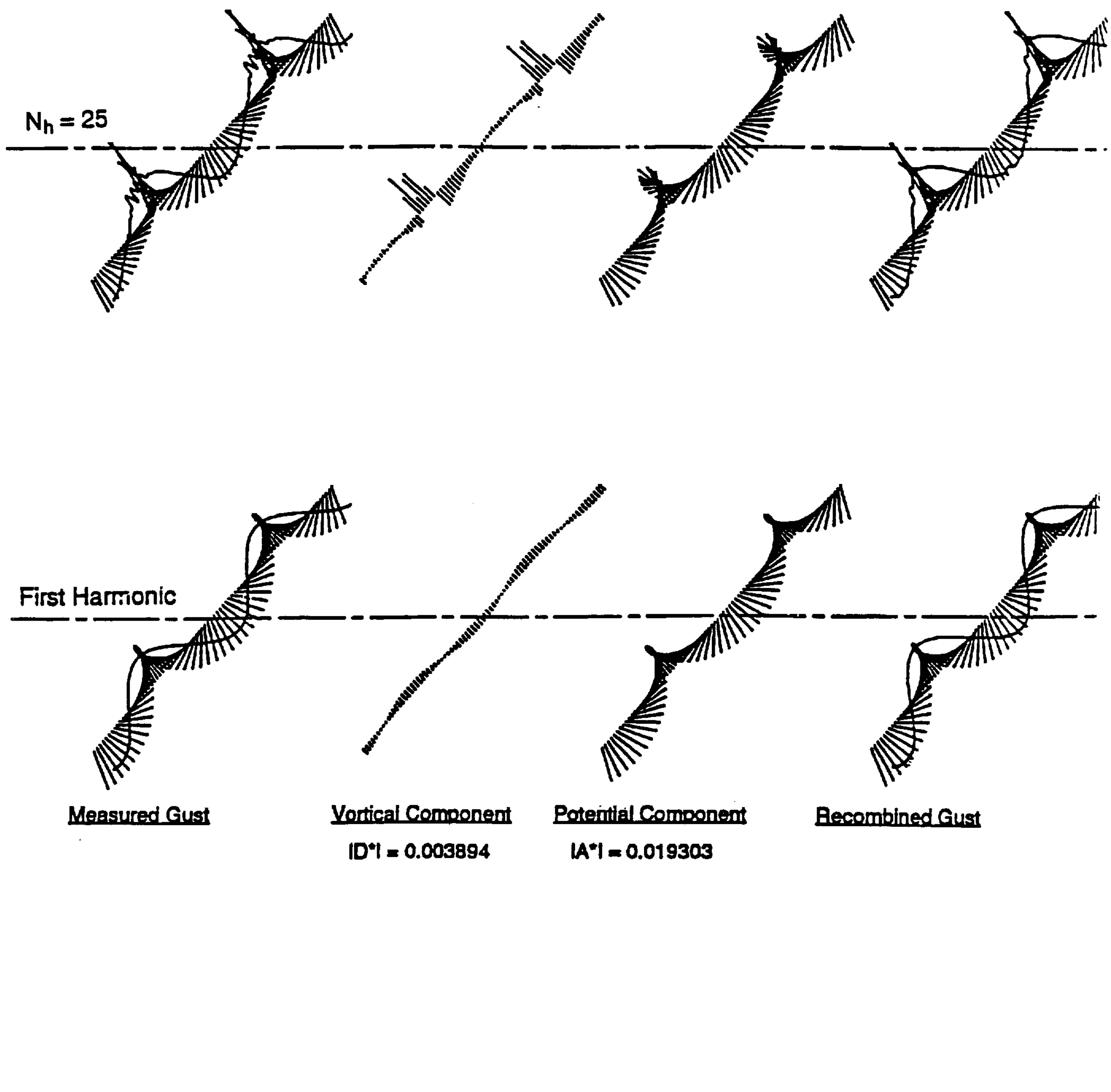

Neutrally Loaded Airfoil
Method P

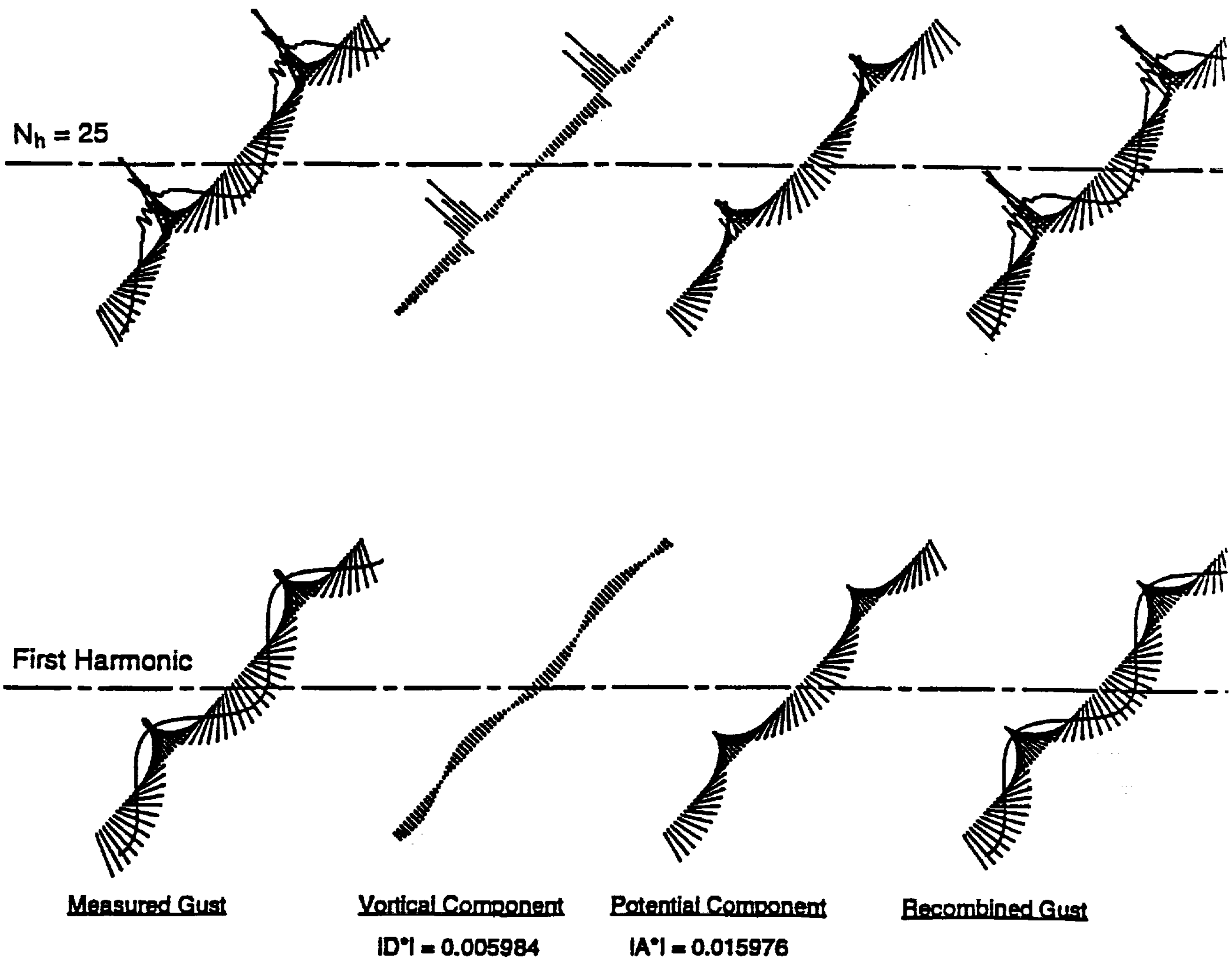

Compressor-Loaded Airfoil
Decayed Potential Field

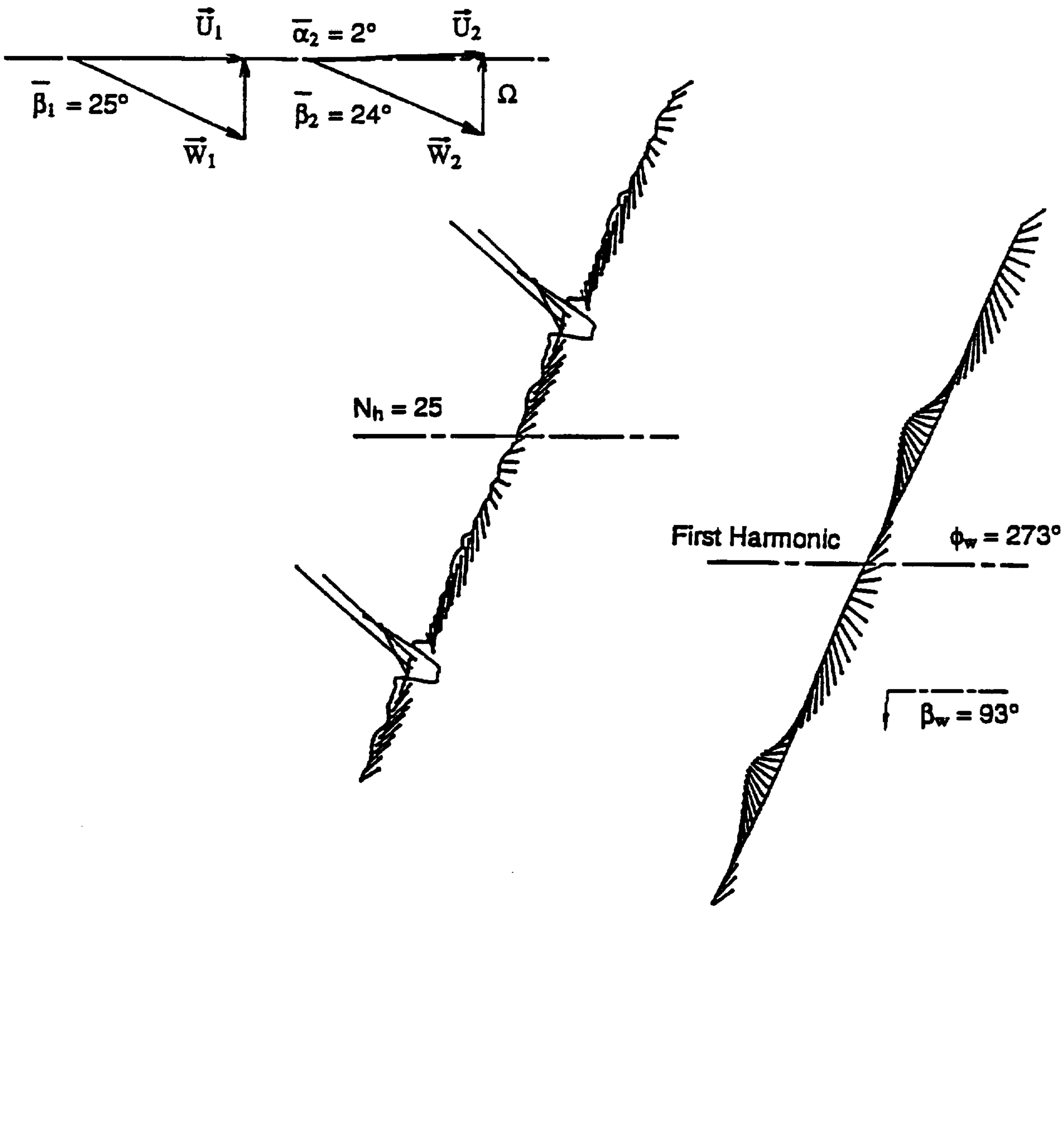

C-2

Compressor-Loaded Airfoil
Decayed Potential Field
Method V

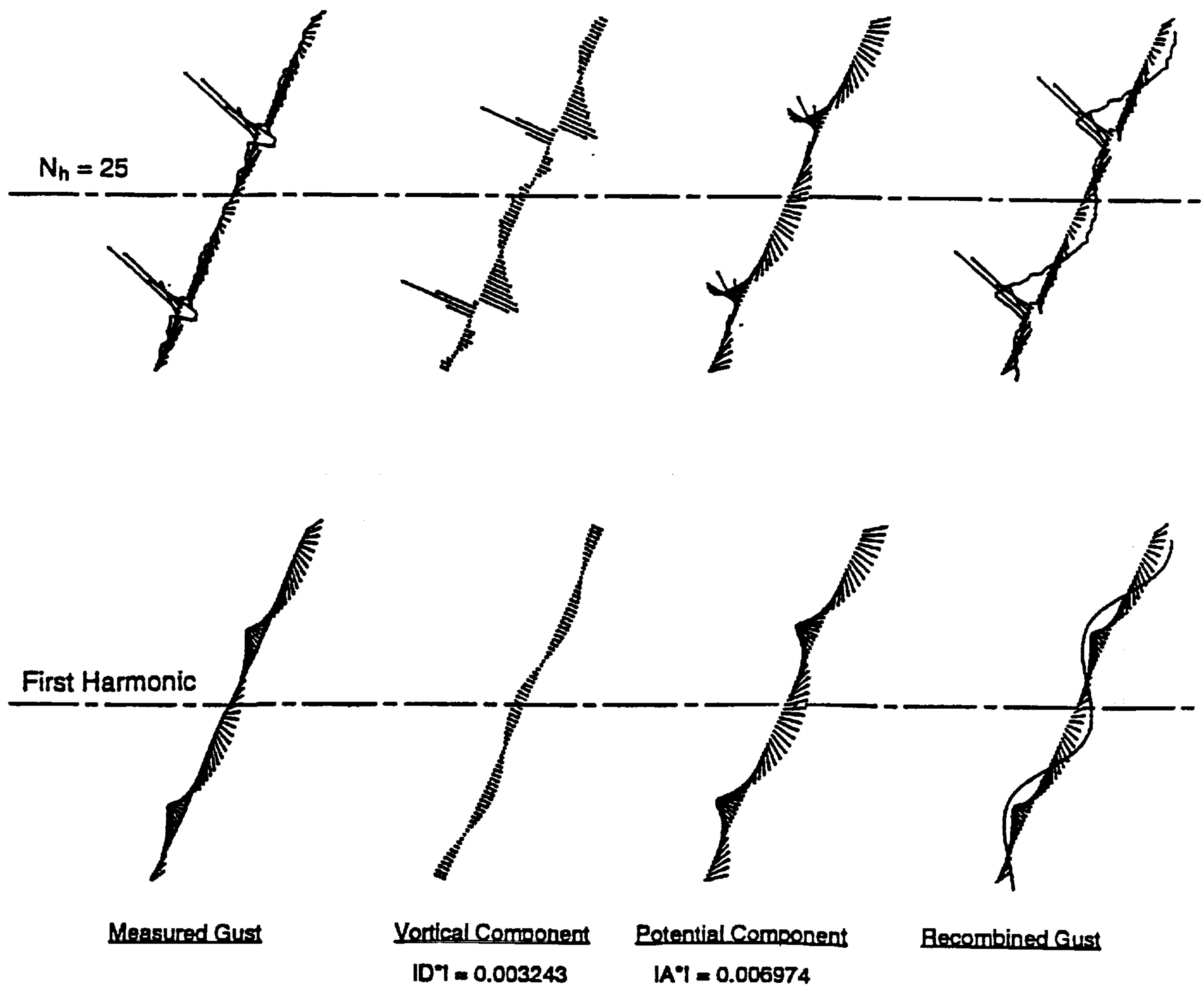

Compressor-Loaded Airfoil
Decayed Potential Field
Method P

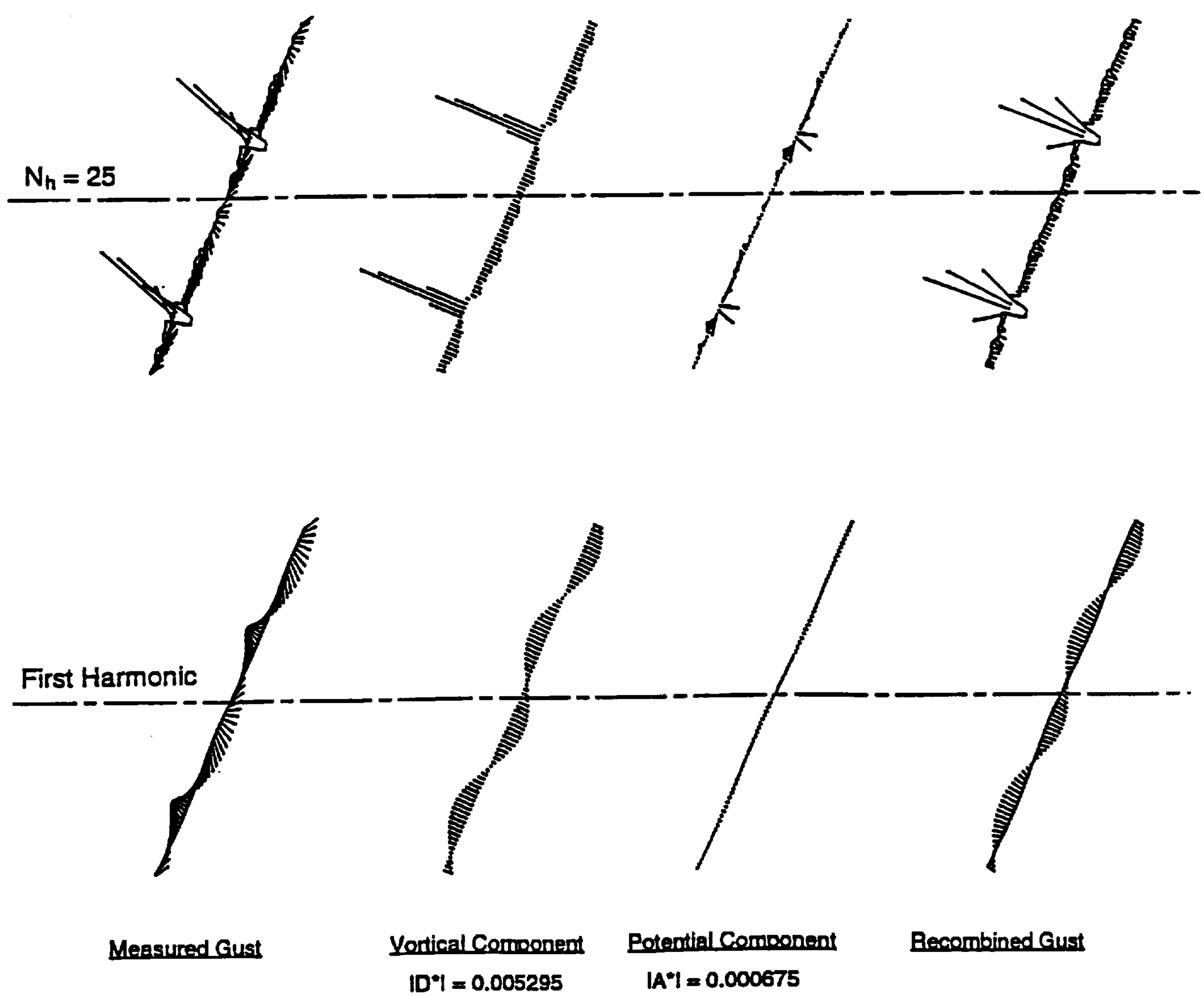

Perforated Plate
Vortical Component

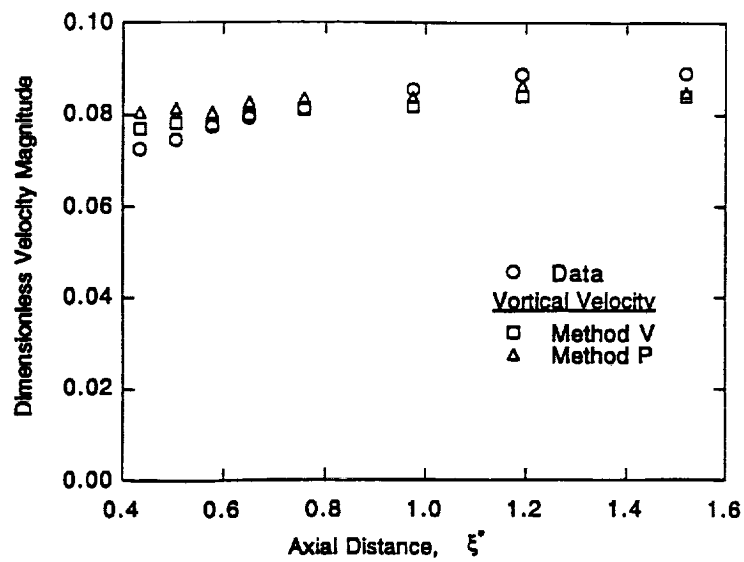

Compressor-Loaded Airfoil
Vortical Component

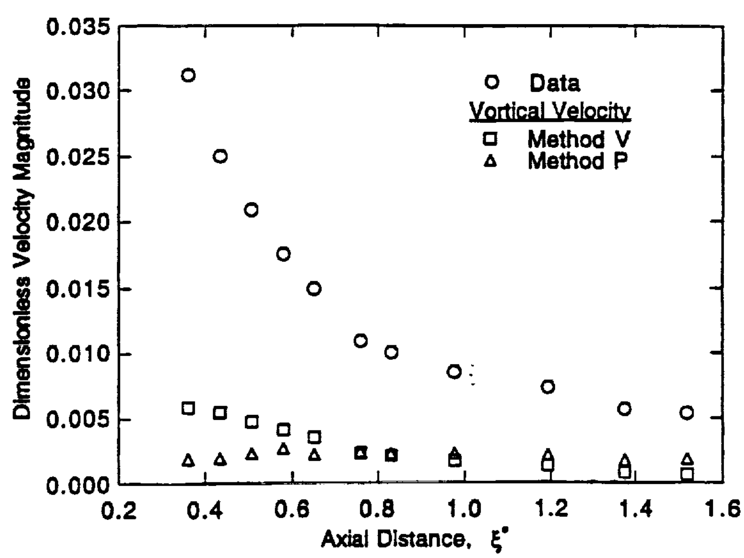

Compressor-Loaded Airfoil
Potential Component

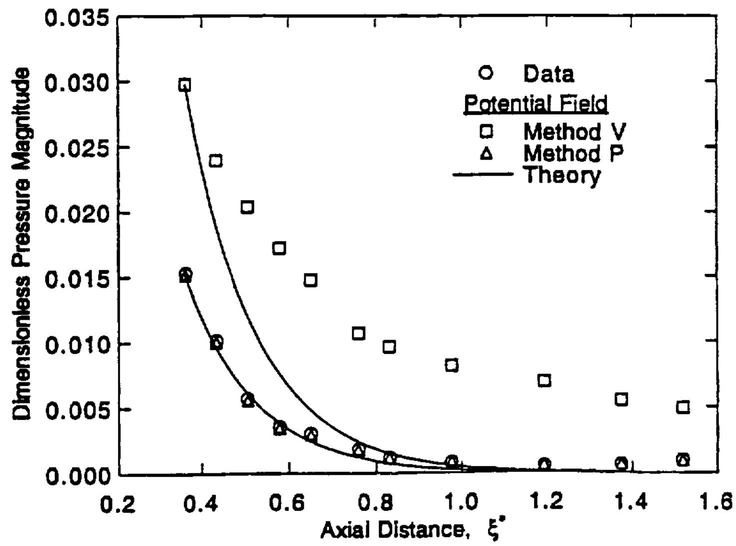

Turbine-Loaded Airfoil
Vortical Component

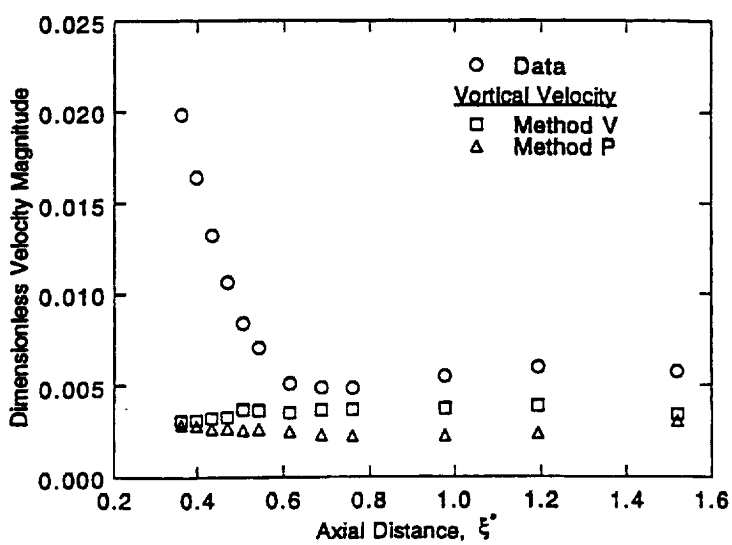

Turbine-Loaded Airfoil
Potential Component

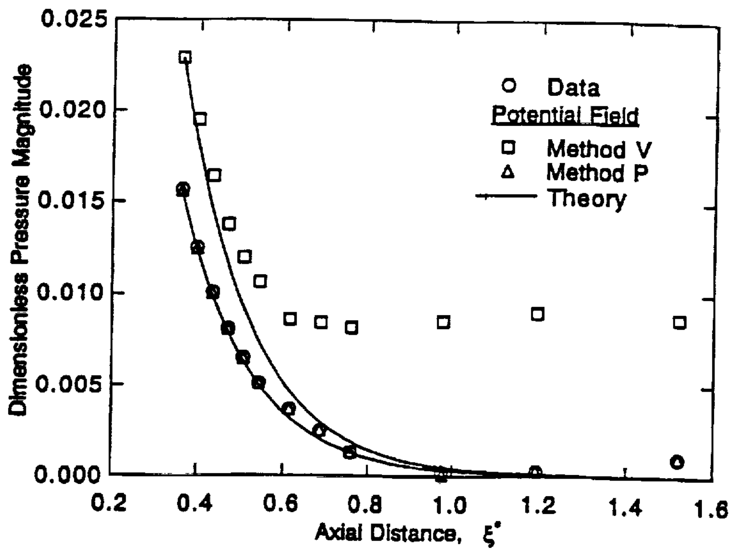

CONCLUSIONS

- **Vortical Gust Constraints Do Not Apply to Combined Vortical/Potential Gusts**

- **Gust Should Not Be Defined Utilizing Only Unsteady Velocity Data**
    - **Forcing Functions Defined by Unsteady Velocity & Pressure**

- **Least Squares Velocity-Pressure Method Produces Results Which Conform to Linear Theory**

N95- 19383

FORCED RESPONSE OF MISTUNED BLADED DISKS

S3-07
370/3
12P

C. Pierre
The University of Michigan
Ann Arbor, Michigan 48109

Mistuning

- Manufacturing tolerances, material non-uniformities, non-identical root fixtures, and in-service degradation result in blade-to-blade differences that destroy cyclic symmetry

- *Small* mistuning can cause large, *catastrophic* changes in blade vibrational response

  - amplitudes of vibration of some blades may increase by several hundred percent, producing "rogue" blades and HCF failure

  - free and forced responses may be highly *sensitive* to mistuning

  - tuned system predictions may be *qualitatively* in error and grossly underestimate blade forced response and overestimate fatigue life

- A credible forced response prediction system for turbomachinery vibration must take mistuning into account

An Example of Mistuning Effects on the Free Aeroelastic Response

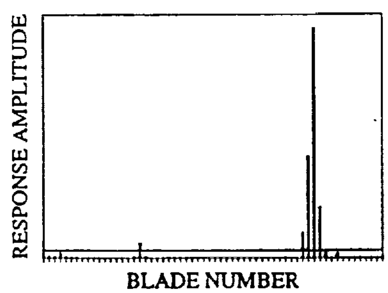

(Pierre and Murthy, 1991)

- ☐ In tuned analysis, all of the blades vibrate with equal amplitudes and share the excitation energy.
- ☐ Real system, with 1% random blade mistuning, has most of the vibration energy confined to 4 blades out of 56.

Mistuning causes *vibration localization*

⟶ much larger amplitudes for some blades

⟶ high stresses

⟶ blade fatigue

If unaccounted for, mistuning could cause cracks and catastrophic blade failures.

Effect of mistuning on forced response for a common blade assembly model

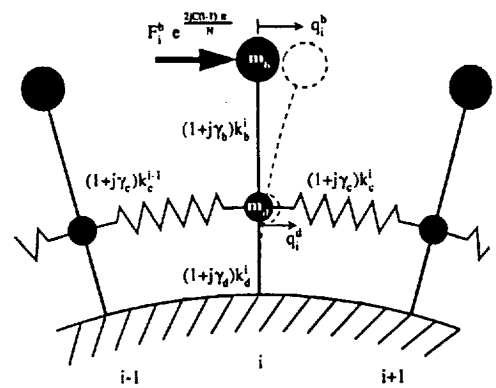

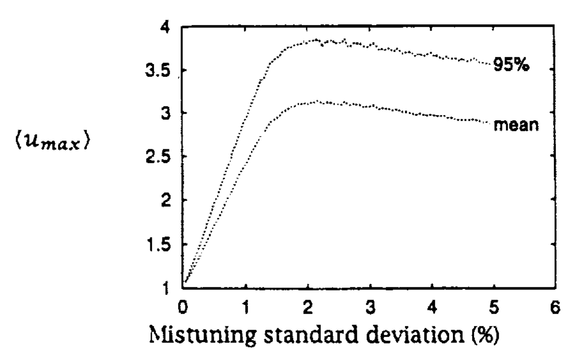

Obstacles

- Mistuned assembly analyses are very expensive. Parametric studies cannot be performed

  ⟶ need for accurate reduced-order models

- Mistuning is random by nature

  - ☐ mistuning pattern (and sometimes mistuning strength) is typically not available
  - ☐ mistuning differs from rotor to rotor
  - ☐ mistuning that results from in-service degradation cannot be modeled deterministically

  ⟶ calls for *statistical* and parametric tools

- Studies of mistuning by Afolabi, Bendiksen, Ewins, Griffin, Kaza, Kielb, Pierre, Sinha, Srinivasan, Mignolet, *etc.*, have led to general conclusions:
  - ☐ helps flutter
  - ☐ increases forced response amplitudes
- However — quantitatively and even qualitatively different findings regarding other issues
  - ☐ blade with largest amplitude
  - ☐ forced response amplitude increase over tuned system

- A new perspective of the mistuning problem (Bendiksen, Pierre):
  - ☐ Mistuning belongs to the broader topic of repetitive structures with periodicity-breaking irregularities
  - ☐ identification of the basic physical mechanism governing mistuning effects: sensitivity of aeroelastic eigensolution to mistuning is inverse proportional to the distance between the eigenvalues

$$\delta^2\lambda_j \propto \frac{1}{\lambda_{oj} - \lambda_{ok}}$$

- ☐ closeness of eigenvalues is governed by the *interblade coupling* and number of blades
  - → weakly coupled assemblies are highly sensitive to mistuning (interblade coupling depends on frequency)
  - → assemblies with many blades are more sensitive
  - → mistuning effects increase with frequency (tip modes)
- ☐ highly sensitive mistuned assemblies feature localized responses

■ Formulation of a preliminary unifying theory of mistuning

■ Demonstration of the importance of considering mistuning effects at the design stage

Objectives

Provide the designer with tools for predicting the forced response amplitudes of real (*i.e.*, mistuned) bladed disks. Incorporate a mistuning analysis capability into forced response prediction system (FREPS)

- ■ develop low-dimensional reduced-order models
- ■ evaluate the significance of mistuning effects in terms of system parameters. Identify key parameters governing sensitivity to mistuning.
- ■ predict the sensitivity of the system dynamics to blade mistuning .
- ■ determine true response amplitudes for typical mistuned bladed disks
- ■ obtain confidence intervals for amplitudes and stresses and estimates of fatigue life

NASA research program thrusts

- Aeroelastic characteristics of mistuned assemblies: mode localization and root locus scattering
- Stochastic measures of sensitivity to mistuning
  - ☐ transfer matrix based
  - ☐ eigenvalue perturbation based
  - ☐ localization factors
  - ☐ composite sensitivity measure for structurally and aerodynamically coupled rotors
- Dynamics of mistuned assemblies with several component modes per blade.
  Effect of close blade modes on tuned and mistuned system dynamics.
- Design for low sensitivity to mistuning: formulation of an optimization constraint.
- Forced response of mistuned assemblies:
  - → physical mechanisms governing mistuning effects
  - → efficient statistical computational methods
- Mistuned bladed disk formulation via component mode analysis and validation of simple models

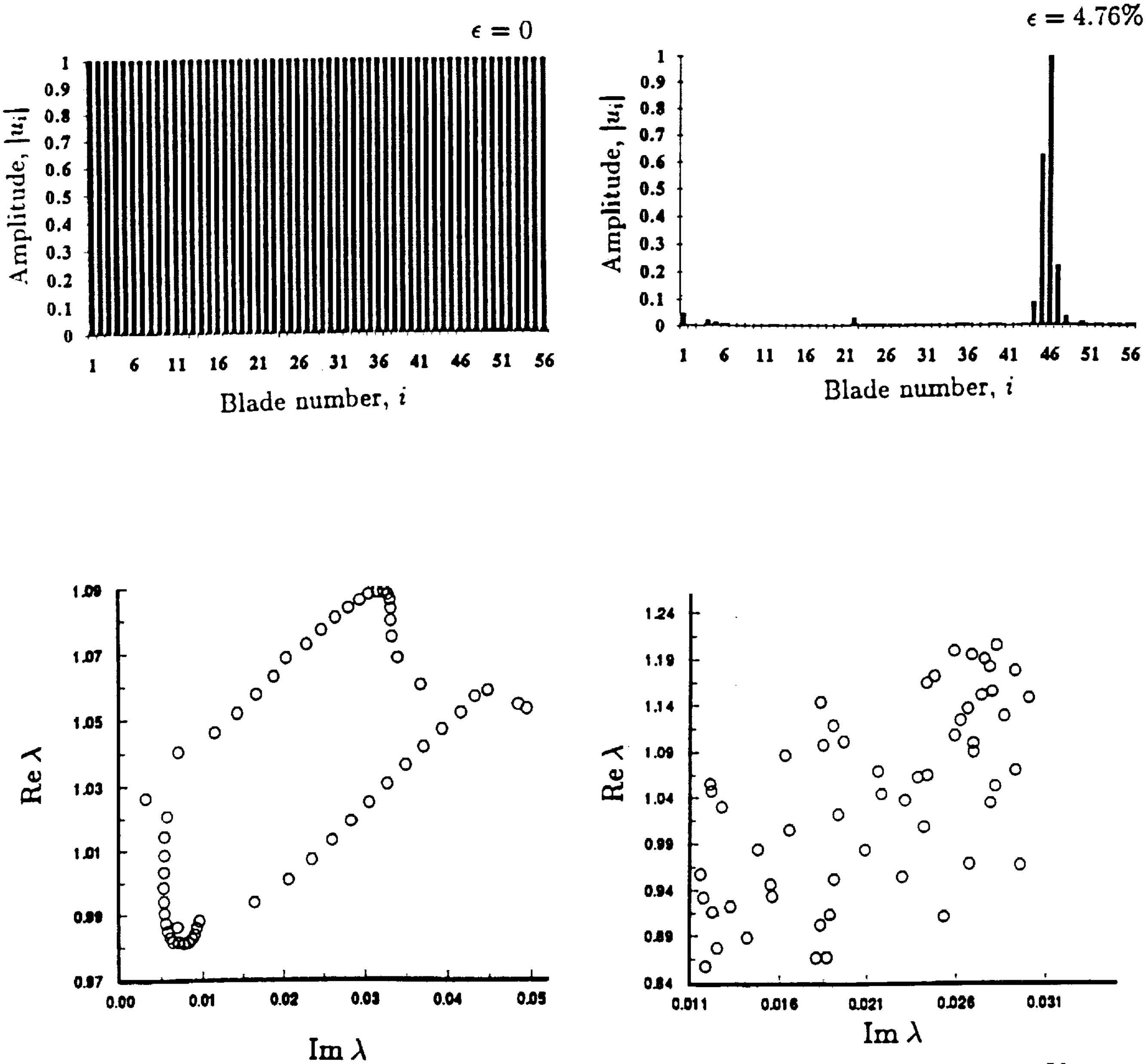

Tuned, $\epsilon = 0$

Mistuned, $\epsilon = 4.76\%$

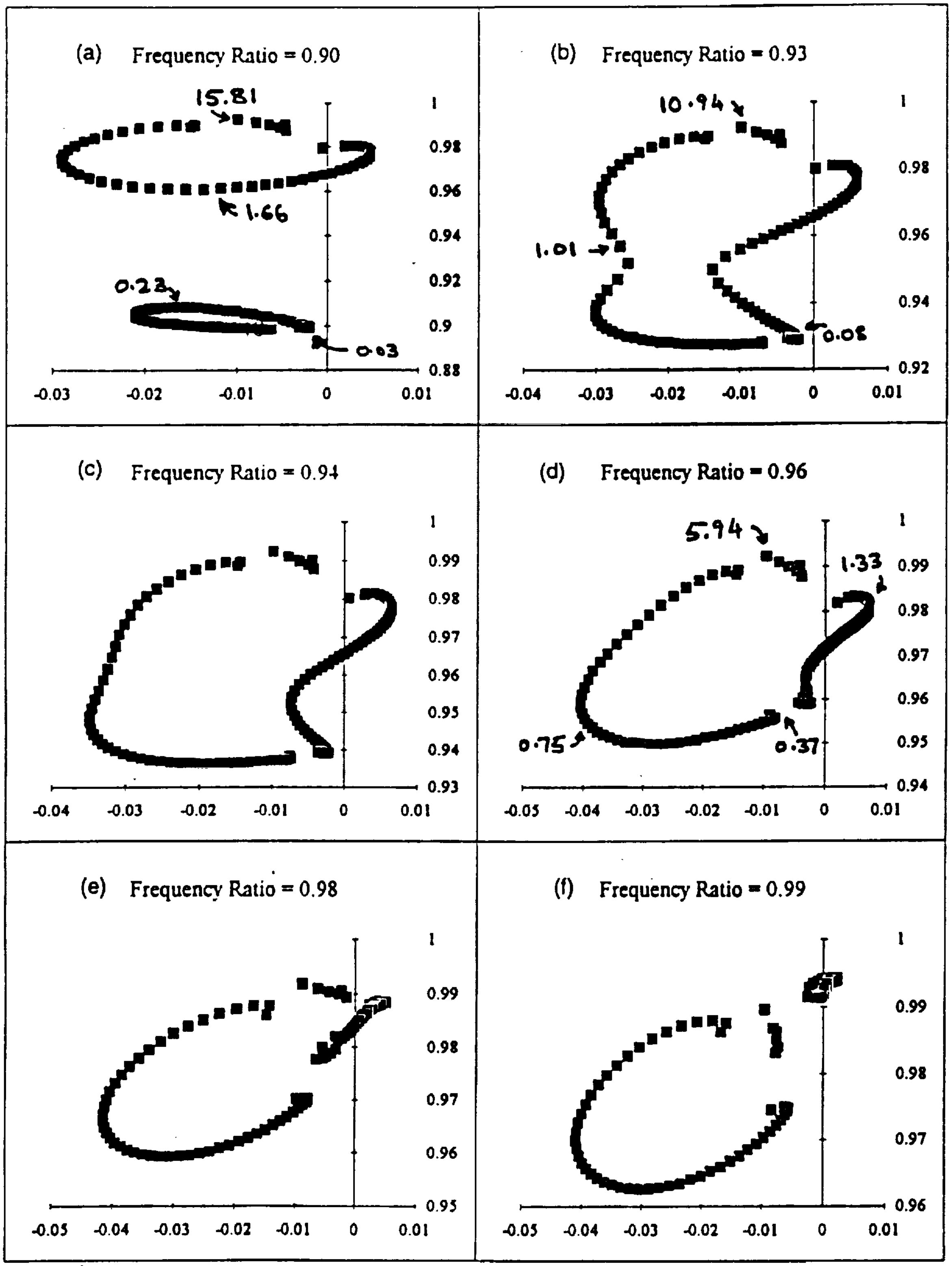

(a) Frequency Ratio = 0.90
15.81
1.66
0.22
0.03
(b) Frequency Ratio = 0.93
10.94
1.01
0.08
(c) Frequency Ratio = 0.94
(d) Frequency Ratio = 0.96
5.94
1.33
0.75
0.37
(e) Frequency Ratio = 0.98
(f) Frequency Ratio = 0.99

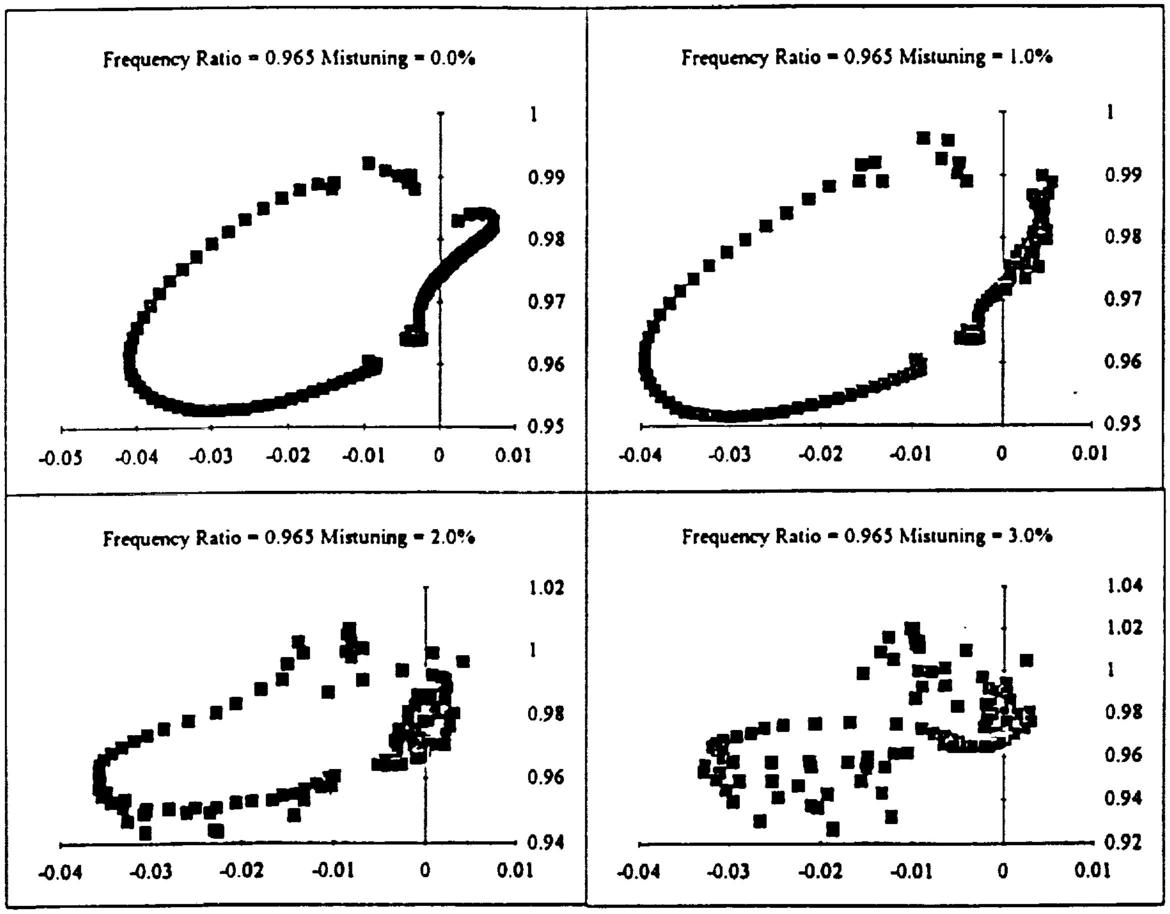

Frequency Ratio = 0.965 Mistuning = 0.0%
1
0.99
0.98
0.97
0.96
0.95
-0.05
-0.04
-0.03
-0.02
-0.01
0
0.01
Frequency Ratio = 0.965 Mistuning = 1.0%
1
0.99
0.98
0.97
0.96
0.95
-0.04
-0.03
-0.02
-0.01
0
0.01
Frequency Ratio = 0.965 Mistuning = 2.0%
1.02
1
0.98
0.96
0.94
-0.04
-0.03
-0.02
-0.01
0
0.01
Frequency Ratio = 0.965 Mistuning = 3.0%
1.04
1.02
1
0.98
0.96
0.94
0.92
-0.04
-0.03
-0.02
-0.01
0
0.01

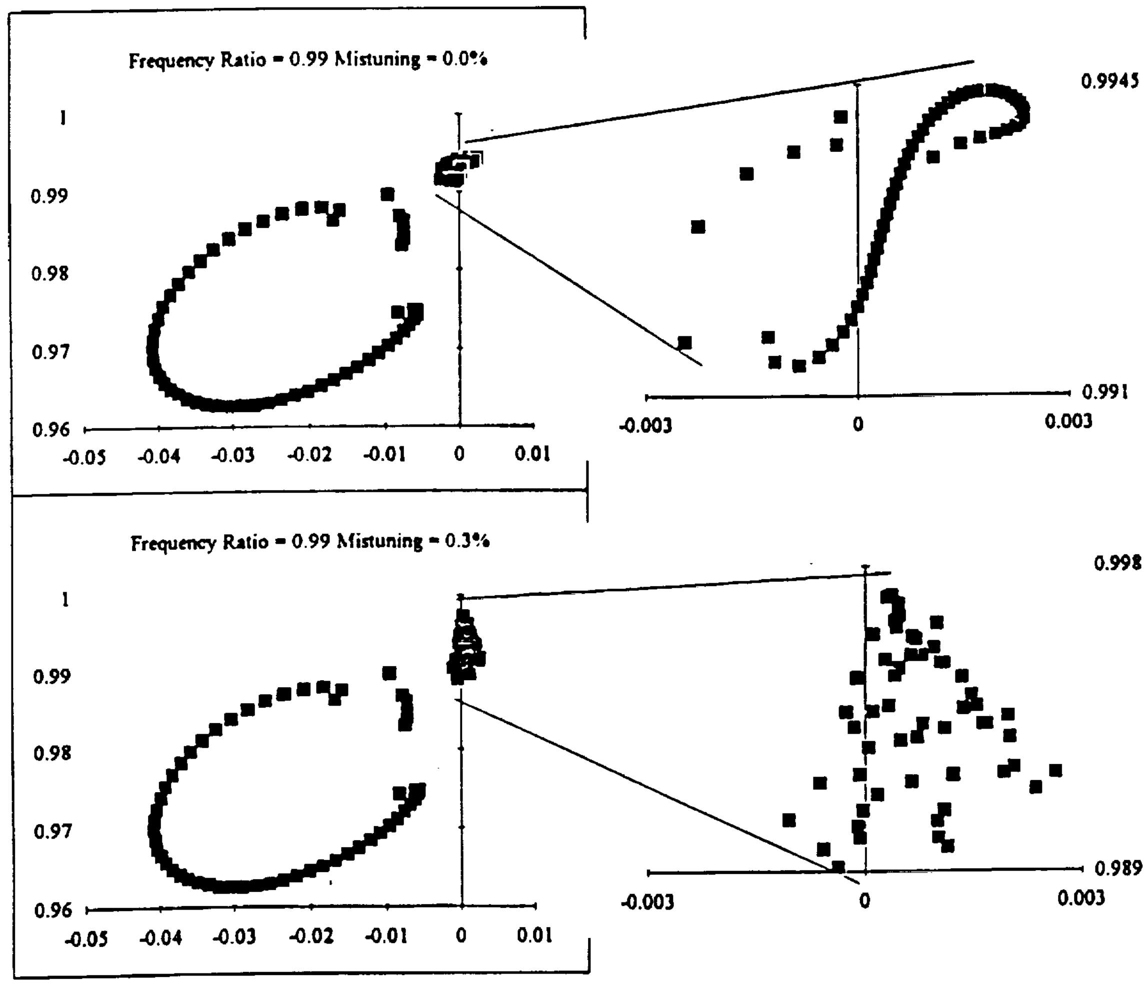
Frequency Ratio = 0.99 Mistuning = 0.0%
1
0.99
0.98
0.97
0.96
-0.05
-0.04
-0.03
-0.02
-0.01
0
0.01
0.9945
0.991
-0.003
0
0.003
Frequency Ratio = 0.99 Mistuning = 0.3%
1
0.99
0.98
0.97
0.96
-0.05
-0.04
-0.03
-0.02
-0.01
0
0.01
0.998
0.989
-0.003
0
0.003

Practical Significance of the Localization Factor

decay according to $e^{-\gamma n}$

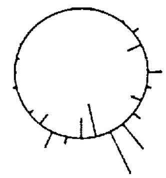

$S_{mid} \simeq 25$
$\gamma = 0.2$
90% amplitude decay
by the 11th blade

- For $\gamma = 0.1$, amplitude decays by a factor $e^{-0.1} \simeq 0.9$ from one bay to the next (on *average*) ·

  56% of the energy is transmitted to the 3rd bay
- For $\gamma = 1.0$, average energy transmitted to next bay is 13.5% and less than 0.25% of the energy reaches the 3rd bay!
- γ is an average quantity and specific realizations of mistuned systems may exhibit different behavior.
- γ can be calculated in terms of a universal sensitivity measure for simple models.

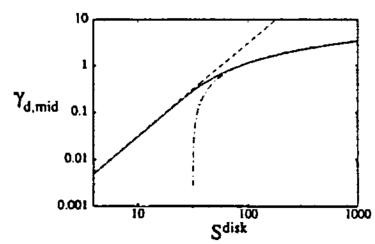

- Use in design:

  Maximum allowable localization strength $\Rightarrow \gamma \Rightarrow S \Rightarrow$ corresponding permitted regions in parameter space.

Forced Response of Mistuned Assemblies

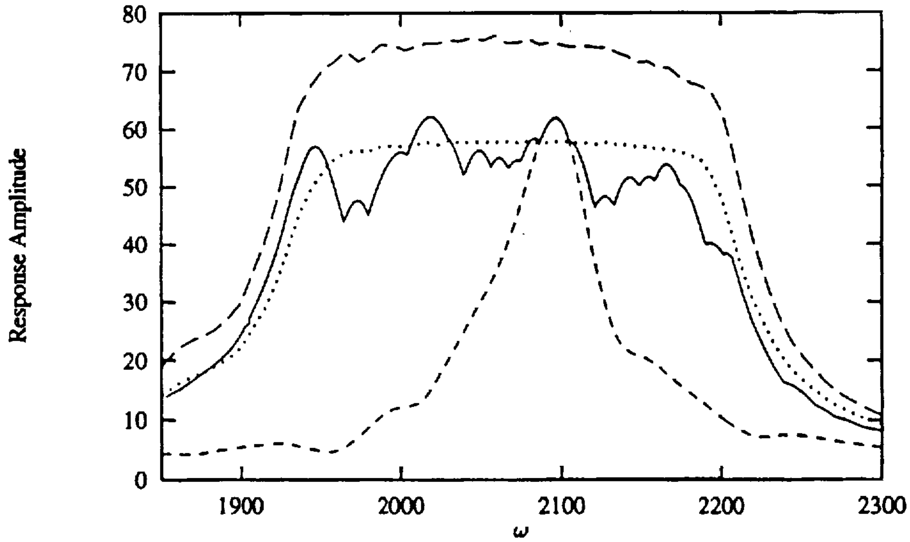

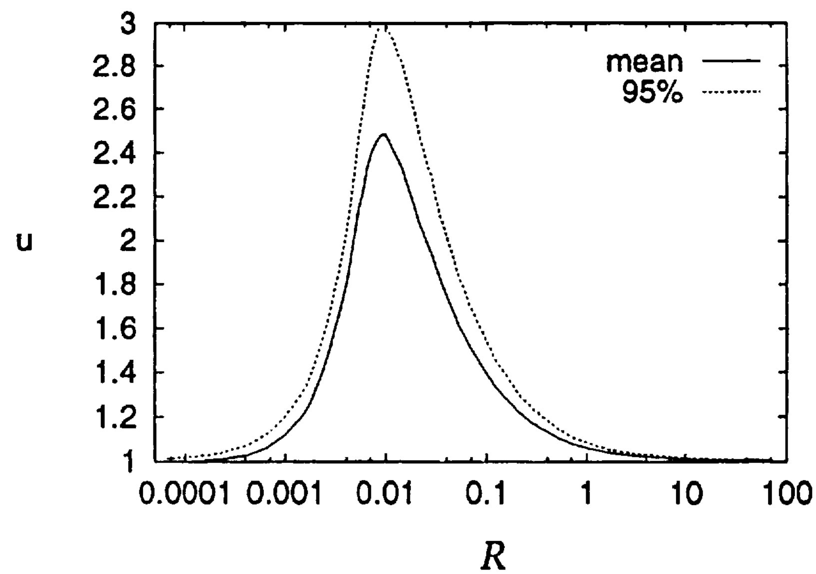

$$u = \frac{\text{Maximum blade amplitude in mistuned system}}{\text{Blade amplitude in tuned system}}$$

Closing

- Because of its potentially catastrophic effects such as single blade failure, mistuning must be accounted for in the design and analysis of blade assemblies
- Simple and effective mistuning capability must be incorporated into FREPS
- Underlying physical mechanisms must be understood to generate proper reduced-order models

Future work:

- Forced response: develop physical understanding and associated efficient computational techniques
- Mistuning experiment: corroborate occurrence of localization and high sensitivity in nonrotating/rotating conditions
- Beneficial mistuning patterns: practical only if mistuning can be controlled

MISTUNING PATTERNS AND FORCED RESPONSE OF BLADED DISKS

omit
14P

B.C. Watson
Georgia Institute of Technology
Atlanta, Georgia 23681

RESEARCH OBJECTIVES

- BETTER UNDERSTANDING OF MISTUNED BLADED DISK ASSEMBLY RESPONSE CHARACTERISTICS
- RELATIONSHIPS BETWEEN MISTUNE PATTERN, EXCITATION MODE, AND RESPONSE AMPLITUDE
- OPTIMIZATION OF MISTUNING PATTERNS SUCH THAT FATIGUE DAMAGE IS MINIMIZED

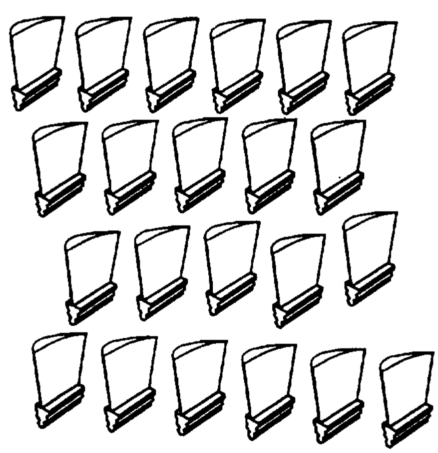

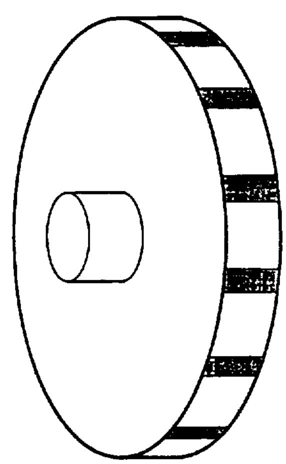

BLADE/DISK MODEL

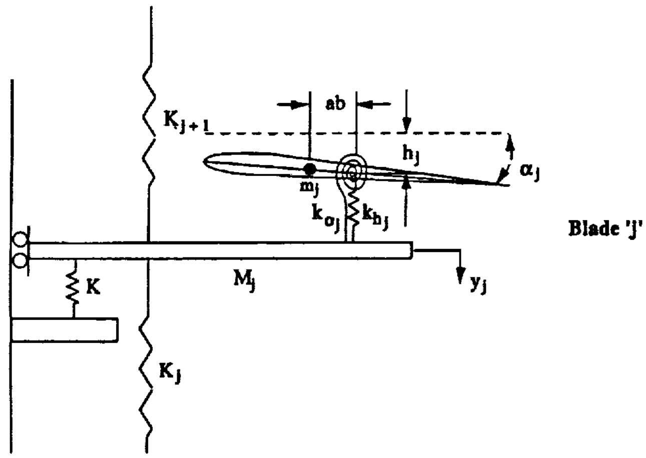

Blade '0' connects to blade 'N' for cyclic periodicity

AERODYNAMIC MODEL

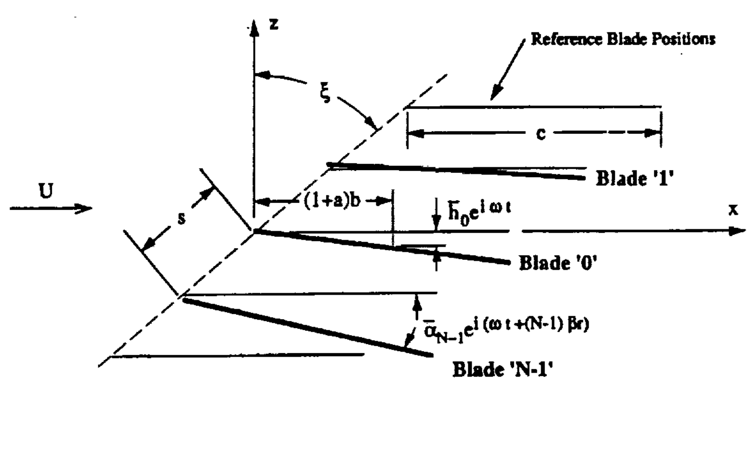

Mistune Modes

$$\gamma_j^2 = \delta_0 + \sum_{i=0}^{\left\lceil \frac{N}{2} \right\rceil - 1} \delta_i \cos(\beta_i j) + \overbrace{\frac{1}{\sqrt{2}} \delta_{\frac{N}{2}} \cos(\beta_{\frac{N}{2}} j)}^{\text{if N is Even}} + \sum_{i=\frac{N}{2}+1}^{N-1} \delta_i \sin(\beta_{i-\frac{N}{2}} j)$$

$$\text{Mean} = \delta_0$$

$$\text{Variance} = \; s^2 = \frac{1}{2} \sum_{i=1}^{N-1} \delta_i^2$$

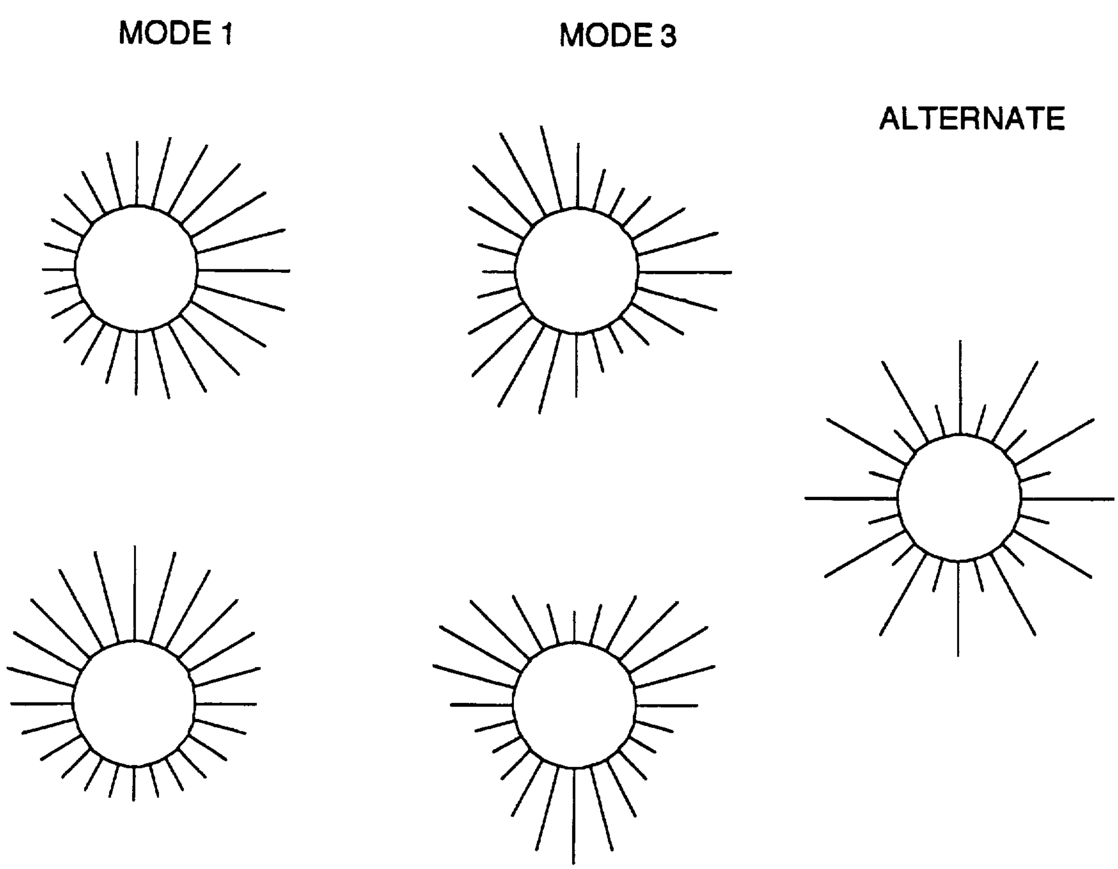

GOVERNING EQUATIONS

$$\begin{bmatrix} \mathbf{B}_{00} & \mathbf{B}_{01} & 0 \\ \mathbf{B}_{10} & \mathbf{B}_{11} & \mathbf{B}_{12} \\ 0 & \mathbf{B}_{21} & \mathbf{B}_{22} \end{bmatrix} \begin{Bmatrix} \mathbf{y}_a^* \\ \mathbf{h}_a^* \\ \alpha_a \end{Bmatrix} = \begin{Bmatrix} 0 \\ \mathbf{R}_1 \\ \mathbf{R}_2 \end{Bmatrix}$$

$\mathbf{y}_a^*$ is the vector of disk element modal amplitudes

$\mathbf{h}_a^*$ is the vector of blade translational modal amplitudes

α_a is the vector of blade torsional modal amplitudes

$$\mathbf{B}_{00} = \left[-\left(\gamma^2 - \gamma_\Omega^2\right)\mathbf{I} + \frac{\mu_t}{V}\gamma_h^2[\mathbf{I} + [C_h]] + 2\gamma_\Phi^2[\mathbf{I} - \cos\beta_1 j] \right]$$

$$\mathbf{B}_{01} = -\frac{\mu_t}{V}\gamma_h^2[\mathbf{I} + [C_h]]$$

$$\mathbf{B}_{10} = -\mu_t\gamma_h^2[\mathbf{I} + [C_h]]$$

$$\mathbf{B}_{11} = \left[-\mu_t\gamma^2\mathbf{I} + \mu_t\gamma_h^2[\mathbf{I} + [C_h]] + \gamma^2[\ell_h]\right]$$

$$\mathbf{B}_{12} = \gamma^2[\ell_\alpha]$$

$$\mathbf{B}_{21} = -\gamma^2[m_h]$$

$$\mathbf{B}_{22} = \left[-\mu_t r_{\alpha t}^2\gamma^2\mathbf{I} + \mu_t r_{\alpha t}^2\gamma_\alpha^2[\mathbf{I} + [C_\alpha]] - \gamma^2[m_\alpha]\right]$$

STRUCTURE OF THE CIRCULANT MISTUNE MATRIX

$$[C_\alpha] = \frac{1}{\delta_0} circ\left[0 \quad \frac{1}{2}\left(\delta_1 - i\delta_{1+\frac{N}{2}}\right) \quad \frac{1}{2}\left(\delta_2 - i\delta_{2+\frac{N}{2}}\right) \quad \cdots \quad \frac{1}{2}\left(\delta_2 + i\delta_{2+\frac{N}{2}}\right) \quad \frac{1}{2}\left(\delta_1 + i\delta_{1+\frac{N}{2}}\right)\right]$$

SMALL MISTUNE PARAMETER

$$[C_h] = \varepsilon\left[\tilde{C}_h\right]$$

$$[C_\alpha] = \varepsilon\left[\tilde{C}_\alpha\right]$$

$$\mathbf{B}_{00} = \hat{\mathbf{B}}_{00} + \varepsilon\,\tilde{\mathbf{B}}_{00}$$
$$\mathbf{B}_{01} = \hat{\mathbf{B}}_{01} + \varepsilon\,\tilde{\mathbf{B}}_{01}$$

etc.

$\hat{\mathbf{B}}_{ij}$ are diagonal matrices
$\tilde{\mathbf{B}}_{ij}$ are circulant matrices

RESPONSE PERTURBATION

$$\mathbf{y}_a^* = \mathbf{y}_{a0}^* + \varepsilon \mathbf{y}_{a1}^* + \varepsilon^2 \mathbf{y}_{a2}^* + \cdots$$

$$\mathbf{h}_a^* = \mathbf{h}_{a0}^* + \varepsilon \mathbf{h}_{a1}^* + \varepsilon^2 \mathbf{h}_{a2}^* + \cdots$$

$$\alpha_a = \alpha_{a0} + \varepsilon \alpha_{a1} + \varepsilon^2 \alpha_{a2} + \cdots$$

PERTURBATION EQUATIONS

$$\left[\hat{\mathbf{B}}\right]\begin{Bmatrix}\mathbf{y}_{a0}^*\\ \mathbf{h}_{a0}^*\\ \alpha_{a0}\end{Bmatrix} - \begin{Bmatrix}0\\ \mathbf{R}_1\\ \mathbf{R}_2\end{Bmatrix} + \varepsilon\left\{\left[\hat{\mathbf{B}}\right]\begin{Bmatrix}\mathbf{y}_{a1}^*\\ \mathbf{h}_{a1}^*\\ \alpha_{a1}\end{Bmatrix} + \left[\tilde{\mathbf{B}}\right]\begin{Bmatrix}\mathbf{y}_{a0}^*\\ \mathbf{h}_{a0}^*\\ \alpha_{a0}\end{Bmatrix}\right\} + \varepsilon^2\left\{\left[\hat{\mathbf{B}}\right]\begin{Bmatrix}\mathbf{y}_{a2}^*\\ \mathbf{h}_{a2}^*\\ \alpha_{a2}\end{Bmatrix} + \left[\tilde{\mathbf{B}}\right]\begin{Bmatrix}\mathbf{y}_{a1}^*\\ \mathbf{h}_{a1}^*\\ \alpha_{a1}\end{Bmatrix}\right\} + \cdots = \begin{Bmatrix}0\\0\\0\end{Bmatrix}$$

$$\left[\hat{\mathbf{B}}\right] = \begin{bmatrix}\hat{\mathbf{B}}_{00} & \hat{\mathbf{B}}_{01} & 0\\ \hat{\mathbf{B}}_{10} & \hat{\mathbf{B}}_{11} & \hat{\mathbf{B}}_{12}\\ 0 & \hat{\mathbf{B}}_{21} & \hat{\mathbf{B}}_{22}\end{bmatrix}$$

$$\left[\tilde{\mathbf{B}}\right] = \begin{bmatrix}\tilde{\mathbf{B}}_{00} & \tilde{\mathbf{B}}_{01} & 0\\ \tilde{\mathbf{B}}_{10} & \tilde{\mathbf{B}}_{11} & 0\\ 0 & 0 & \tilde{\mathbf{B}}_{22}\end{bmatrix}$$

FIRST ORDER EXCITATION MODES

FOR EXCITATION MODE p
and
SINGLE MISTUNE MODE r

$$p_1 = (p-r) \bmod N$$

$$p_2 = (p+r) \bmod N$$

POSSIBLE RESPONSE MODES

FOR MISTUNE MODE *S* WHICH DIVIDES *N*

$$(p + j\, N/S) \bmod N; \quad j = 0, 1, 2, \ldots, S-1$$

MODE 11 MISTUNE OFF RESONANCE

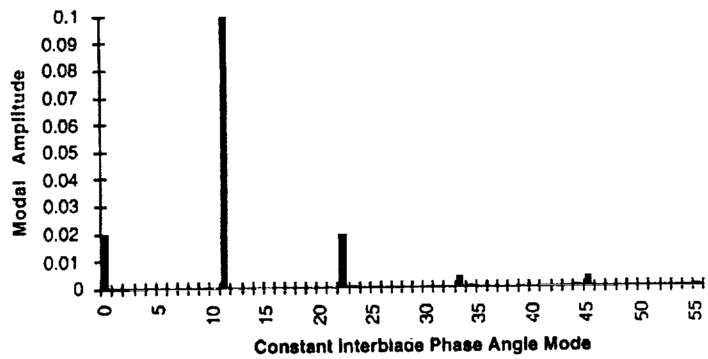

MODE 11 MISTUNE NEAR RESONANCE

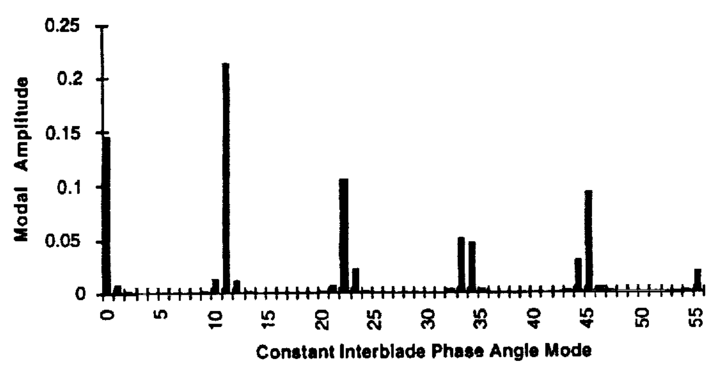

DESIGN PROBLEM

Given a set of (mistuned) blades, find an arrangement (blade - slot pairing) such that the forced response amplitudes are minimized.

Note: For an assembly with N blades, there are (N-1)! possible arrangements

TWO PHASE SYSTEM

- Phase One

  Continuous optimization to find Mistune Mode Parameters with a constraint on mistune strength

- Phase Two

  Find the arrangement that best matches the pattern desribed by mistune mode parameters

CONSTRAINTS

FOR A GIVEN SET OF BLADES, THE MEAN AND THE STANDARD DEVIATION ARE FIXED

- FIXED MEAN --> DETERMINES δ_0
- FIXED STANDARD DEVIATION --> DETERMINES $\sqrt{\sum_{r=1}^{N-1} \delta_r^2}$

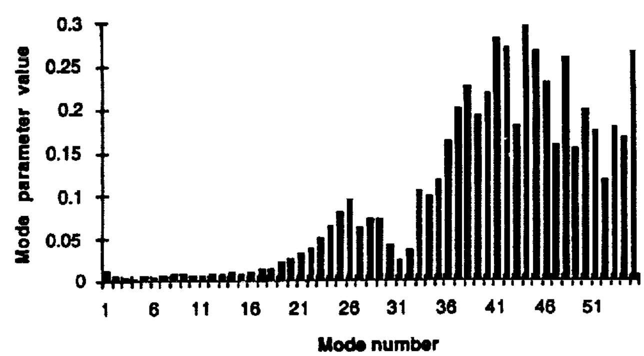

Optimal mistune mode parameters for $\gamma = 0.99$

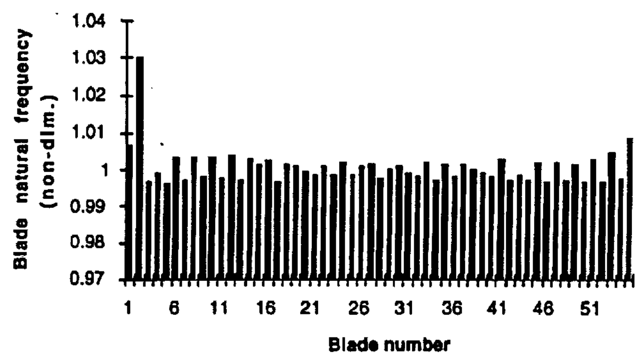

Optimal blade natural frequencies for $\gamma = 0.99$

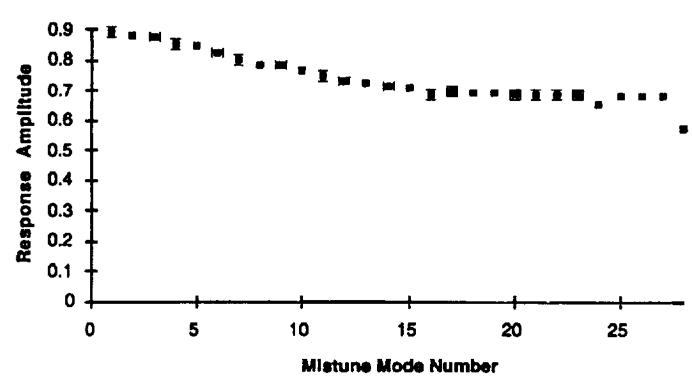

Objective function values for single mode mistune cases for $\gamma=0.99$

BLADE-SLOT ASSIGNMENT

- Find $\{\delta\}$ such that $\|\delta-\bar{\delta}\|_2$ is minimized
- Classic Linear Sum Assignment Problem

Minimize $\sum_{j=0}^{N-1}\sum_{k=0}^{N-1} a_{jk}c_{jk}$ subject to: $\sum_{j=0}^{N-1} a_{jk} = 1$ and $\sum_{k=0}^{N-1} a_{jk} = 1$

Where:

$$c_{jk} = \left(\gamma_{bj}^2 - \bar{\gamma}_{bk}^2\right)^2$$

$$a_{jk} = \begin{cases} 1; & \text{if blade j is at slot k} \\ 0; & \text{otherwise} \end{cases}$$

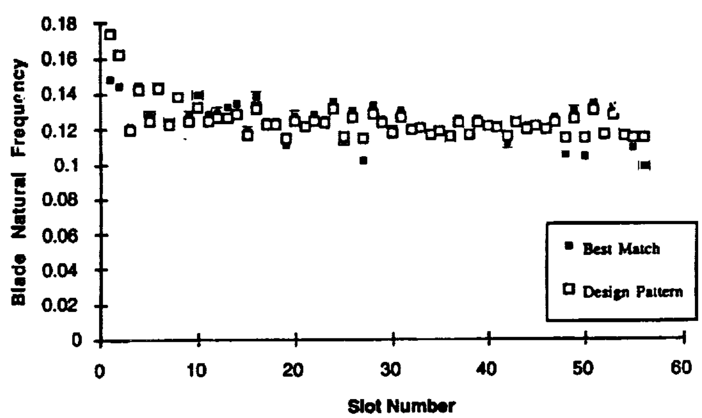

Best blade arrangement for optimal mistune pattern

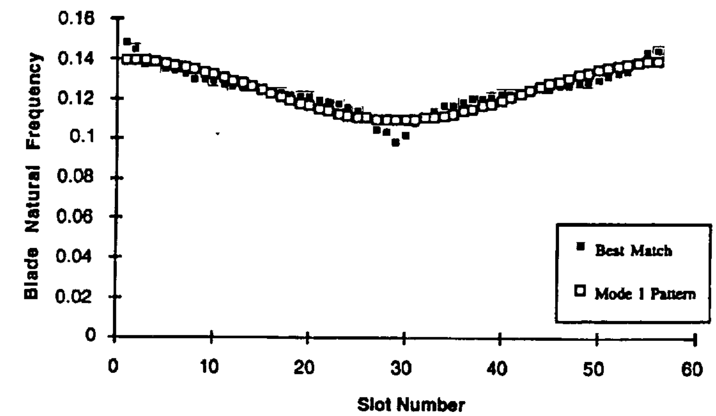

Best blade arrangement for mode 1 mistune pattern

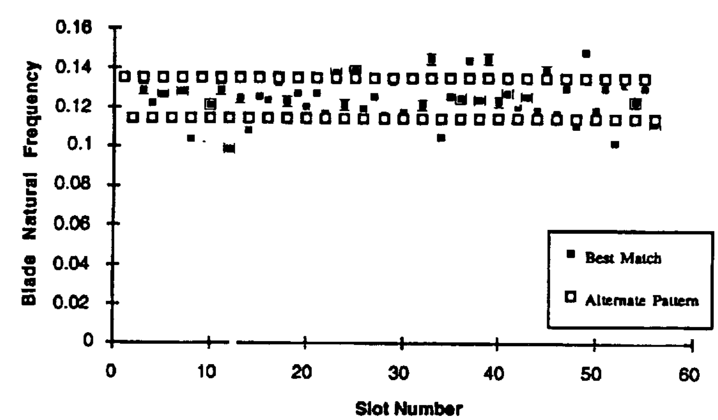

Best blade arrangement for alternate mistune pattern

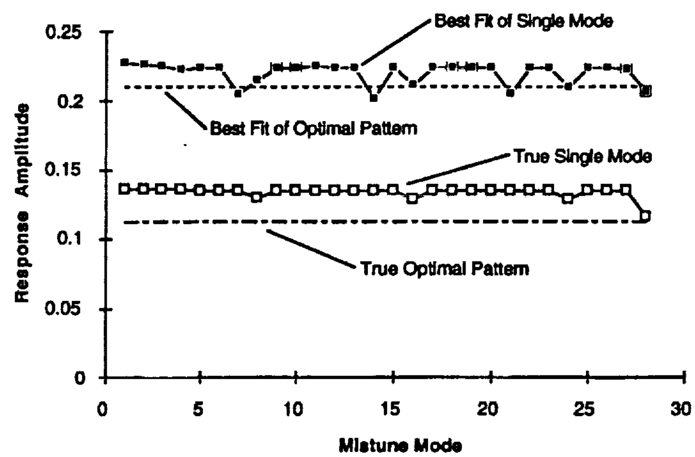

Response amplitudes of best fit to mistune patterns

LOCALIZATION

- Localized physical blade amplitudes can imply non-localized modal amplitudes

- Localized modal amplitudes implies non-localized physical blade amplitudes

FREPS CODE DEMONSTRATION

omit to END 9

M.R. Morel
NYMA, Inc.
Brook Park, Ohio 44142

and

D.V. Murthy*
NASA Lewis Research Center
Cleveland, Ohio 44135

FREPS Analysis Options

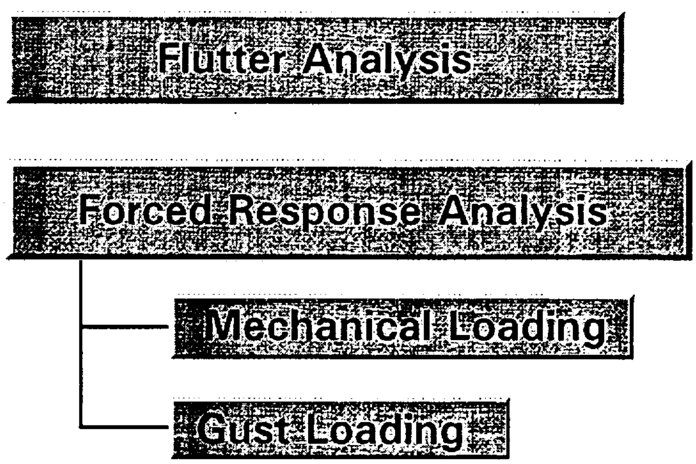

*NASA Resident Research Associate at Lewis Research Center.

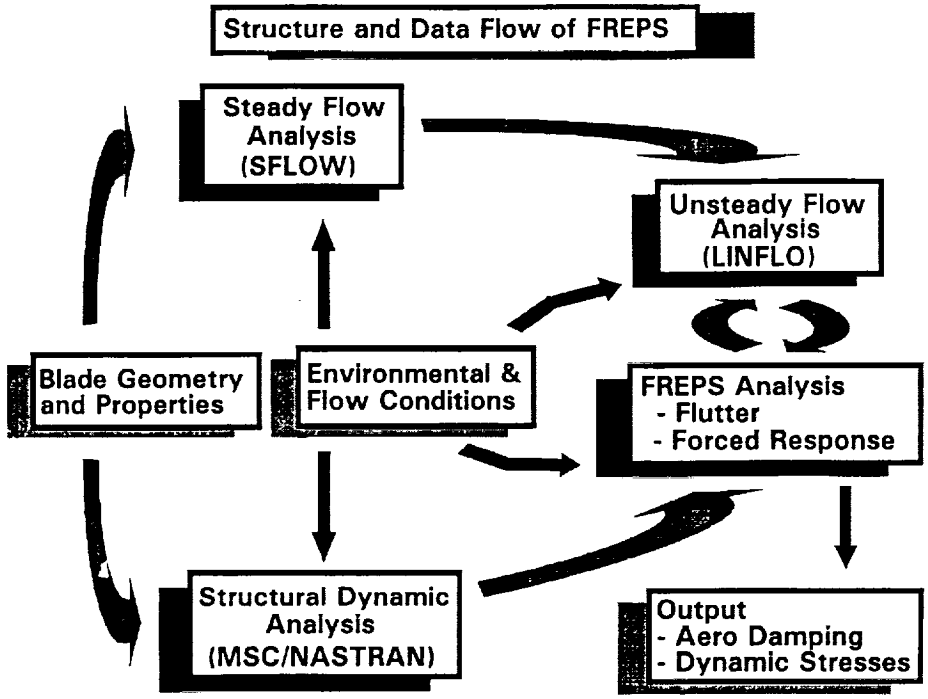

FREPS Input/Output File Structure

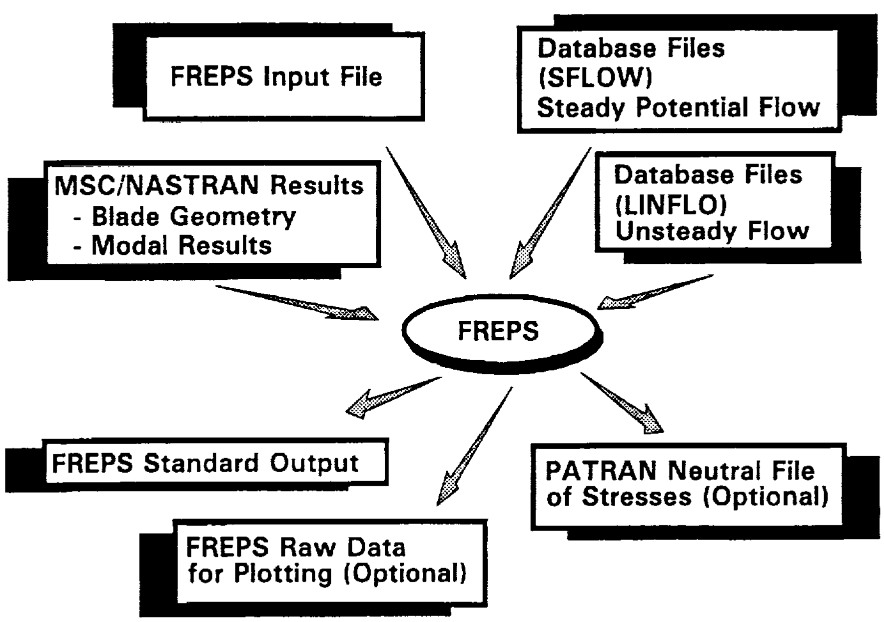

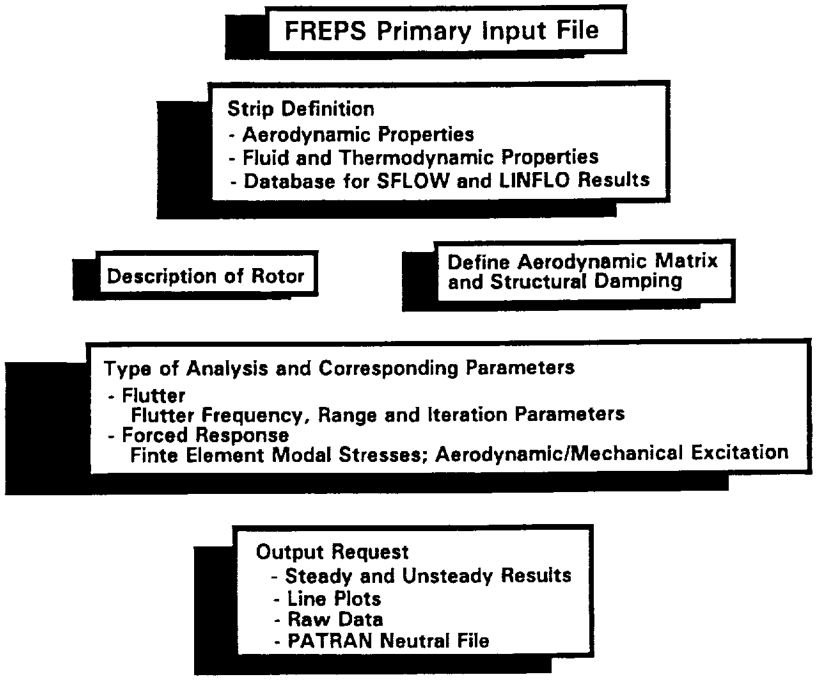
FREPS Primary Input File
Strip Definition
- Aerodynamic Properties
- Fluid and Thermodynamic Properties
- Database for SFLOW and LINFLO Results
Description of Rotor
Define Aerodynamic Matrix and Structural Damping
Type of Analysis and Corresponding Parameters
- Flutter
Flutter Frequency, Range and Iteration Parameters
- Forced Response
Finte Element Modal Stresses; Aerodynamic/Mechanical Excitation
Output Request
- Steady and Unsteady Results
- Line Plots
- Raw Data
- PATRAN Neutral File

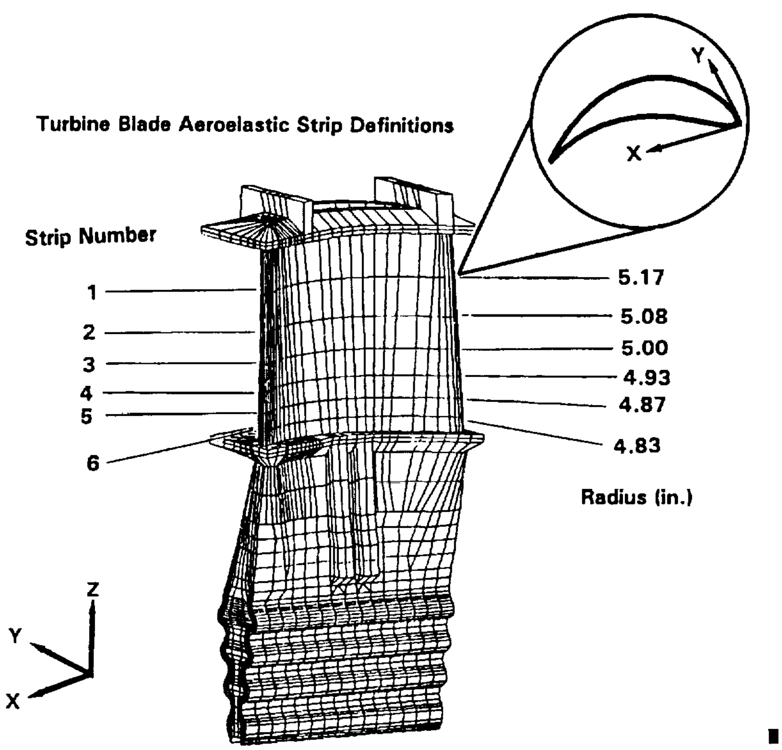
Turbine Blade Aeroelastic Strip Definitions
Y
X
Strip Number
1
2
3
4
5
6
5.17
5.08
5.00
4.93
4.87
4.83
Radius (in.)
Z
Y
X

FREPS Sample Input

```
1 ..........................................80

TITLE   TURBINE BLADE -- FORCED RESPONSE ANALYSIS

$
$   STRIP DEFINITION
$
$        nodal points defining locus
STRIP  1     3   27   75  159  243  327  411
STRIP  1   495  579  663  747  831  915  999
STRIP  1  1083 1206 1321 1394 1397 1401 1405
STRIP  1  1409 1413 1417 1421 1424 1427 1428
STRIP  1  1426 1422 1419 1414 1410 1406 1402
STRIP  1  1398 1318 1203 1080  996  912  828
STRIP  1   744  660  576  492  408  324  240
STRIP  1   156   72   26    3
```

FREPS Sample Input

```
$
$   FLUID AND AERO DESCRIPTION FOR STRIPS
$
$          fluidID  T(°R)   p(psi)  ρ(lbm/in³)  a(fps)  γ
SFLUID      100    518.69, 14.69,   0.0000,    1116.4, 1.4
$
$          stripID   θ
SROTATE     1       0.0
$
$          aeroID  W       β       M       H
SAERO       100,   0.0,    114.0,  0.3800, 0.225
$
$          groupID    stripID aeroID fluidID
SGROUP      100         1      100     100
$
$   STRIP DATABASE DEFINITIONS
$
$              stripID filename
DATABASE        1      airfoil_1
```

FREPS Sample Input

```
$
$   ROTOR DESCRIPTION
$
$           NofBLADES     Ω(rpm)  hubRADIUS     tipRADIUS
ROTOR         50          6000.0    4.79          5.29
$
$   AEROELASTIC SET DEFINITIONS
$     groupIDs
AESET    100
$
$   INTERBLADE PHASE ANGLE
$
$           n_σ   σ
AESIGMA  1    72.0
$
$   GUST  LOADS
$
$       stripID  V_G
GUST     1      25.0
$
$   FREQUENCY RANGE
$                f_low    f_high       Δf
FREQUENCY  9700.0  10100.0     20.00
```

FREPS Sample Input

```
$
$   NODAL DISPLACEMENTS
$
$                    nodes
NODEOUT      7851    7860
$
$   ELEMENT STRESSES
$
$                    elements
ELEMOUT      2886     2917     2892
$
$   MSC/NASTRAN PUNCH FILE OF STRESSES
$
$           iounit    filename
STRFILE      1       hp104.data
$
$   FORCED RESPONSE ANALYSES REQUESTED
$
RESPONSE
$
END
```

FREPS Output Files

FREPS Output
- Summarize Input
- Strip Geometry & Properties
- Steady Aerodynamic Results
- Unsteady Aerodynamic Results
- Aero Damping
- Dynamic Stresses
- Line Plots

FREPS Raw Data
(Optional)
- Airfoil Contour
- Steady Data
- Unsteady Data
- Root Locus Data

PATRAN Neutral File
(Optional)
Dynamic Principal Stresses for the Elements

Space Shuttle Main Engine (SSME) Blade

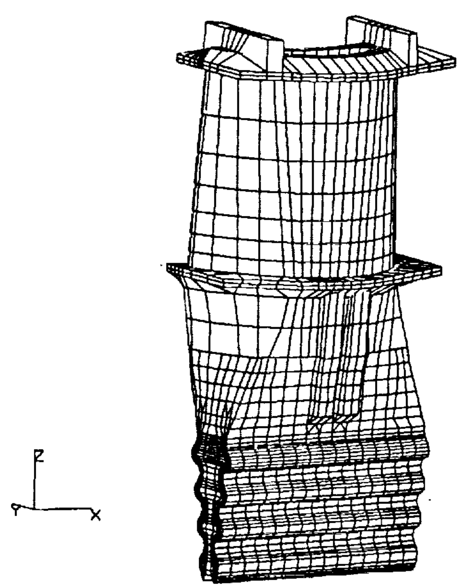

10,014 Nodal Points
7758 3-D Elements

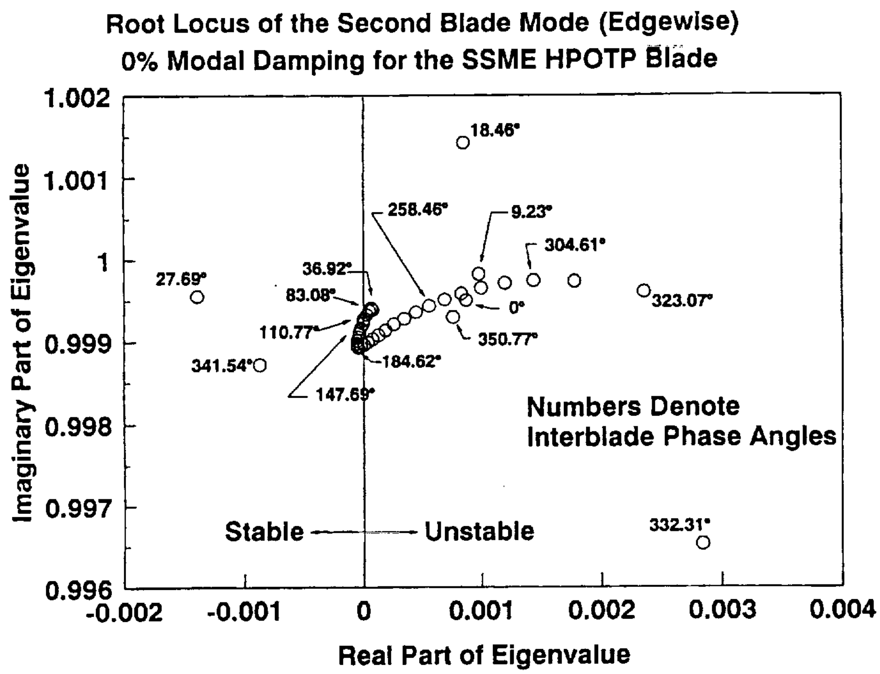
Root Locus of the Second Blade Mode (Edgewise)
0% Modal Damping for the SSME HPOTP Blade
Imaginary Part of Eigenvalue
Real Part of Eigenvalue
1.002
1.001
1
0.999
0.998
0.997
0.996
-0.002
-0.001
0
0.001
0.002
0.003
0.004
18.46°
258.46°
9.23°
304.61°
27.69°
36.92°
83.08°
0°
323.07°
110.77°
350.77°
184.62°
341.54°
147.69°
Numbers Denote
Interblade Phase Angles
Stable
Unstable
332.31°

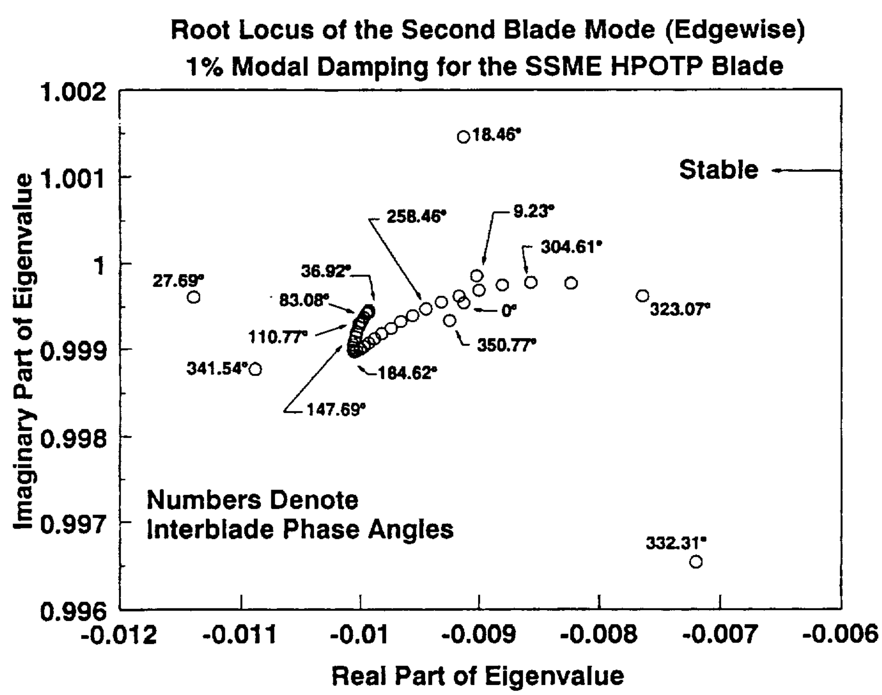
Root Locus of the Second Blade Mode (Edgewise)
1% Modal Damping for the SSME HPOTP Blade
Imaginary Part of Eigenvalue
Real Part of Eigenvalue
1.002
1.001
1
0.999
0.998
0.997
0.996
-0.012
-0.011
-0.01
-0.009
-0.008
-0.007
-0.006
18.46°
Stable
258.46°
9.23°
304.61°
27.69°
36.92°
83.08°
0°
323.07°
110.77°
350.77°
341.54°
184.62°
147.69°
Numbers Denote
Interblade Phase Angles
332.31°

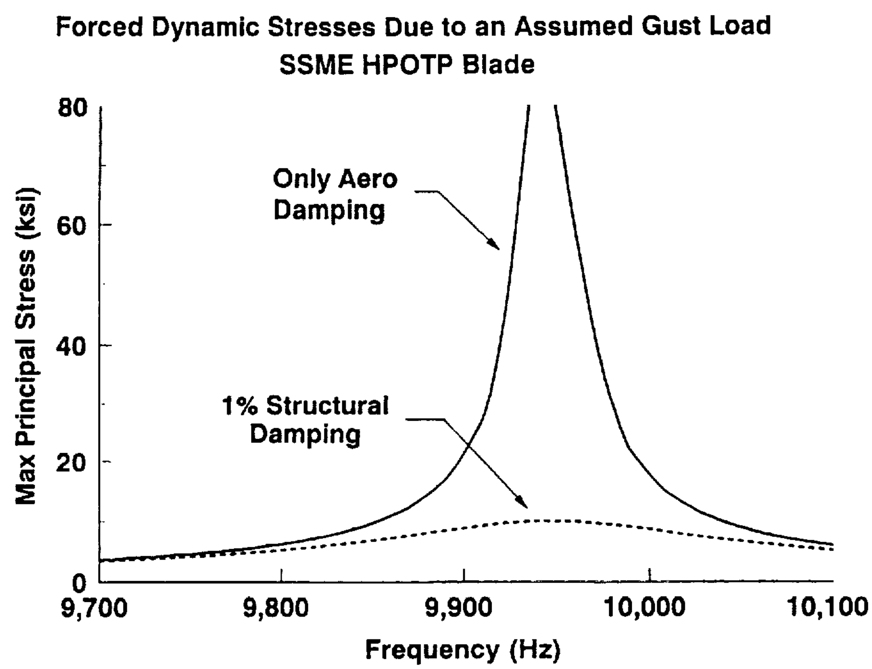
Forced Dynamic Stresses Due to an Assumed Gust Load
SSME HPOTP Blade
Max Principal Stress (ksi)
80
60
40
20
0
Only Aero Damping
1% Structural Damping
9,700
9,800
9,900
10,000
10,100
Frequency (Hz)

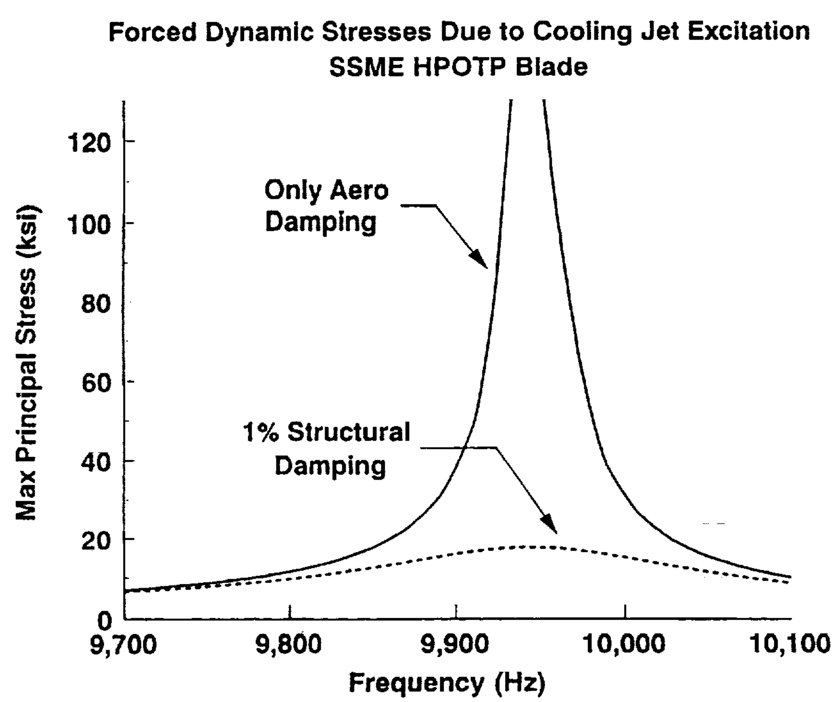
Forced Dynamic Stresses Due to Cooling Jet Excitation
SSME HPOTP Blade
Max Principal Stress (ksi)
120
100
80
60
40
20
0
Only Aero Damping
1% Structural Damping
9,700
9,800
9,900
10,000
10,100
Frequency (Hz)

REPORT DOCUMENTATION PAGE

Form Approved
OMB No. 0704-0188

1. AGENCY USE ONLY (*Leave blank*)	2. REPORT DATE	3. REPORT TYPE AND DATES COVERED
	December 1994	Conference Publication

4. TITLE AND SUBTITLE

NASA Lewis Research Center Workshop on Forced Response in Turbomachinery

5. FUNDING NUMBERS

WU-505-63-5B

6. AUTHOR(S)

G.L. Stefko, D.V. Murthy, M. Morel, D. Hoyniak, and J.W. Gauntner, compilers

7. PERFORMING ORGANIZATION NAME(S) AND ADDRESS(ES)

National Aeronautics and Space Administration
Lewis Research Center
Cleveland, Ohio 44135-3191

8. PERFORMING ORGANIZATION REPORT NUMBER

E-9111

9. SPONSORING/MONITORING AGENCY NAME(S) AND ADDRESS(ES)

National Aeronautics and Space Administration
Washington, D.C. 20546-0001

10. SPONSORING/MONITORING AGENCY REPORT NUMBER

NASA CP-10147

11. SUPPLEMENTARY NOTES

Proceedings of a conference sponsored by the NASA Lewis Research Center, the Structural Dynamics Branch, Structures Division; the Turbomachinery Technology Branch, Propulsion Systems Division, and the Launch Vehicle Propulsion Branch, Space Propulsion Technology Division and held at the NASA Lewis Research Center, Cleveland, Ohio, August 11, 1993. Responsible person, George Stefko, organization code 5230, (216) 433-3920.

12a. DISTRIBUTION/AVAILABILITY STATEMENT

Unclassified - Unlimited
Subject Category 07

12b. DISTRIBUTION CODE

13. ABSTRACT ***(Maximum 200 words)***

This document serves as a summary of the NASA Lewis Research Center (LeRC) Workshop on Forced Response in Turbomachinery in August of 1993. The workshop was sponsored by the following NASA organizations: Structures, Space Propulsion Technology, and Propulsion Systems Divisions of NASA LeRC and the Aeronautics and Advanced Concepts & Technology Offices of NASA Headquarters. In addition, the workshop was held in conjunction with the GUIde (Government/Industry/Universities) Consortium on Forced Response. The workshop was specifically designed to receive suggestions and comments from industry on current research at NASA LeRC in the area of forced vibratory response of turbomachinery blades which includes both computational and experimental approaches. There were eight presentations and a code demonstration. Major areas of research included aeroelastic response, steady and unsteady fluid dynamics, mistuning, and corresponding experimental work.

14. SUBJECT TERMS

Forced response; Turbomachinery; Blades; Computational fluid dynamics

15. NUMBER OF PAGES

143

16. PRICE CODE

A07

17. SECURITY CLASSIFICATION OF REPORT	18. SECURITY CLASSIFICATION OF THIS PAGE	19. SECURITY CLASSIFICATION OF ABSTRACT	20. LIMITATION OF ABSTRACT
Unclassified	Unclassified	Unclassified	

NSN 7540-01-280-5500

Standard Form 298 (Rev. 2-89)
Prescribed by ANSI Std. Z39-18
298-102